NSF/CEE-81014

PB82-104217

INVESTIGATION OF REINFORCED BRICK MASONRY BUILDINGS UNDAMAGED BY THE SAN FERNANDO EARTHQUAKE

THIS MATERIAL IS BASED UPON WORK SUPPORTED BY THE NATIONAL SCIENCE FOUNDATION UNDER GRANT NUMBER PFR-7900013. ANY OPINIONS, FINDINGS, AND CONCLUSIONS OR RECOMMENDATIONS EXPRESSED IN THIS PUBLICATION ARE THOSE OF THE AUTHOR AND DO NOT NECESSARILY REFLECT THE VIEWS OF THE NATIONAL SCIENCE FOUNDATION.

May 1981

Prepared under

National Science Foundation Grant No. PFR-7900013

AGBABIAN ASSOCIATES

El Segundo, California

INFORMATION RESOURCES
NATIONAL SCIENCE FOUNDATION

REPRODUCED BY
NATIONAL TECHNICAL
INFORMATION SERVICE
U.S. DEPARTMENT OF COMMERCE
SPRINGFIE...

50272-101

REPORT DOCUMENTATION PAGE	1. REPORT NO. NSF/CEE-81014	2.	3. Recipient's Accession No.

4. Title and Subtitle Investigation of Reinforced Brick Masonry Buildings Undamaged by the San Fernando Earthquake	5. Report Date May 1981
	6.
7. Author(s) S.A. Adham	8. Performing Organization Rept. No.
9. Performing Organization Name and Address Agbabian Associates 250 North Nash Street El Segundo, CA 90245	10. Project/Task/Work Unit No.
	11. Contract(C) or Grant(G) No. (C) (G) PFR7900013
12. Sponsoring Organization Name and Address Directorate for Engineering (ENG) National Science Foundation 1800 G Street, N.W. Washington, D.C. 20550	13. Type of Report & Period Covered
	14.

15. Supplementary Notes
Submitted by: Communications Program (OPRM)
National Science Foundation
Washington, D.C. 20550

16. Abstract (Limit: 200 words)

Behavior of the buildings of the Sepulveda Veterans Administration Hospital during the 1971 San Fernando earthquake was examined. The study explored why these buildings sustained minimal structural damage while other buildings in close proximity sustained major damage. A literature review was conducted and seismic input motions at the site during the earthquake were estimated. Verifications of seismic analysis techniques, using a two-dimensional finite element model, were determined through studies of observed earthquake damage to a six-story building. Relative displacements were calculated at the expansion joints and compared to damage of the flexible joints. Also verified were seismic analysis techniques through a study of observed earthquake damage to the boiler house building. A two-dimensional finite element analysis was conducted, followed by simple hand calculations. Results of both analyses were compared to observed cracks from overstress conditions. The calibrated motions were used as input to a three-dimensional model of a reinforced brick masonry building. The building's behavior and the effects of expansion joints on its performance were evaluated. Performance criteria were developed for assessing the response of masonry buildings during the earthquake and evaluating the effect of expansion joints on relieving internal stresses. Conclusions and recommendations are provided.

17. Document Analysis a. Descriptors

Earthquake resistant structures	Reinforcement (structures)
Buildings	Numerical analysis
Brick structures	Masonry
Earthquakes	Damage assessment

b. Identifiers/Open-Ended Terms

San Fernando Earthquake
Finite element analysis
Sepulveda Veterans Administration Hospital

c. COSATI Field/Group D,S

18. Availability Statement	19. Security Class (This Report)	21. No. of Pages
NTIS	20. Security Class (This Page)	22. Price

(See ANSI-Z39.18) See Instructions on Reverse OPTIONAL FORM 272 (4-77)
(Formerly NTIS-35)
Department of Commerce

ATTENTION

AS NOTED IN THE NTIS ANNOUNCEMENT, PORTIONS OF THIS REPORT ARE NOT LEGIBLE. HOWEVER, IT IS THE BEST REPRODUCTION AVAILABLE FROM THE COPY SENT TO NTIS.

i.a

INVESTIGATION OF REINFORCED BRICK MASONRY BUILDINGS UNDAMAGED BY THE SAN FERNANDO EARTHQUAKE

THIS MATERIAL IS BASED UPON WORK SUPPORTED BY THE NATIONAL SCIENCE FOUNDATION UNDER GRANT NUMBER PFR-7900013. ANY OPINIONS, FINDINGS, AND CONCLUSIONS OR RECOMMENDATIONS EXPRESSED IN THIS PUBLICATION ARE THOSE OF THE AUTHOR AND DO NOT NECESSARILY REFLECT THE VIEWS OF THE NATIONAL SCIENCE FOUNDATION.

May 1981

Prepared under

National Science Foundation Grant No. PFR-7900013

AGBABIAN ASSOCIATES
El Segundo, California

1.b

INTENTIONALLY BLANK

PREFACE

This final report was prepared by Agbabian Associates under NSF Grant No. PFR-7900013. This 12-month program supported the objectives of the Disaster and National Hazard Research conducted under the Earthquake Hazard Mitigation program of the National Science Foundation. The objective of work covered by this report is to investigate a group of reinforced brick masonry buildings undamaged by the 1971 San Fernando earthquake.

The cognizant NSF Program Official for this grant is Dr. John B. Scalzi. Principal Investigator for Agbabian Associates is Dr. Samy A. Adham. The Project Engineer for this study is Dr. Y. C. Lee, assisted by O. Babakhanian and M. Kundu.

Preceding page blank

INTENTIONALLY BLANK

CONTENTS

Preceding page blank

CONTENTS (CONTINUED)

CONTENTS (CONTINUED)

SECTION 1

INTRODUCTION

Numerous investigations have been made of damaged buildings in past earthquakes in order to understand how they responded to the ground shaking and how they might have been designed to eliminate or minimize the resulting damage. But little attention has been paid to undamaged structures in the immediate area that were also exposed to the same ground motion environment. Understanding why a structure was not damaged can contribute significantly to our knowledge of earthquake engineering and to the design and construction of earthquake-resistant structures.

This report analyzes and evaluates the behavior of the buildings of the Sepulveda Veterans Administration Hospital during the February 9, 1971 San Fernando earthquake. The buildings were constructed of reinforced concrete and reinforced grouted brick masonry (Guard, 1974) and were subjected to strong ground motions that greatly exceeded the original design assumptions. However, these buildings did not sustain major structural damage (Dickey, 1972). The facility is located in close proximity to three hospitals that were badly damaged in the earthquake: the San Fernando VA Hospital, the Holy Cross Hospital, and the Indian Hills Medical Center. Also, there was structural damage to many other buildings in the immediate area (Lew et al., 1971).

The remainder of this introductory section will provide background information for the study of the Sepulveda VA Hospital and its responses to the 1971 San Fernando earthquake. The objectives, scope, and organization of this report are included at the end of this section.

1.1 BACKGROUND

The construction of the Sepulveda Veterans Administration Hospital was completed in 1955. The hospital is located near the community of Sepulveda on a 160-acre site in the heart of the San Fernando Valley section of the City of Los Angeles (Figs. 1-1, 1-2, and 1-3). The unit numbers and titles used in this report are the same as those currently employed by the hospital

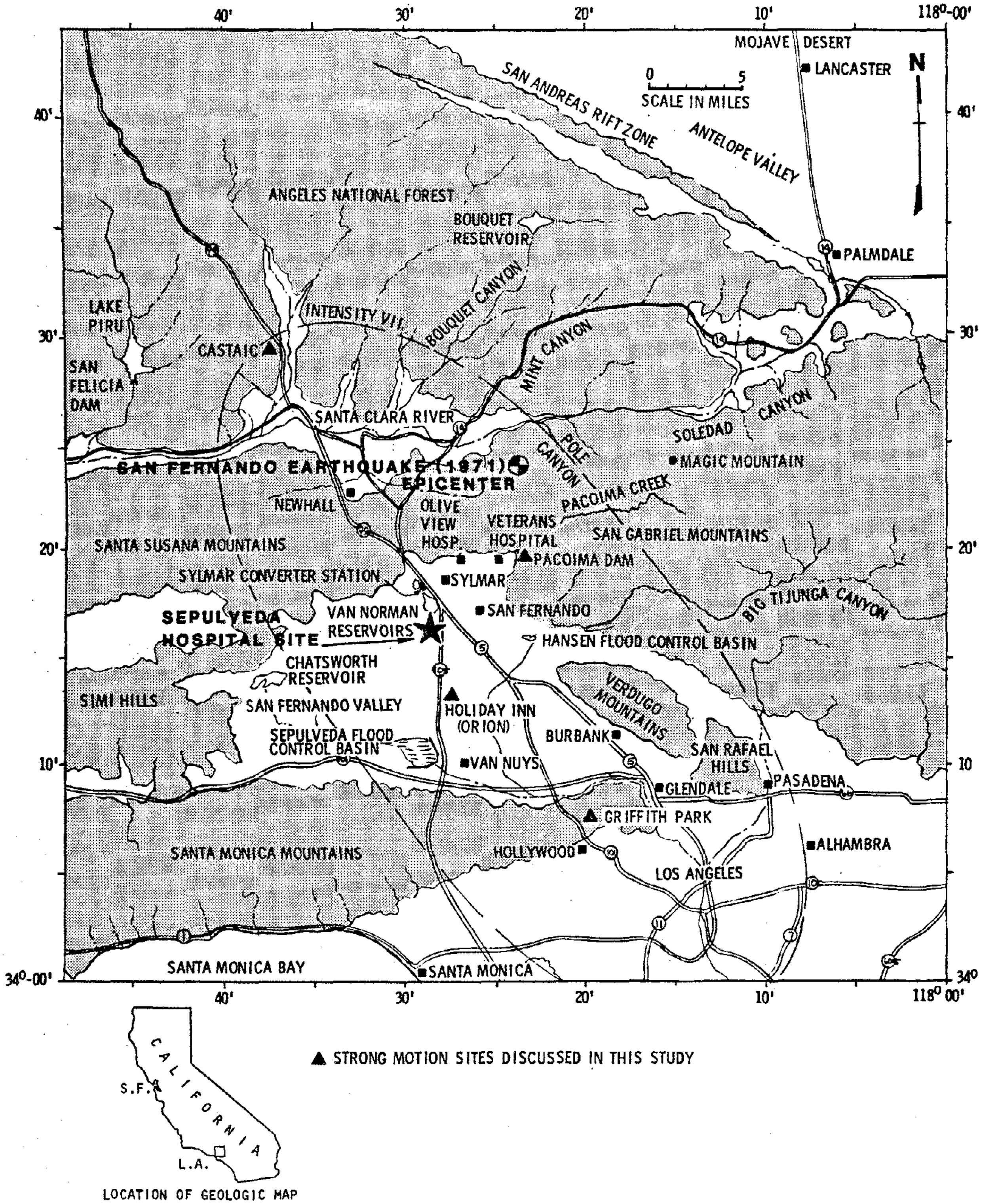

FIGURE 1-1. GENERAL MAP SHOWING PHYSIOGRAPHICAL FEATURES OF SAN FERNANDO VALLEY AND SURROUNDING MOUNTAIN AREAS AND LOCATION OF SEPULVEDA HOSPITAL

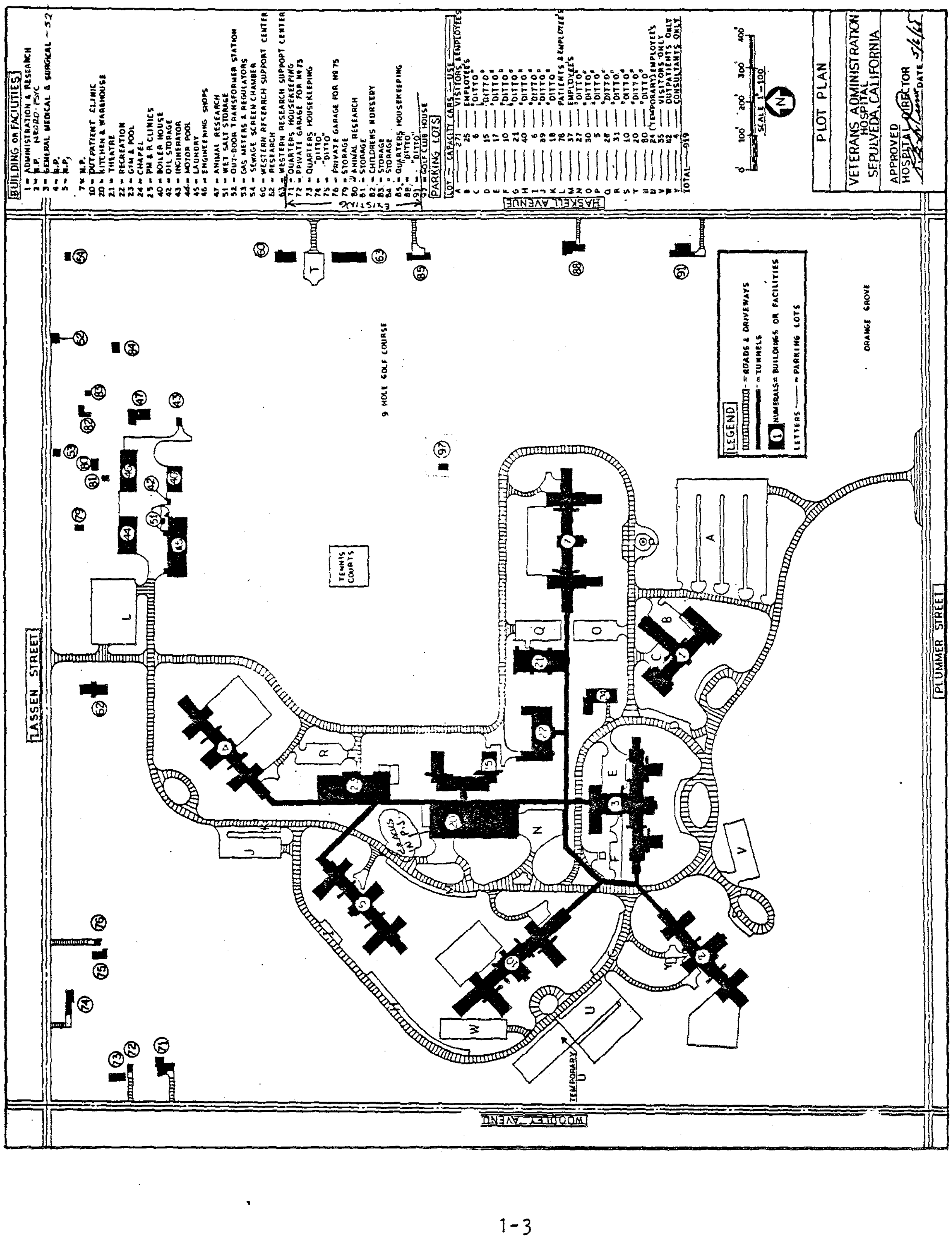

FIGURE 1-2. GENERAL LAYOUT OF SEPULVEDA VA HOSPITAL

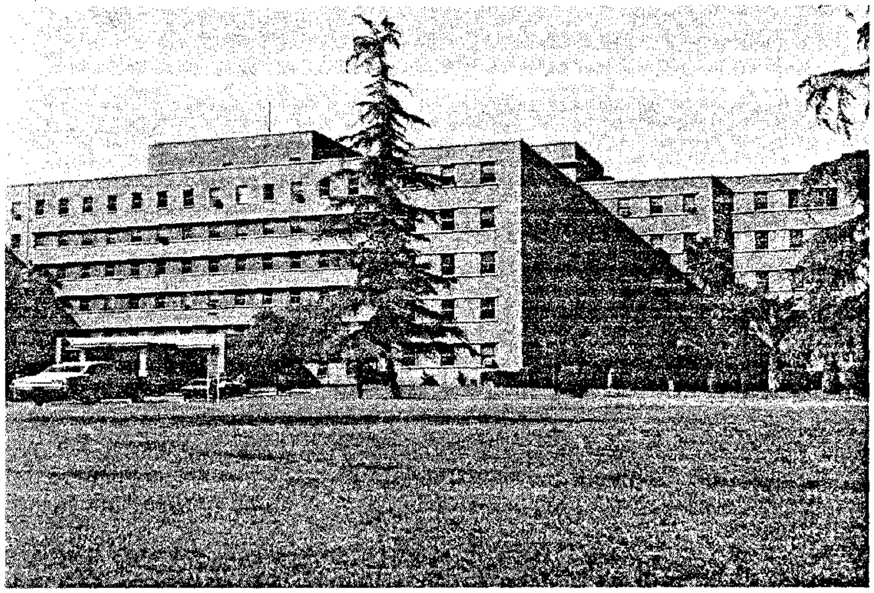

(a) Building 3

(a) Building 4

FIGURE 1-3. VIEW OF TYPICAL HOSPITAL BUILDINGS administration. It should be noted that the unit numbers are not necessarily consecutive, as illustrated in Figure 1-2 and Table 1-1 taken from a report by Brandow and Johnston (1972). The group of buildings of concern in this study are 22 buildings and 5 support facilities ranging in height between one and six stories (Table 1-1). At the time the hospital was constructed in 1955, it was reported as probably the largest single project utilizing reinforced brick masonry construction ever built in the United States.

A survey of the hospital buildings immediately after the 1971 San Fernando earthquake was reported by Lew et al. (1971):

> One of the six-story buildings experienced considerable damage to the seismic (flexible) joints between building segments. However, it was observed that these joints did minimize the damage which could have occurred. Another six-story building sustained minimal cracking in structural concrete walls and extensive plaster cracking, particularly on the fifth and sixth floors. Several buildings sustained visible cracking in reinforced concrete joist and slab floor systems. A number of elevators sustained damage to the cast iron counterweight guide shoes and rail brackets. Several other elevators sustained additional damage to hoisting machine drive motors.
>
> Overall, there was only minimal structural damage to the Sepulveda V.A. Hospital. The operation of the hospital was not interrupted. However, extensive elevator and plaster repairs were required and a number of seismic joints required replacement.

The earthquake-resistant design of the Sepulveda VA Hospital included expansion joints. These expansion joints were used to separate large and irregular structural configurations into separate and symmetrical buildings. Four-inch expansion joints were used for the six-story buildings while 3-inch expansion joints were used for one-and two-story buildings.

The violence of ground shaking was evidenced by extensive damage to the flexible expansion joints in Building 3 and jolting out-of-place of window jambs in the sixth floor. In addition, a permanent displacement of approximately 1 inch was reported at the six-floor level of Segment B of

TABLE 1-1. SCHEDULE OF BUILDINGS CONSTRUCTED UNDER THE AUSPICES OF THE VETERAN'S ADMINISTRATION (Brandow and Johnston, 1972)

BUILDING NUMBER	YEAR CONST.	NO. OF STORIES	BASEMENT	PIPE ACCESS	VERTICAL LOAD CARRYING ELEMENTS															SHEAR WALL CONSTRUCTION
					RC						RM		SS					W		
					os	rs	b	a	c	bw	c	bw	d	j	b	t	c	s	r/j	
1	1955	2	yes	no		●	●		●			●								RM
2	1955	4	yes	yes		●	●		●	●										RC
3	1955	6	yes	yes		●	●		●	●										RC
4	1955	2	yes	yes		●	●		●			●								RM
5	1955	2	yes	yes		●	●		●			●								RM
7	1955	1	yes	yes		●	●		●			●								RM
10	1955	2	yes	yes		●	●		●			●								RM
20	1955	2	no	no		●	●		●			●								RM
21	1955	2	yes	no	●		●		●							●	●			RC
22	1955	2	yes	no	●	●	●		●						●	●				RM
23	1955	2	yes	yes	●	●	●								●	●	●			RM
24	1955	1	yes	yes		●	●				●	●								RM
25	1955	1	yes	yes		●	●		●			●								RM
40	1955	1	no	no		●		●												RM
43	1955	1	no	no	●		●					●								RM
44	1955	1	no	no		●	●				●	●								RM
45	1955	1	no	yes	●	●	●	●			●									RM
46	1955	1	no	no		●	●				●	●								RM
47	1962	1	no	no								●	●	●						RM
60	1955	1	no.	yes		●			●			●								RM
62	1955	2	no	yes		●			●			●								RM
63	1955	1	no	yes								●			●			●	●	RM

SYMBOLS

RC - REINFORCED CONCRETE
RM - REINFORCED MASONRY (BRICK)
SS - STRUCTURAL STEEL
W - WOOD
a - ARCHES

b - BEAMS
bw - BEARING WALLS
c - COLUMNS
d - DECKING
j - JOISTS

os - ONE-WAY SLABS
rs - RIBBED SLABS
r/j - RAFTERS AND/OR JOISTS
s - SHEATHING
t - TRUSSES

Building 3 (see Section 3 for details). Visible cracks were also reported in the reinforced concrete frames supporting the boiler house roof (see Section 4 for details) and the chimney of the incinerator (Building 43) as illustrated in Figure 1-4.

1.2 OBJECTIVES

The objectives of this study are:

a. To evaluate the performance of the Sepulveda Hospital during the San Fernando earthquake

b. To assess response of reinforced grouted brick masonry structures to strong earthquake shaking

c. To provide information of effectiveness of expansion joints in large and/or irregular buildings

d. To evaluate wall-to-slab connections and detailing

1.3 SCOPE

The scope of this study includes the following activities:

1. Develop ground motion for the site that duplicates the actual motions during the 1971 San Fernando earthquake.

2. Analyze Building 3 (six-story reinforced concrete) for the input developed in Step 1 and revise input until calculated deflections provide reasonable correlation with the post-earthquake observations made of estimated building motions.

3. Analyze Building 40 (reinforced concrete structure with exterior brick walls) for the seismic input calibrated in Step 2. Compare analysis results with observed crack pattern in the frames. Provide an additional calibration of seismic input.

4. Construct a three-dimensional finite-element model of Building 10 (two-story reinforced brick masonry) and analyze the building for the revised earthquake input of Steps 2 and 3.

5. Construct a three-dimensional model of Building 10 with various parts tied together (no expansion joints) and analyze for the same earthquake input used in Steps 2 and 3.

6. Examine failure theories of brick masonry and develop a method for evaluating shear wall performance.

7. Evaluate response of Building 10 with and without expansion joints using method developed in Step 6.

8. Examine wall-to-slab connections and construction details and compare to current standard practice.

9. Provide conclusions and recommendations for brick masonry construction in highly seismic areas.

1.4 REPORT ORGANIZATION

Section 2 of this report describes development of seismic input for the analysis of Buildings 3, 40, and 10. Section 3 describes the two-dimensional seismic analysis of Building 3 and provides a comparison with observed response during the earthquake. Section 4 illustrates two types of analyses performed for Building 40 and provides a correlation with observed overstress in this building. Section 5 provides for the analysis of two three-dimensional models of the brick masonry Building 10. The first model represents Building 10 with expansion joints while the second model assumes the various segments of Building 10 to be tied together. Section 6 includes a discussion of both shear and biaxial failure theories. Section 7 contains an evaluation of the response of Building 10 and assessment of connections and construction details. Section 8 provides conclusions and recommendations derived from this study. References are listed in Section 9.

Reproduced from best available copy.

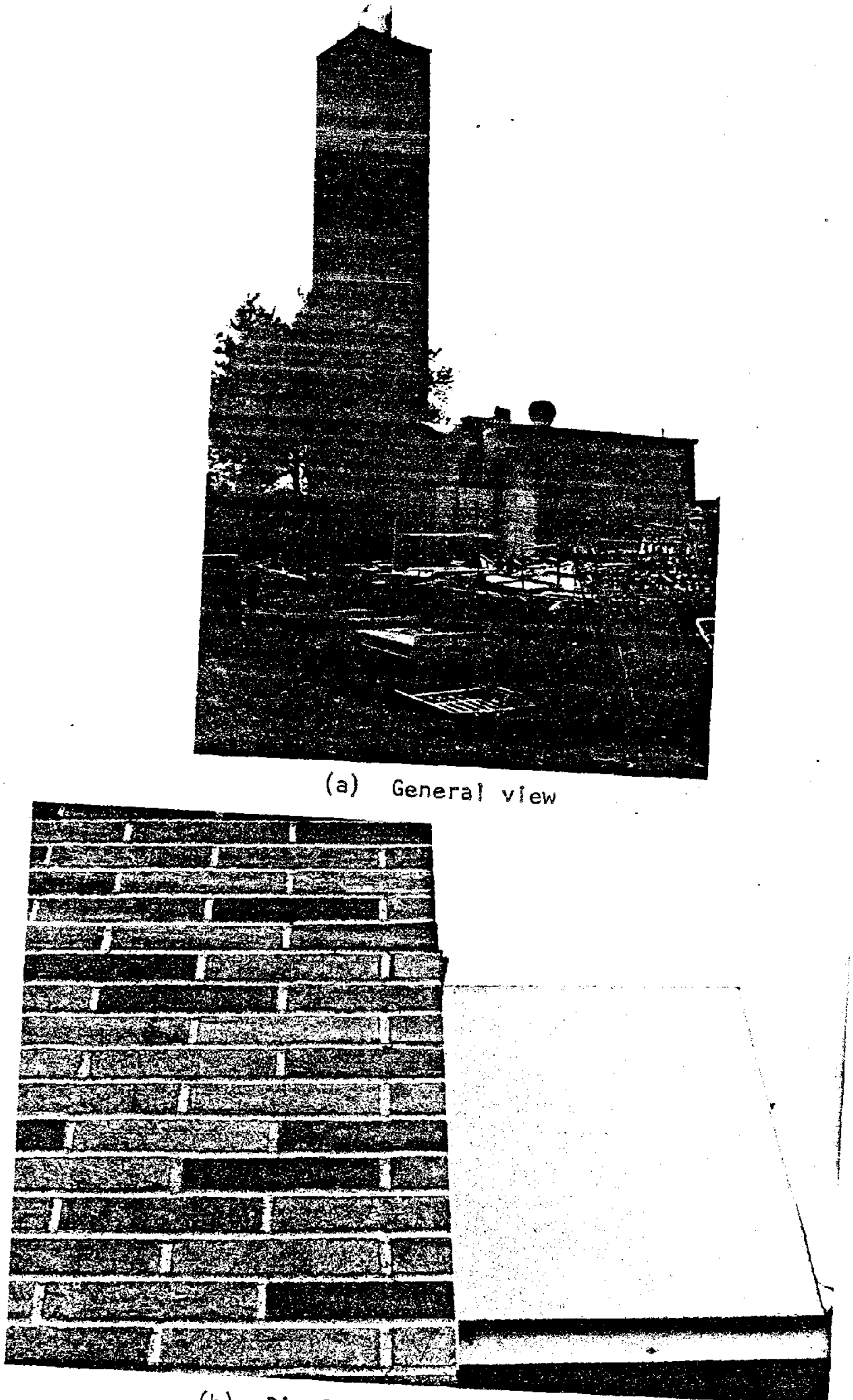

(a) General view

(b) Displaced brick — chimney

FIGURE 1-4. INCINERATOR BUILDING (NO. 43)

SECTION 2

ESTIMATES OF EARTHQUAKE GROUND MOTIONS AT THE SITE DURING THE 1971 SAN FERNANDO EARTHQUAKE

2.1 INTRODUCTION

An estimate of the earthquake ground motions experienced at the site during the San Fernando earthquake of 9 February 1971 is given in this section. It is based on a study of strong motion earthquake records available from nearby stations, the geology and seismic characteristics of the area, and the local soil conditions. The extent of regional and local faulting that has been identified is also given.

Information sources for this study were published reports and papers on the San Fernando earthquake, in addition to specific reports on the subject buildings.*

2.2 GEOLOGY

The physiographical features of the San Fernando Valley and the surrounding area are shown in Figure 1-1. The site is located in the northern-central part of the San Fernando Valley. The San Gabriel and Santa Susana Mountains lie to the east and north of the site, and the Santa Monica Mountains lie some 15 miles to the south across the San Fernando Valley. The epicenter of the 9 February 1971 earthquake and its position relative to the San Andreas Rift Zone are shown in Figure 1-1. The epicenter and the rift zone are about 10 miles and 27-1/2 miles, respectively, northeast of the site.

A generalized geologic map of Los Angeles-San Fernando Valley area showing epicenter and rupture zone along San Fernando fault, 9 February 1971, is provided as Figure 2-1. A geologic section along line N-S is shown in Figure 2-2.

---

*Murphy (1973), Lew et al. (1971), Allen et al. (1973), Jennings and Strand (1969), Wentworth and Yerkes (1971), Oakeshott (1958), Veterans Administration (1952), Agbabian Associates (1973), Woodward-Lundgren (1975).

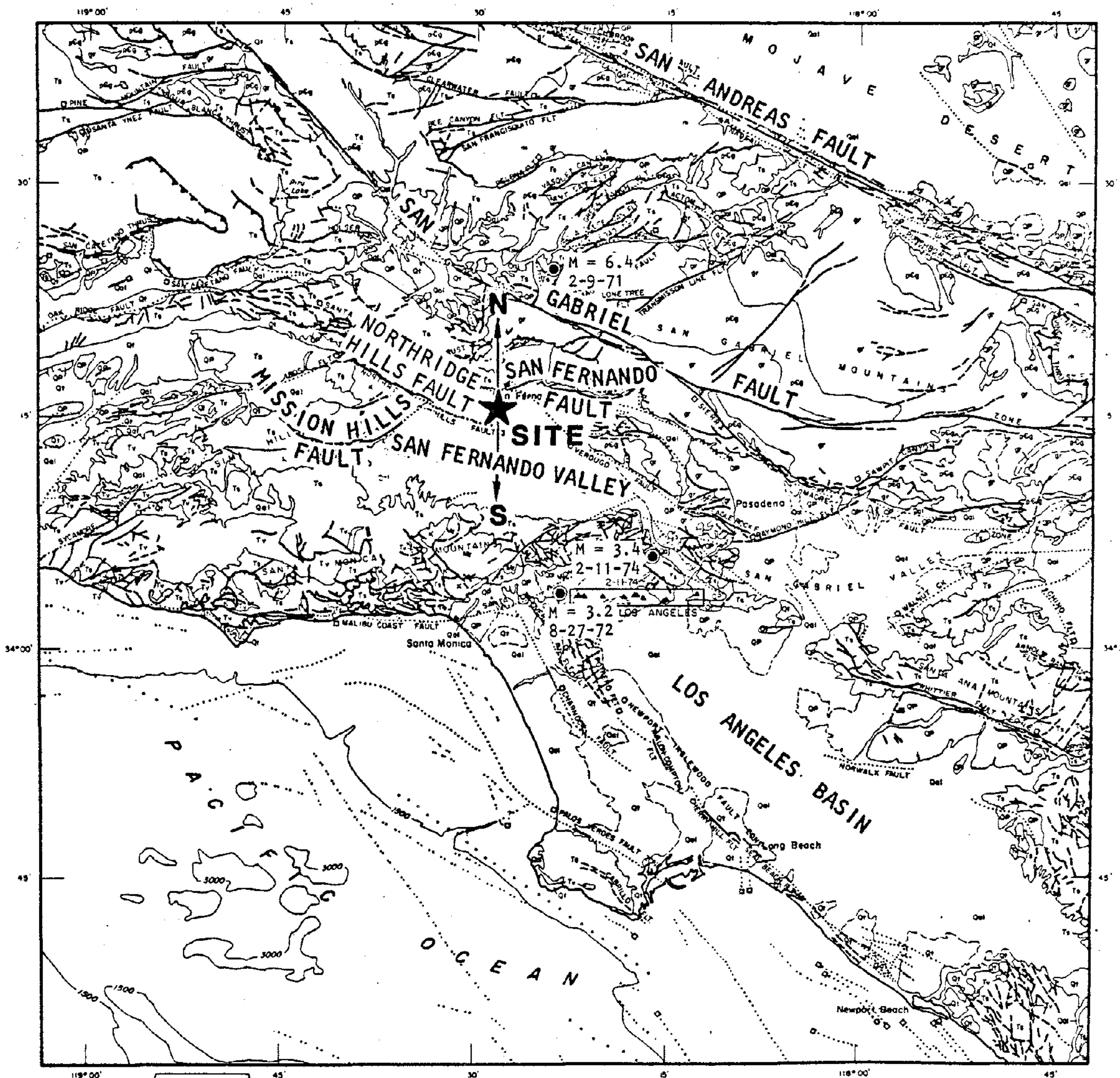

LOCATION OF GEOLOGIC MAP

FIGURE 2-1. GEOLOGIC MAP OF LOS ANGELES — SAN FERNANDO AREA (SW/AA, 1978)

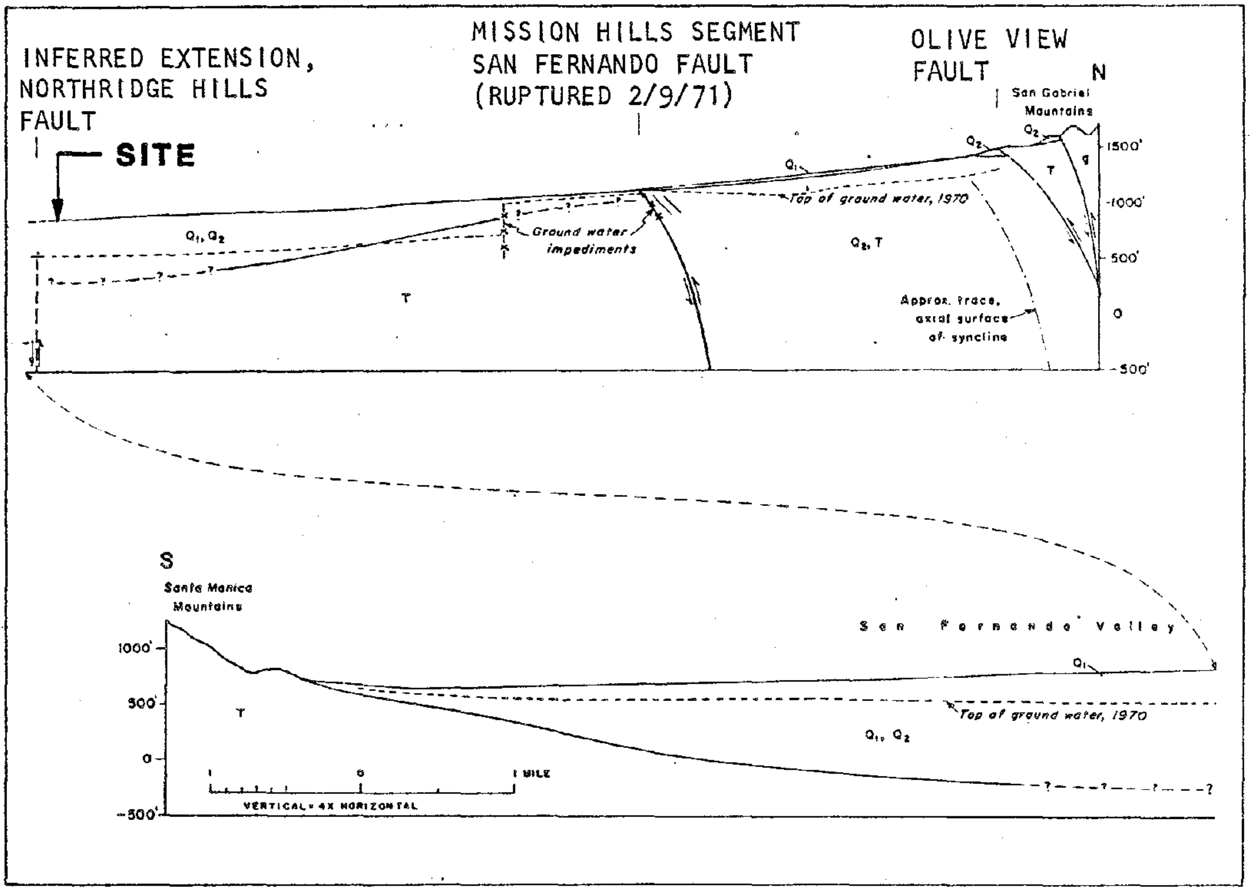

FIGURE 2-2. NORTH-SOUTH GEOLOGIC SECTION ACROSS SAN FERNANDO VALLEY (Yerkes, 1973)

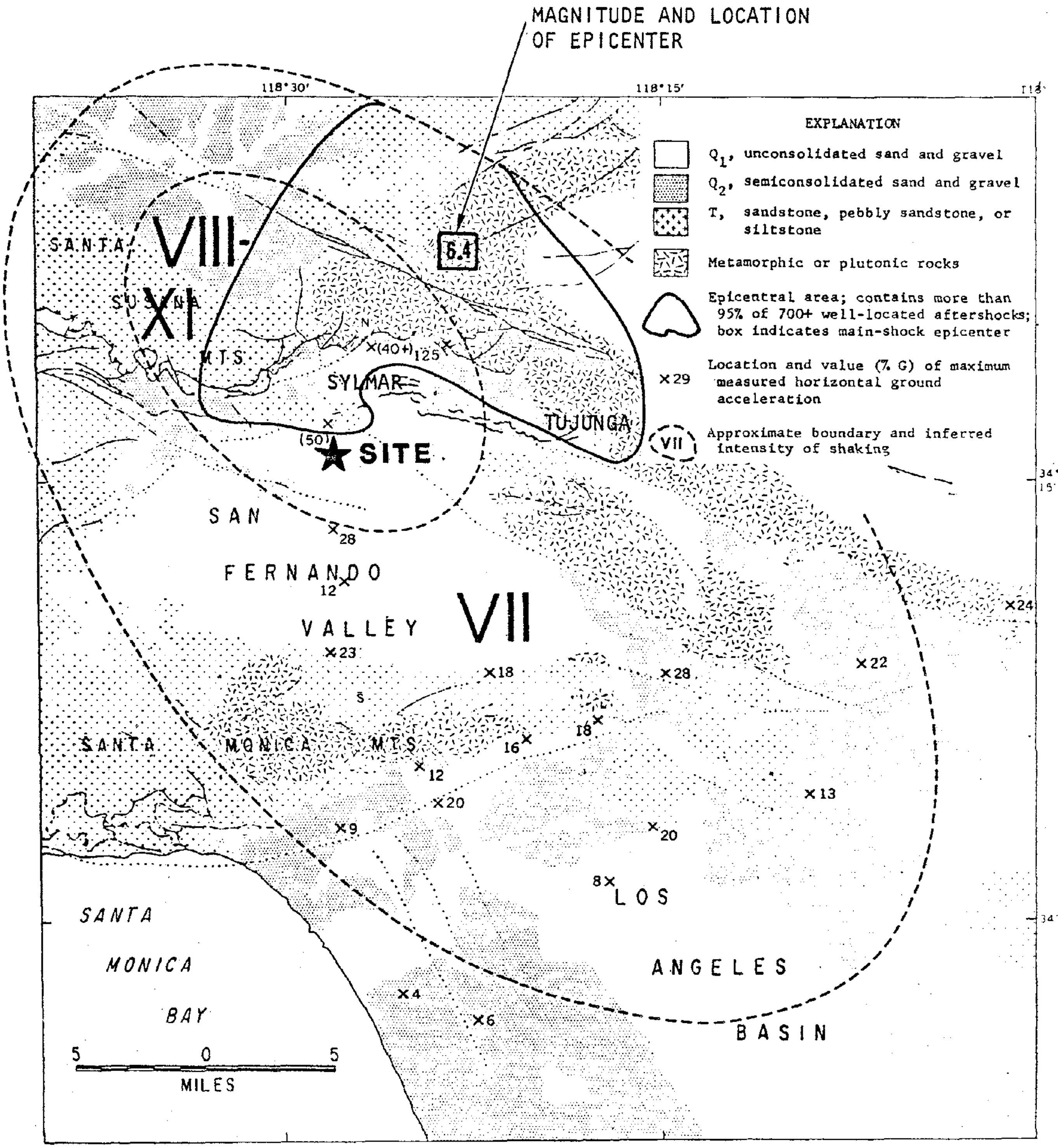

FIGURE 2-3. MAP OF TRANSITORY EFFECTS OF FEBRUARY 9 (1971) EARTHQUAKE (Yerkes, 1973)

A detailed description of effects of the San Fernando earthquake as related to geology is given by Yerkes (1973), shown in Figures 2-2 and 2-3. This report locates the epicenter of the moderate (magnitude 6.4) San Fernando earthquake only 40 miles northeast of the urbanized San Fernando Valley. Unusually severe shaking, locally exceeding 50% of g, characterized the mountain-front belt. Measured horizontal accelerations of 10 to 20% of g extended southward into the downtown areas of Los Angeles and Pasadena 25 miles from the epicenter.

The San Fernando earthquake is attributed to displacement on a buried north-dipping fault beneath the southwesternmost San Gabriel Mountains, north of the San Fernando Valley. The cross section of the epicenteral area is shown in Figure 2-4. The dip of the San Fernando fault is such that it intersected the surface as a zone of tectonic ruptures along the north margin of San Fernando Valley. The displacement of the San Fernando earthquake was reverse in nature--the mountainous block north of the fault moved relatively southward, up and over the San Fernando Valley south of the fault.

The San Fernando Valley area (Figs. 2-1, 2-2, and 2-3) is located in a depositional basin that dates from middle Miocene time (about 15 million years ago, Fig. 2-4); the basin is floored and bounded on the north, east, and south by cyrstalline basement rocks (Wentworth and Yerkes, 1971). The basin is believed to be 15,000 to 20,000 ft deep in its central part; the upper 50 to 1,000 ft of basin fill are relatively unconsolidated alluvial sands and gravels (Yerkes, 1973).

2.3 FAULTING MECHANISM OF THE SAN FERNANDO EARTHQUAKE

The San Fernando earthquake occurred on 9 February 1971. Allen et al. (1973) assigned it a local magnitude M_L of 6.4, a location at $34^{o}24.7'N$, $118^{o}24.0'W$, and a focal depth $h = 8.4$ km. They estimated the hypocenter to be within 4 km horizontally and 8 km vertically. Hanks (1972) suggested a hypocentral depth of 12 to 14 km on the basis of his analysis of the Pacoima Dam accelerograms and distance recordings. Canitez and Toksoz (1972) concluded that $h = 14$ km yielded the best fit to teleseismic surface wave spectra.

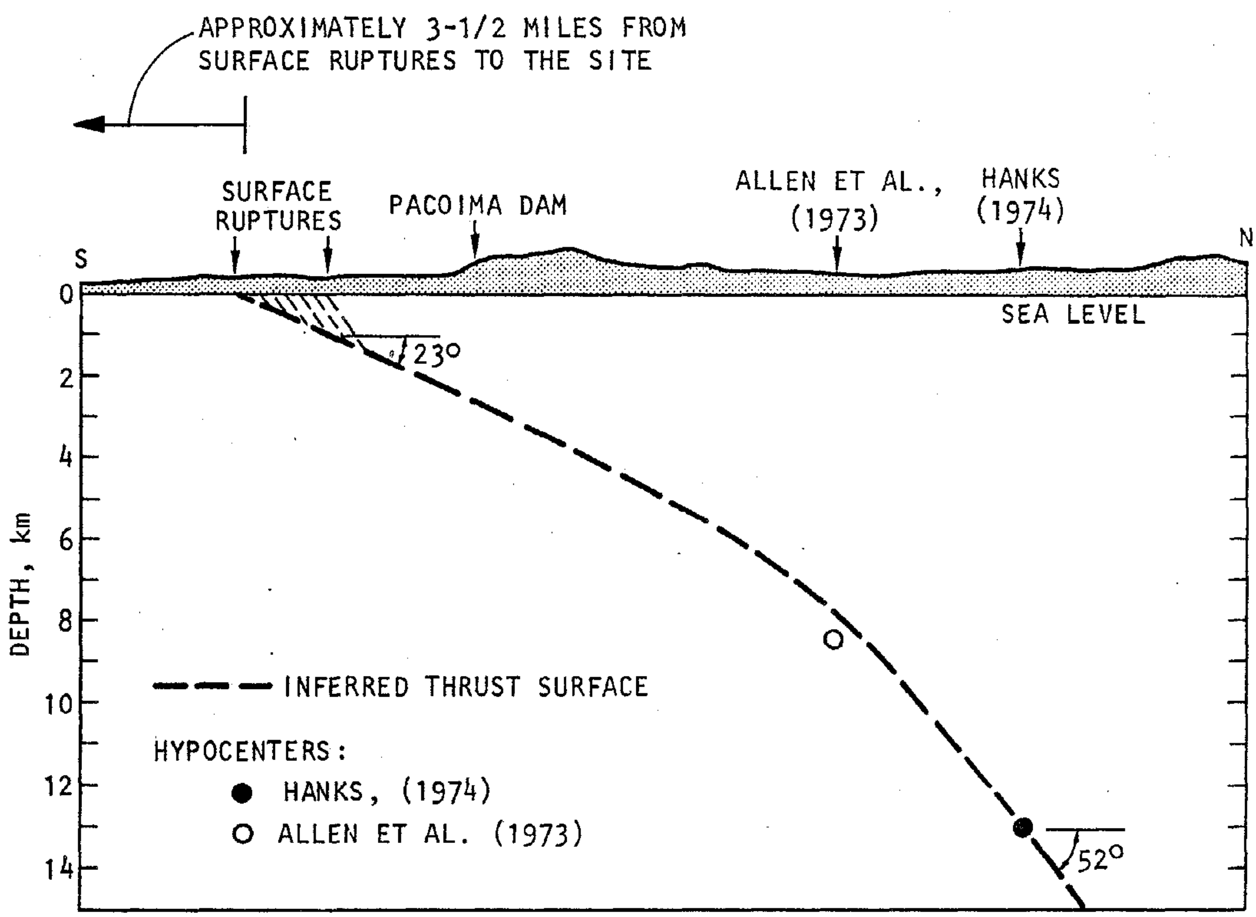

FIGURE 2-4. A NORTH-SOUTH CROSS SECTION OF THE EPICENTRAL AREA (Adapted from Hanks, 1974)

Even though these estimates place the point of initial rupture at depths of 12 to 14 km, they are within the range given by Allen et al. (1973).

As described by Hanks (1974), the faulting initiated beneath the San Gabriel Mountains, in the vicinity of $34^{\circ}27.0'$N, $118^{\circ}24.0'$W, and $h = 13$ km along the preferred fault plane, striking N$67^{\circ}\pm6^{\circ}$W and dipping $52^{\circ}\pm3^{\circ}$ to the northeast. Faulting then proceeded southward and upward along the main thrust plane, the trace of which on a north-south cross section is schematically indicated in Figure 2-4, to intersect the earth's surface along the Sylmar and Tujunga fault segments (Fig. 2-5). The dip of the thrust plane indicated in Figure 2-4 steepens from south to north. At the earth's surface there is some evidence that the thrust plane dips at an angle considerably shallower than 52°. To describe where the Tujunga fault segment is clearly expressed, Kamb et al. (1971) report that it is a thrust fault dipping 20° to 25° to the north. Proctor et al. (1972) also present two cross sections revealing a near-surface dip of 20° to 22° for the Tujunga thrust fault. Thus, the surface and near-surface expressions of this fault support the indicated curvature of the main thrust plane depicted in Figure 2-4.

2.4 SUBSURFACE CONDITIONS

The subsurface conditions have been discussed in several reports, with specific site information provided by Woodward-Lundgren & Associates (1975). Data from these reports indicate that the soils at this site consist of a surficial layer of clayey sand underlain by sand and gravel with interspersed layers of clay. No free ground water was encountered in the borings to the maximum depth explored. The well log indicates the water level at a depth of approximately 250 ft. Penetration results indicate that in most cases soil layers are dense (Fig. 2-6).

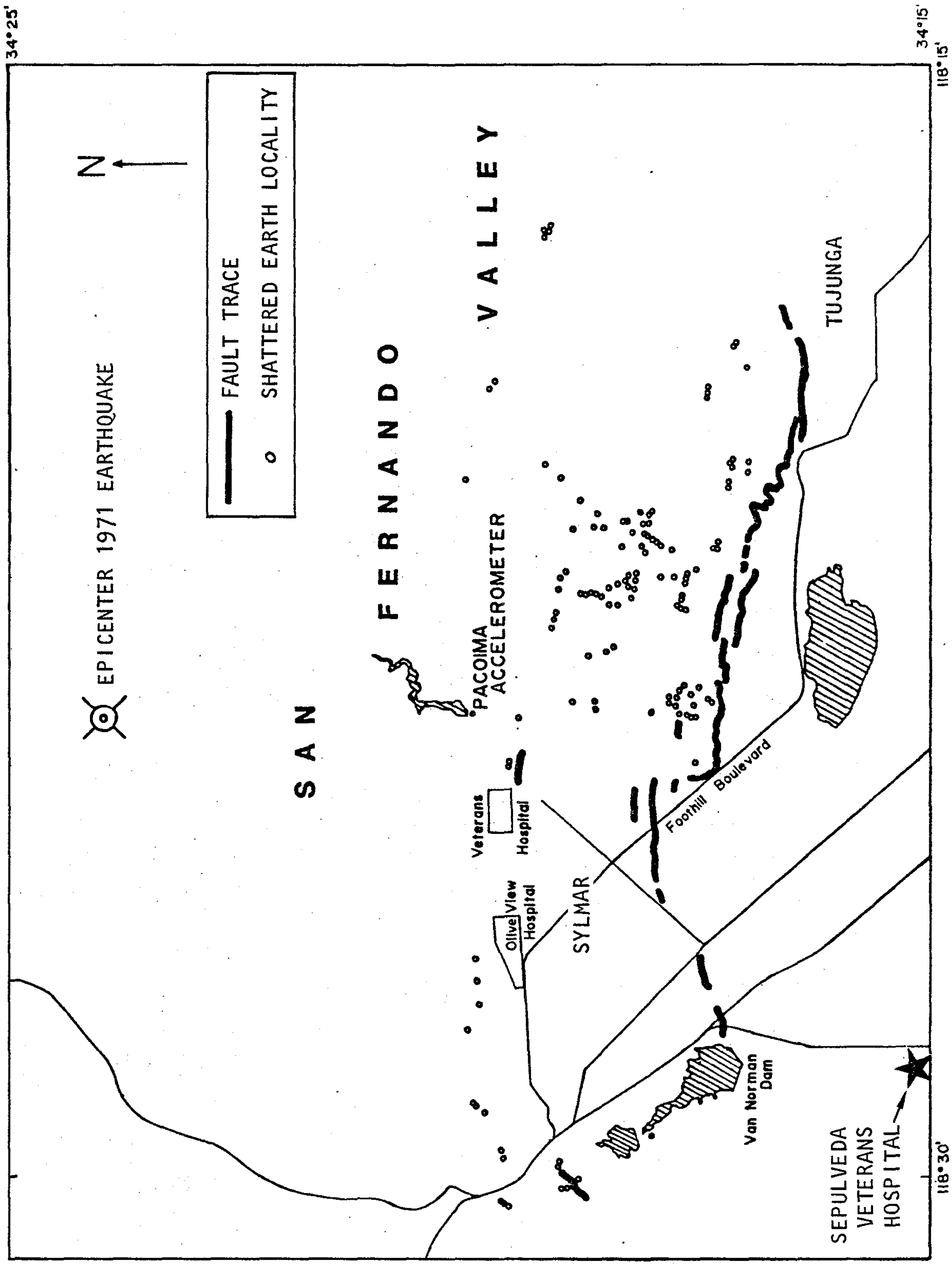

FIGURE 2-5. MAP OF SHATTERED EARTH LOCALITIES AND SURFACE FAULT TRACES, SAN FERNANDO EARTHQUAKE (after Barrows et al., 1971)

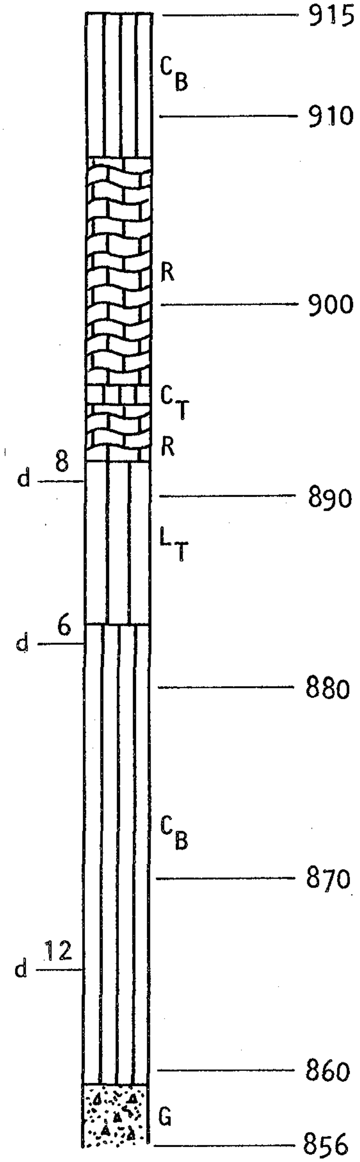

Legend		
Symbol	Abbreviation	Classification
	C_B - Brown C_T - Tan	Clayey sand
	L_B - Brown L_T - Tan	Fine to medium silty sand
	S_B - Brown S_T - Tan	Fine to medium sand
	G	Coarse sand and gravel
	R	Coarse sand, gravel, and rock fragments

FIGURE 2-6. BORING NO. 3-4 AT BUILDING 3 SITE (Veterans Administration, 1952)

In general, this soil profile would not cause any significant sudden changes in seismic waves passing through the site.

2.5 SHAKING EFFECTS

Sylmar was the center for about 7 sec of very strong shaking (Modified Mercalli intensities VIII-XI and measured horizontal accelerations greater than 25% of g) over an area of about 140 sq miles. About 10 sec of moderately strong shaking (intensity VII and measured horizontal accelerations between 8 and 15% of g) covered an additional area of about 835 sq miles that includes all of San Fernando Valley, the northern part of the Los Angeles Basin, and nearby parts of the Santa Clara River Valley (Fig. 2-3).

2.6 STRUCTURAL DAMAGE

The plots of damage (Figs. 2-7 and 2-8) represent primarily the areal distribution and density of significant damage to structures; these plots and the following paragraphs were given by Yerkes (1973).

> These maps are based on field observations and on lists supplied by the cities of Los Angeles and San Fernando, Los Angeles City School District, and Los Angeles County. Only one of these lists separates structural from architectural damage; others give only the estimated cost of repairs to the structures or identify only those structures that were posted as unsafe for occupancy.
>
> None of the lists indicate the age or type of construction. Thus, it was impossible to normalize the data satisfactorily; instead, the plots include all individual structures intended for some degree of occupancy for which repairs were estimated to equal or to exceed $2,000. Eight pre-1933 school buildings that were damaged beyond economic repair are differentiated; the plots also include the wood frame dwellings in the northern San Fernando Valley that were examined and plotted by Steinbrugge et al. (1971).

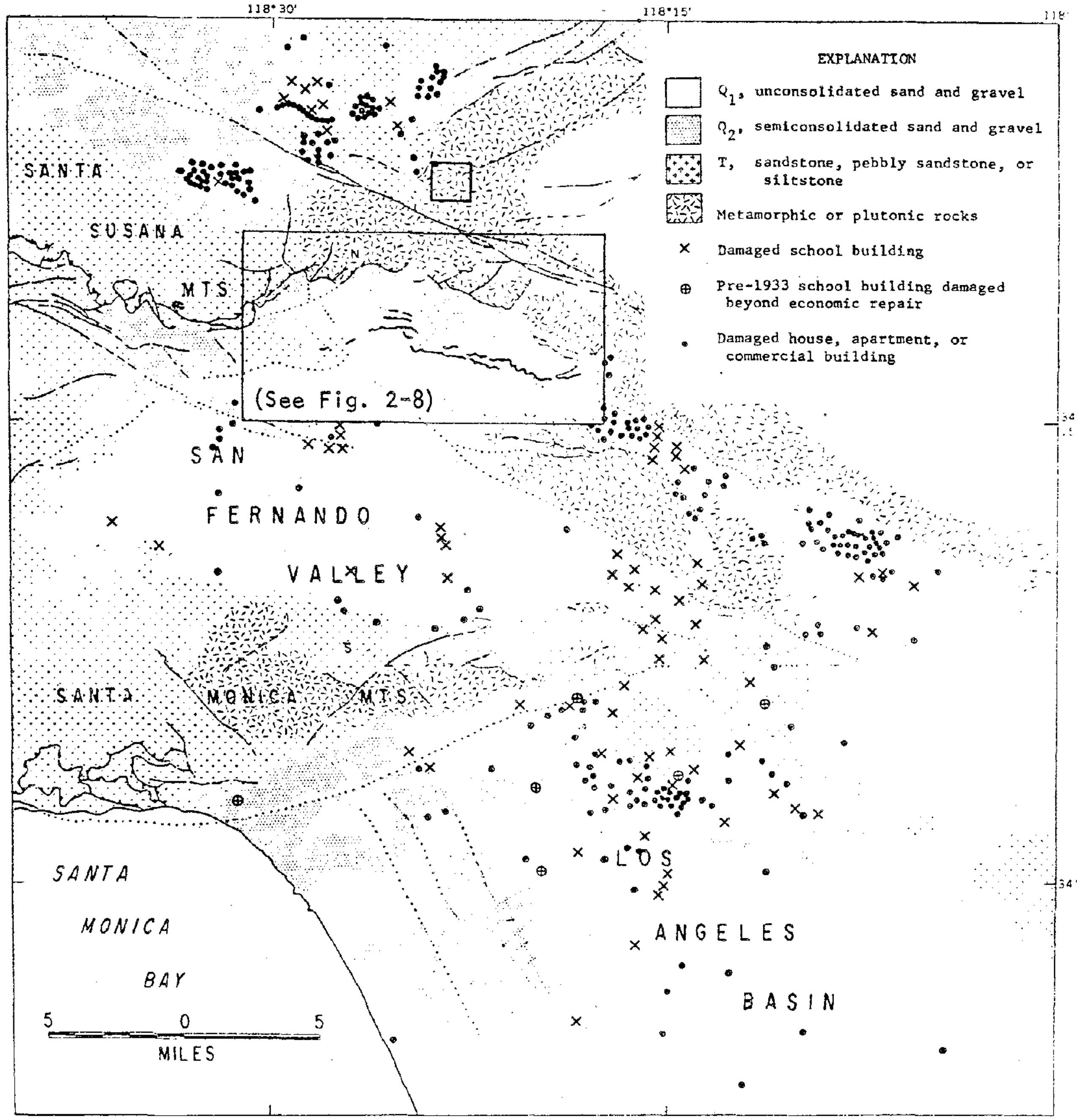

FIGURE 2-7. MAP OF SAN FERNANDO VALLEY, LOS ANGELES BASIN AREA, SHOWING DISTRIBUTION OF STRUCTURAL DAMAGE RELATIVE TO GEOLOGY (Yerkes, 1973)

Reproduced from best available copy.

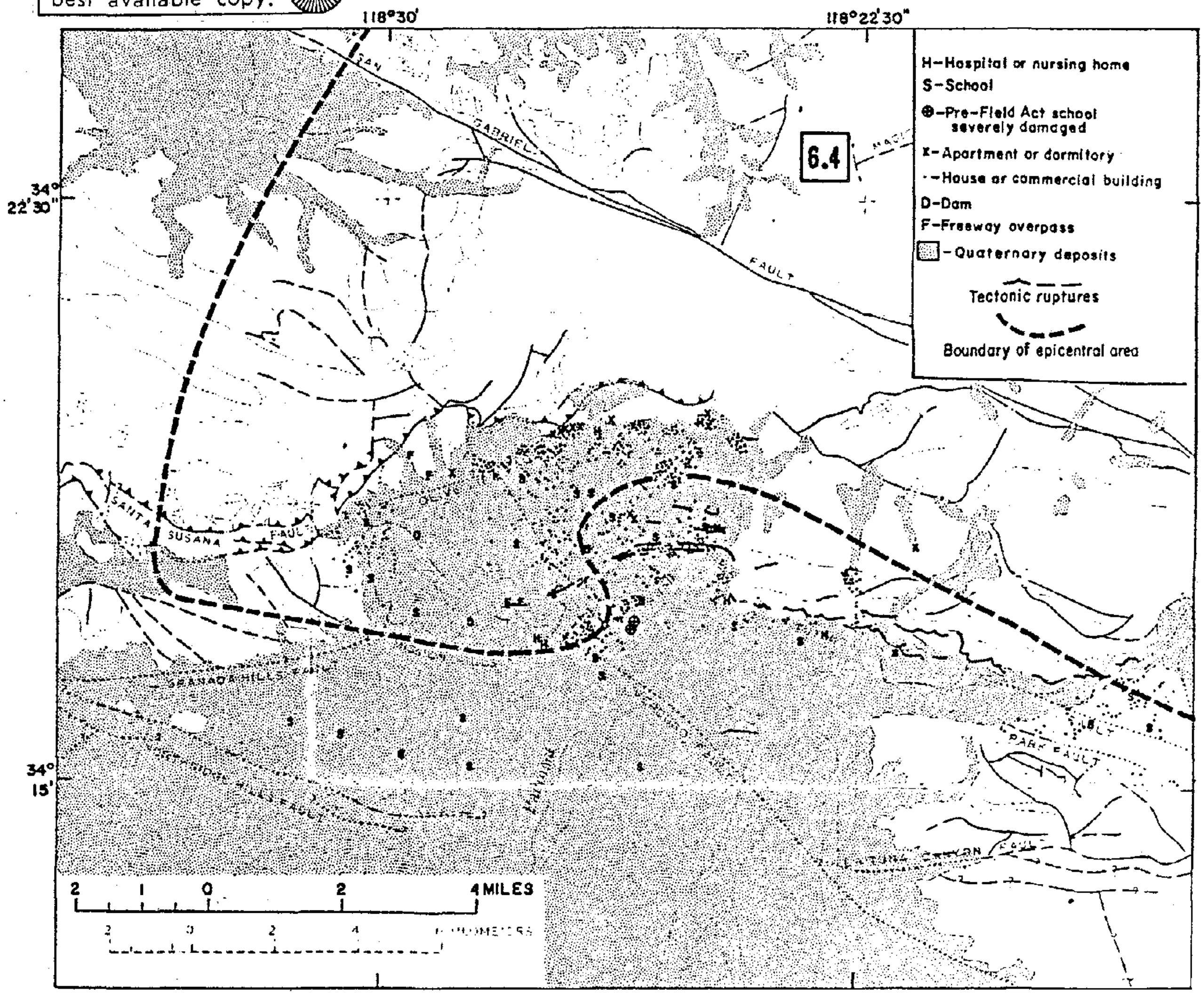

FIGURE 2-8. INSET FROM FIG. 2-7: MAP OF NORTHERN SAN FERNANDO VALLEY AREA, SHOWING DISTRIBUTION OF STRUCTURAL DAMAGE RELATIVE TO GEOLOGY (Yerkes, 1973)

2.7 STRONG-MOTION ACCELEROGRAPH RECORDS FROM THE 1971 SAN FERNANDO EARTHQUAKE

Strong-motion accelerograph records were obtained from 241 instruments between 8 and 369 km of the San Fernando earthquake epicenter (Maley and Cloud, 1973; Fig. 2-9). Selected free-field and building basement records from the San Fernando earthquake are given in Table 2-1. The Orion record provides the closest measured record to the subject site. The peak horizontal acceleration measured at the ground level was 0.27 g. However, this value was modified by Trifunac and Brady (1973) to 0.25 g using baseline correction techniques. In addition to the above 241 records, 144 seismoscope-recorded data were recovered (Morrill, 1973). Morrill summarized the significant results of the strong-motion recording from the San Fernando earthquake as:

1. The highest earthquake accelerations ever measured, 1.25 g horizontally and 0.72 g vertically, were recorded on the abutment of Pacoima Dam, 8 km from the epicenter.

2. Except for the anomalously high Pacoima Dam results, attenuation of maximum horizontal ground accelerations from all recording sites is, for the most part, consistent with the equation, $\log (a/g) = 3.5 - 2 \log (D + 80)$, calculated by Cloud and Perez for past earthquakes (see Fig. 2-10).

3. The range of maximum ground accelerations recorded at different localities in the Los Angeles area was relatively similar, generally about 0.10 to 0.25 g, although the measured values fell off rapidly beyond 45 km.

4. Peak accelerations exceeding 0.3 g were recorded on the top floors of 20 different high-rise buildings, including a 17-story tower 41 km from the epicenter where a maximum of 0.5 g was observed.

5. In 80 percent of the buildings where the base accelerations were 0.10 g or greater, the top-floor accelerations were 1.1 to 2.3 times those recorded at the ground level.

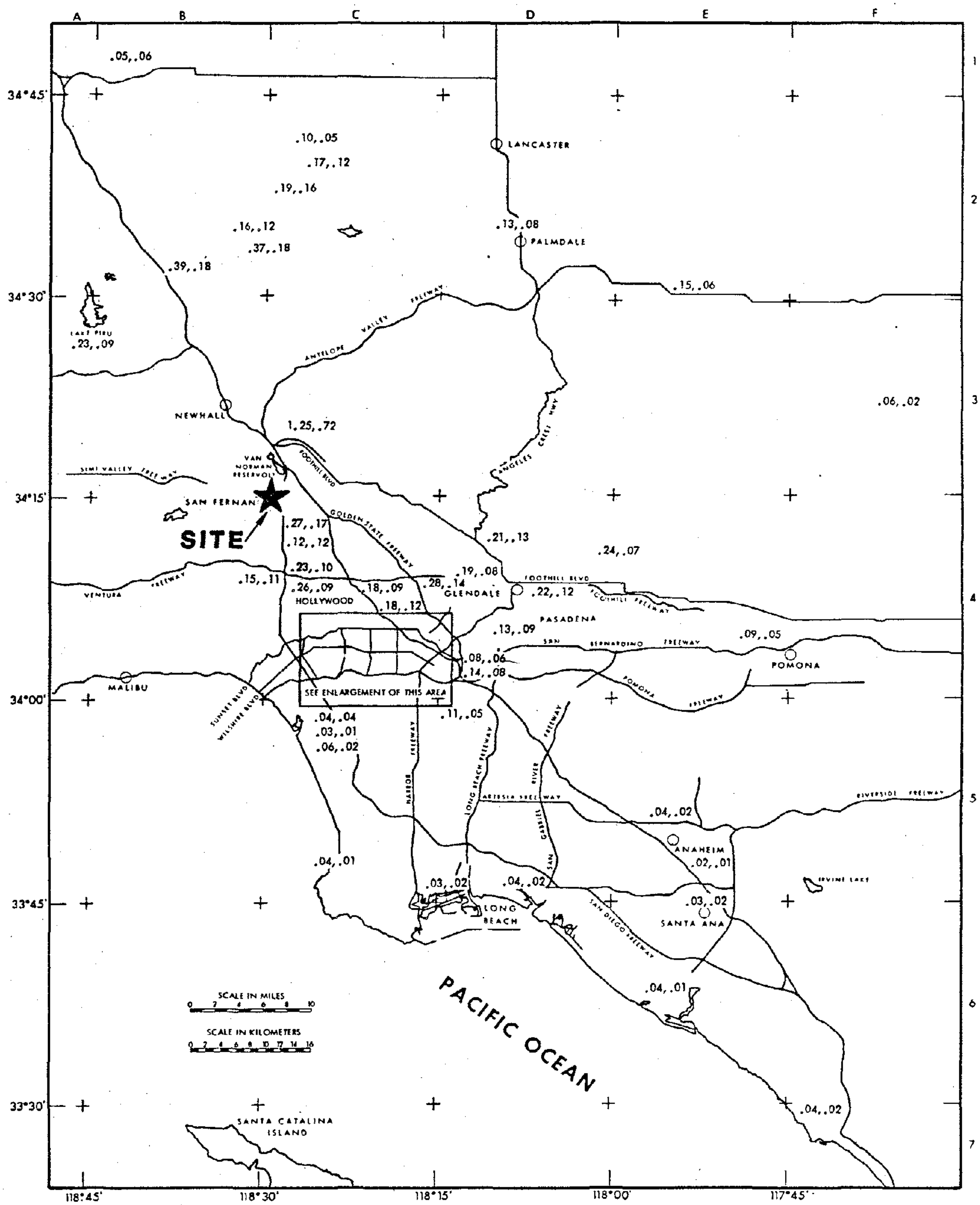

FIGURE 2-9. MAXIMUM HORIZONTAL AND VERTICAL GROUND-ACCELERATION VALUES IN EXTENDED LOS ANGELES AREA DURING SAN FERNANDO EARTHQUAKE (Morrill, 1973)

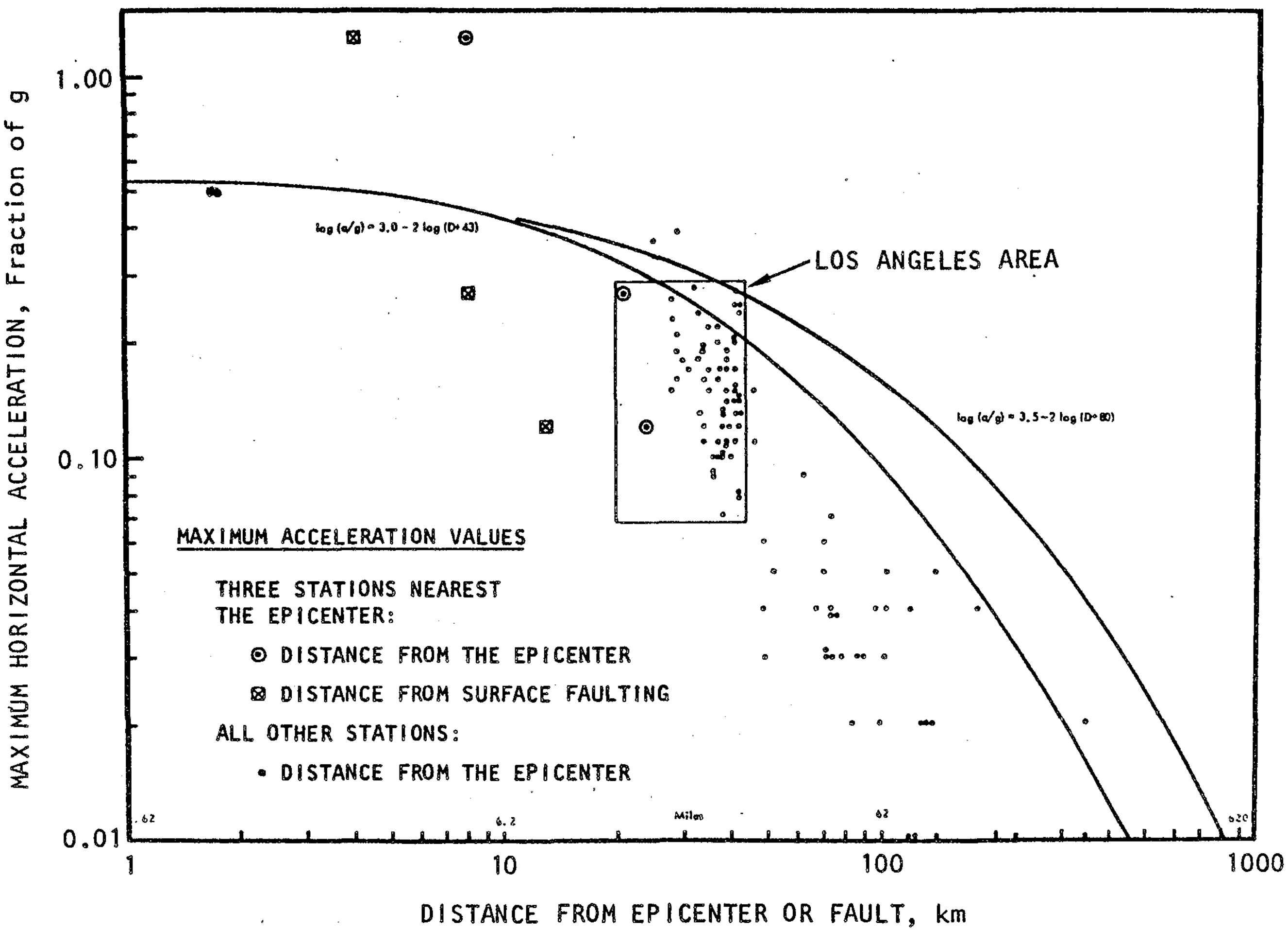

FIGURE 2-10. MAXIMUM HORIZONTAL GROUND ACCELERATIONS RECORDED DURING SAN FERNANDO EARTHQUAKE (VALUES $\geq$ 0.01 g) COMPARED TO ATTENUATION CURVES DEVELOPED BY CLOUD AND PEREZ (Maley and Cloud, 1973)

TABLE 2-1. SELECTED FREE-FIELD AND BUILDING BASEMENT RECORDS FROM THE 1971 SAN FERNANDO EARTHQUAKE

Recording Station	USGS Station Number	Distance from Epicenter, km	Peak Acceleration CIT — cm/sec^2 USGS Files, g			CIT Record
Pacoima Dam, San Fernando	279	8	S14W 1148.1	N76W 1054.9	Down 696.0	C-041
Los Angeles 8244 Orion	241-3	20	N00W 250.0	S90W 131.7	Down 167.5	C-048
Castaic, Old Ridge Rt.	110	29	N21E 309.4	N69W 265.4	Down 153.3	D-056
Griffith Park Observatory, L.A.	141	33	S0W 176.9	S90W 167.4	Down 120.3	0.198

2.8 FACTORS AFFECTING THE DEVELOPMENT OF SEISMIC WAVES AT THE SITE DURING THE SAN FERNANDO EARTHQUAKE

The characteristics of the seismic waves appearing on the strong ground motion accelerograph records at a site depend on the excitation of the source and overall propagation-path geology. The records at Orion, Castaic, and Griffith Park from the 1971 San Fernando earthquake are considered free-field motion records because they were recorded at the basement or first-floor levels of the building, and the effects of the soil/structure interaction are assumed to be small. With the local subsurface conditions indicating no anomalies at the site, local soil modifying effects are not considered significant in our free-field study at this site. Therefore, the site will be considered as one part of the total propagation path.

2.8.1 RADIATION PATTERN OF SEISMIC WAVES

The generation of seismic waves at source depends on the details of the faulting. The faulting of the San Fernando earthquake has been thoroughly studied. Therefore, the radiation pattern of the earthquake can be computed based on a faulting model incorporating the known details. A Rayleigh wave radiation pattern of the San Fernando earthquake at a period of 8 sec based on the source model of Alewine (1974) is shown in Figure 2-11.

The strong north-south asymmetry of the surface wave radiation pattern is primarily the result of the rupture propagation from north to south. The source-station azimuths of Orion and Griffith Park sites are south of the epicenter. The contribution of Rayleigh waves generated at source towards these sites is very large.

The source-station azimuth of Castaic is in a direction very close to the nodal line of the radiation pattern (Fig. 2-11). Therefore, the contribution of a Rayleigh wave generated from the source toward the Castaic site is very small.

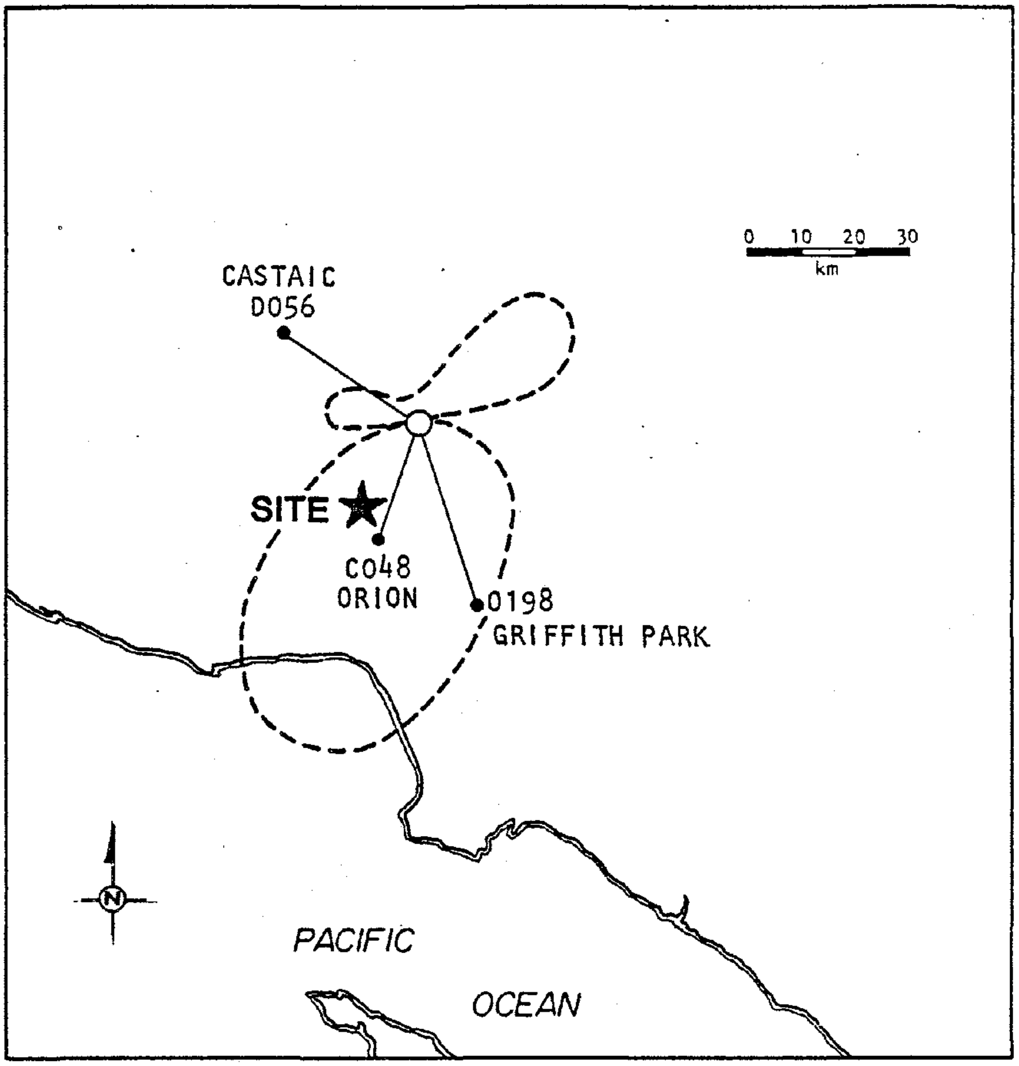

FIGURE 2-11. RADIATION PATTERN OF 8-SEC RAYLEIGH WAVES OF SAN FERNANDO EARTHQUAKE (Adapted from Hanks, 1975)

2.8.2 EFFECT OF PROPAGATION PATH

The propagation paths from the epicenter to Orion and Griffith Park sites are mostly in the San Fernando Valley (Fig. 1-1). The great depth of low-velocity sedimentary cover in the area of San Fernando Valley south of the epicenter served as the wave guide for the propagation. Therefore, the presence of surface waves on the records of Orion and Griffith Park sites is to be expected.

2.8.3 ANALYSIS OF STRONG GROUND MOTION RECORDS AT ORION, CASTAIC, AND GRIFFITH PARK

The acceleration, velocity, and displacement of the ground motion at Orion, Castaic, and Griffith Park are shown in Figures 2-12, 2-13, and 2-14, respectively. The P-wave, S-wave, and surface wave arrived in sequence on the records. The S-wave arrivals can be recognized from the records. The S-wave arrival can be identified on the transverse component in a much cleaner way than that of the other two components.

The surface waves (Rayleigh wave and Love wave) may be recognized on the displacement records. From the vertical component of displacement at Orion (Fig. 2-12) and the S00°W component of the displacement at Griffith Park site (Fig. 2-14), it is clear that the surface wave contribution at these two stations is significant.

All three records--Orion, Castaic, and Griffith Park--are suitable choices for developing the seismic input at the subject site. For the purposes of this study, the advantages of selecting the Orion record are:

1. It is the closest accelerograph strong motion record to the site.

2. Both Orion site and the subject site are located in the San Fernando Valley and have similar subsurface environment of deep alluvial deposits.

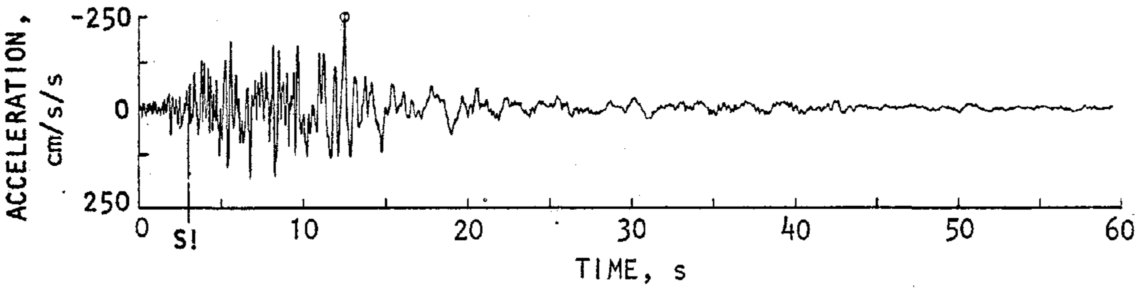

(a) Comp N00W

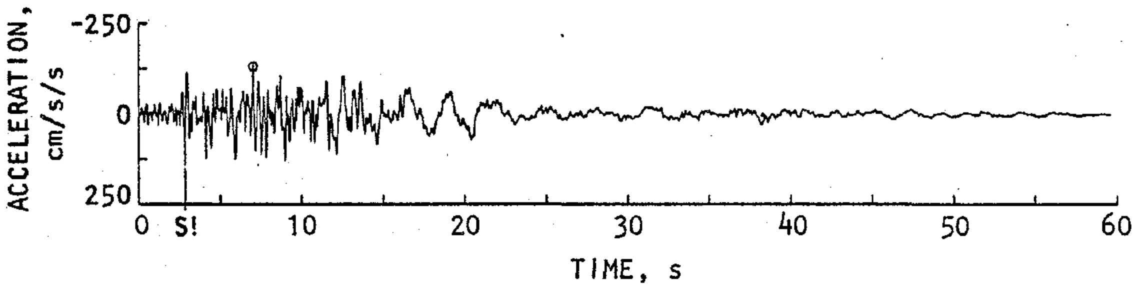

(b) Comp S90W

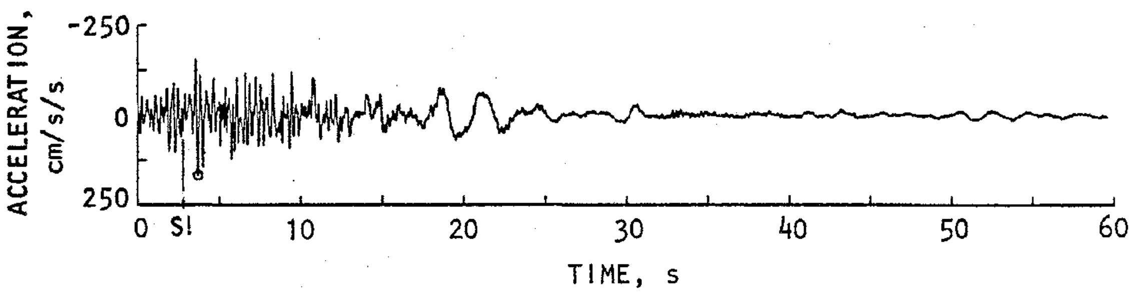

(c) Comp down

FIGURE 2-12. THREE COMPONENTS OF GROUND MOTION AT ORION SITE

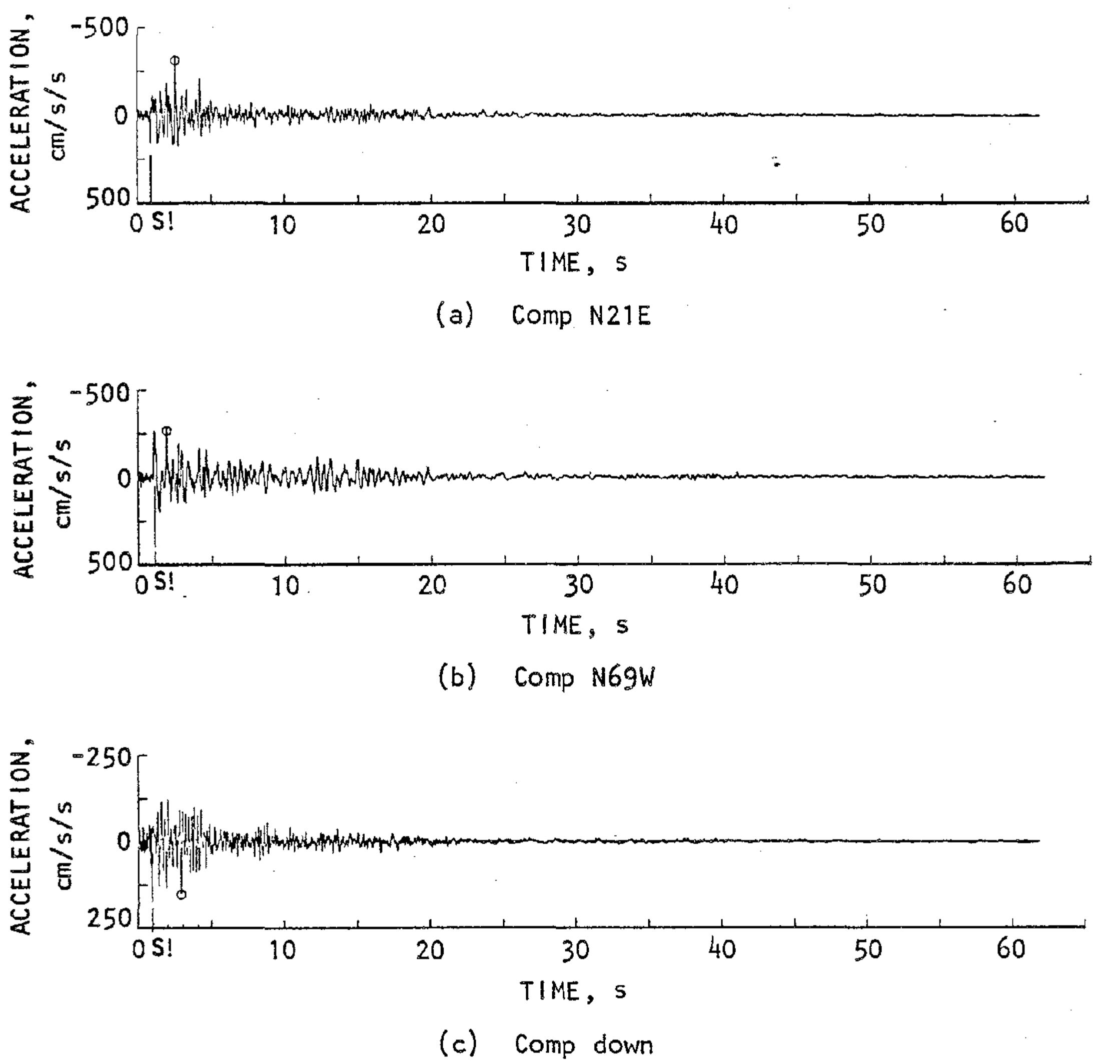

FIGURE 2-13. THREE COMPONENTS OF GROUND MOTION AT CASTAIC SITE

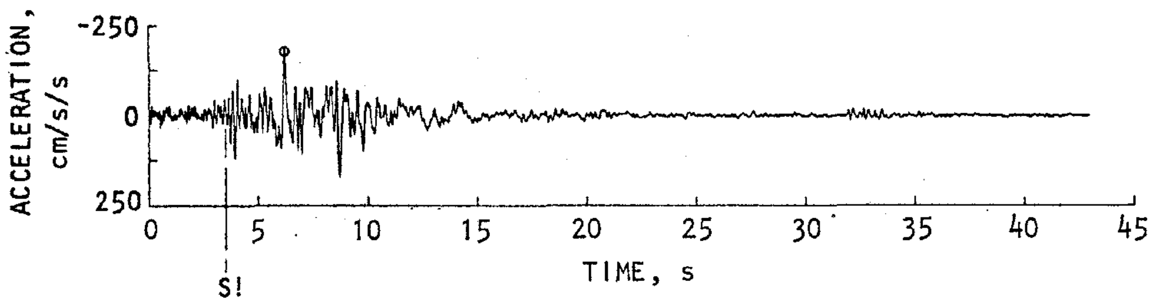

(a) Comp S00W

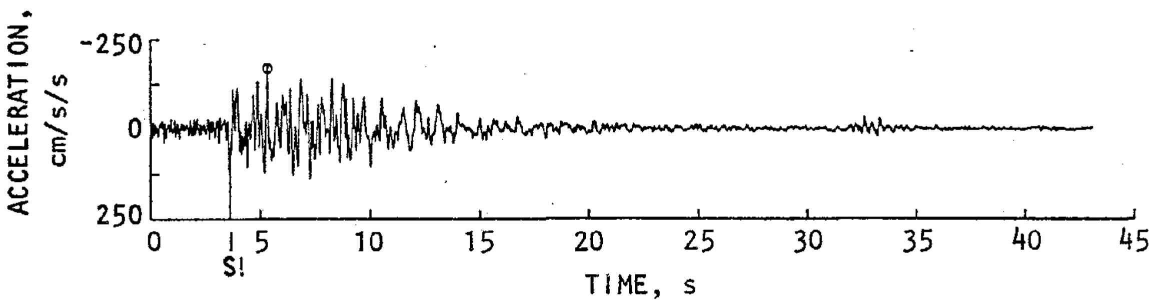

(b) Comp S90W

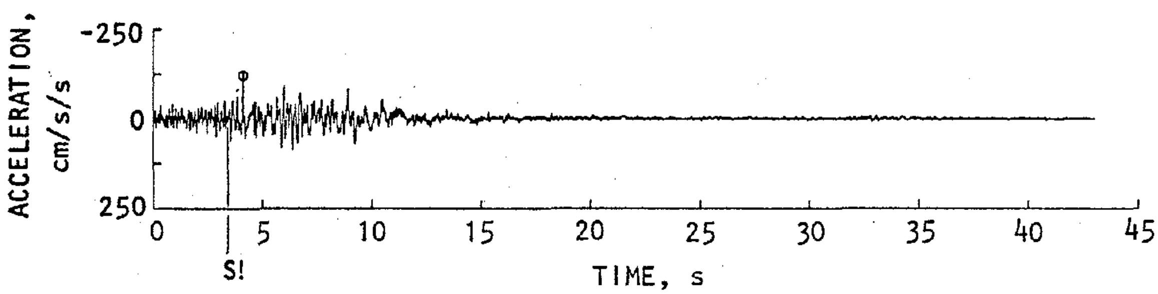

(c) Comp down

FIGURE 2-14. THREE COMPONENTS OF GROUND MOTION AT GRIFFITH PARK SITE

2.9 ESTIMATE OF PEAK GROUND ACCELERATION AT THE SITE

Prediction of peak ground acceleration at the site has been based upon several sources as illustrated in Table 2-2 and Figures 2-10 and 2-15. The data provided by SW/AA (1979) represent the results of an extensive study of parametric effects on earthquake ground motions. Regression analysis was used to compute statistical bounds on the relationship between peak acceleration and distance for the 1971 San Fernando earthquake records (Fig. 2-15). The peak recorded horizontal acceleration at Orion is 0.255 g. However, regression analysis of the San Fernando earthquake records indicates accelerations of 0.30 g at Orion.

Since the peak horizontal acceleration at Orion was 0.255 g, the results of regression analysis for horizontal acceleration should be scaled by a ratio of $\frac{0.255}{0.30}$. Therefore, the 0.50 g obtained from regression analysis at the Sepulveda site was scaled to 0.40 g to represent the peak horizontal acceleration at the Sepulveda site during the earthquake. The peak vertical acceleration recorded at the Orion site is equal to the peak vertical acceleration calculated from regression analyses. Therefore, the peak vertical acceleration of 0.29 g obtained from regression analysis for the Sepulveda site will be used as the peak vertical acceleration at the site during the San Fernando earthquake.

2.10 SELECTED EARTHQUAKE GROUND MOTION AT THE SITE DURING THE 1971 SAN FERNANDO EARTHQUAKE

The Orion record, which best represents the conditions at the Sepulveda Hospital, was scaled to 0.40 g and 0.29 g peak horizontal and vertical accelerations, respectively. The scaled record is assumed to provide the free-field earthquake ground motions that could be used as input to mathematical models of the hospital structures. The time-history record for Orion is shown in Figure 2-12. The response spectra for the scaled horizontal and vertical components are shown in Figures 2-16 and 2-17.

TABLE 2-2. SUMMARY OF DATA NEEDED TO ESTIMATE PEAK GROUND ACCELERATION AT THE SITE DURING THE 1971 SAN FERNANDO EARTHQUAKE

Station Name	Distance from Epicenter, km	Recorded Motions		Maley and Cloud, (1973) (Fig. 2-11)	Regression Analysis (SW/AA, 1979)	Max. Acceleration, g Based on Correlation with Earthquake Damage	Intensity of Shaking	Maximum Acceleration, g Estimated
		Component	Maximum Acceleration, g					
Pacoima	8	S16E S74W Down	1.171 1.076 0.710	0.54	0.95		VIII-XI	
Olive View Hospital	9			0.48	0.75	0.50*	VIII-XI	
Sylmar Converter Station	10.7			0.43	0.65	0.50†	VIII-XI	
Lower Van Norman Dam	12		0.50‡	0.42	0.55	0.50§	VIII-XI	
Sepulveda Hospital	14			0.40	0.50		VIII-XI	0.40 ‡‡
8244 Orion	20	N00W S90W Down	0.255 0.134 0.171	0.35	0.30		VII	

AA10362

*Structural Engineers Association of Southern California, 1971

†Agbabian Associates (1973)

‡Seismoscope Record

§Seed et al. (1973)

‡‡ Using Regression Analysis: Peak Acceleration at Sepulveda $= \frac{0.50}{0.30} \times 0.255 \cong 0.40$

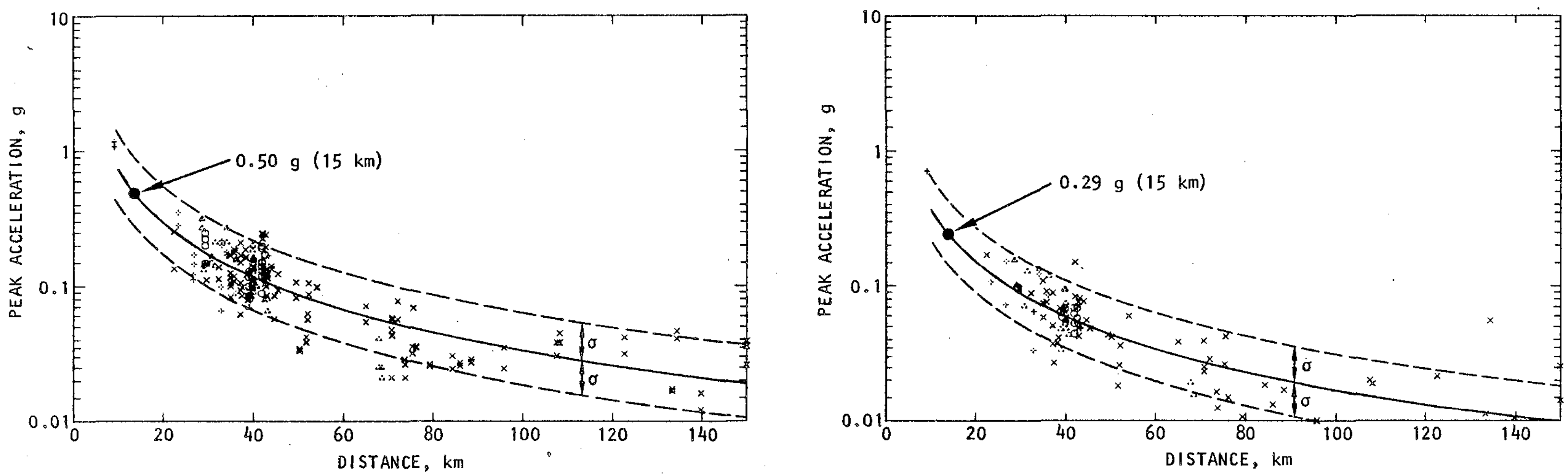

(a) Horizontal (b) Vertical

LEGEND:

DATA POINTS

- ○ DEEP SOIL SITE
- △ INTERMEDIATE SITE
- \+ ROCK SITE
- × UNDEFINED SITE CONDITIONS

REGRESSION ANALYSIS

- ——— 50th PERCENTILE (ALL SITE CONDITIONS)
- — — — 16th PERCENTILE AND 84th PERCENTILE BOUNDS (ALL SITE CONDITIONS)

NOTE:

σ = STANDARD DEVIATION OF ℓn(PEAK ACCELERATION)

FIGURE 2-15. ATTENUATION OF PEAK GROUND ACCELERATIONS RECORDED DURING THE 1971 SAN FERNANDO EARTHQUAKE (SW/AA, 1979)

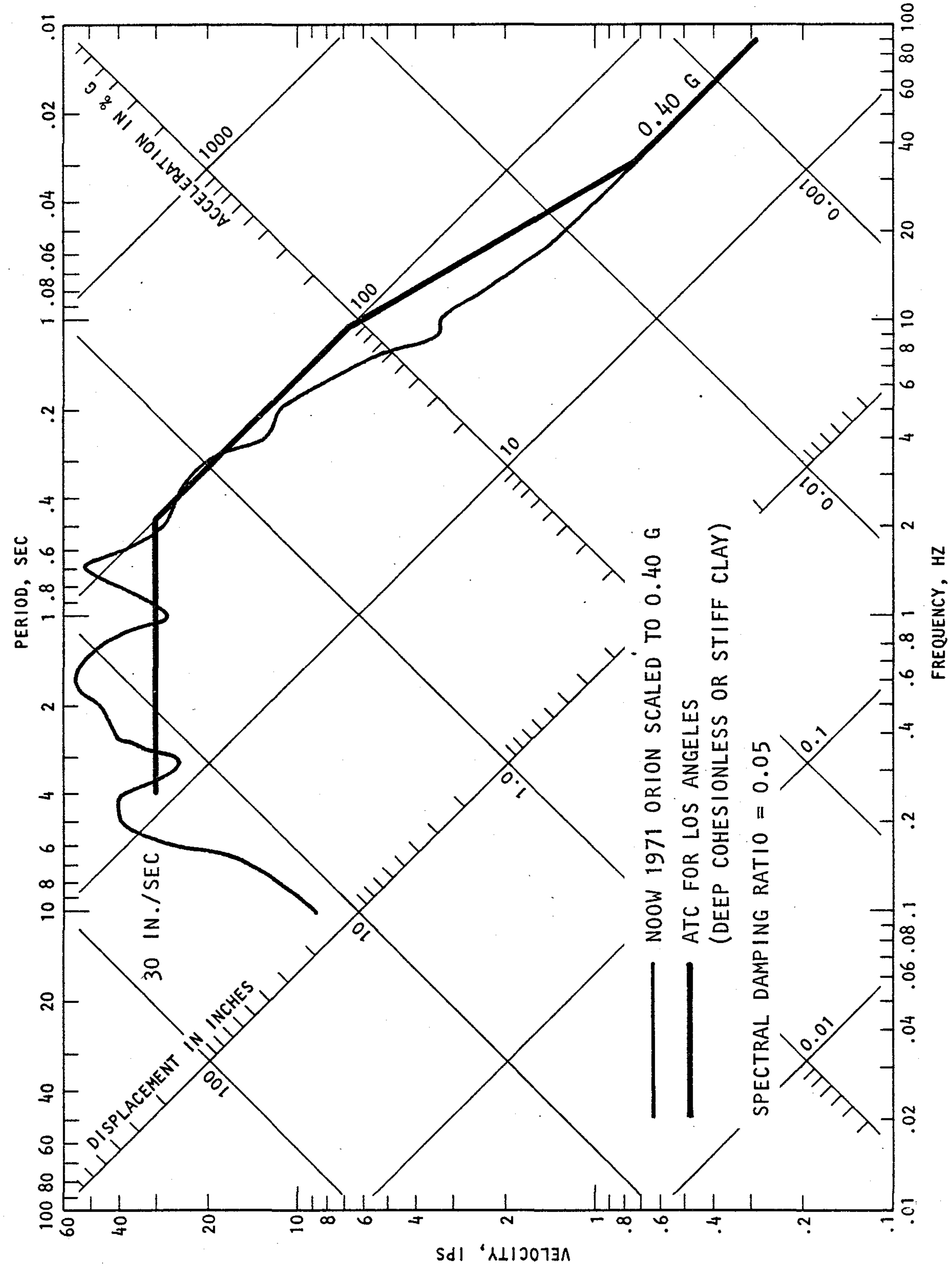

FIGURE 2-16. COMPARISON OF RESPONSE SPECTRA FOR 0.40 G SCALED NOOW 1971 ORION AND ATC FOR LOS ANGELES AREA

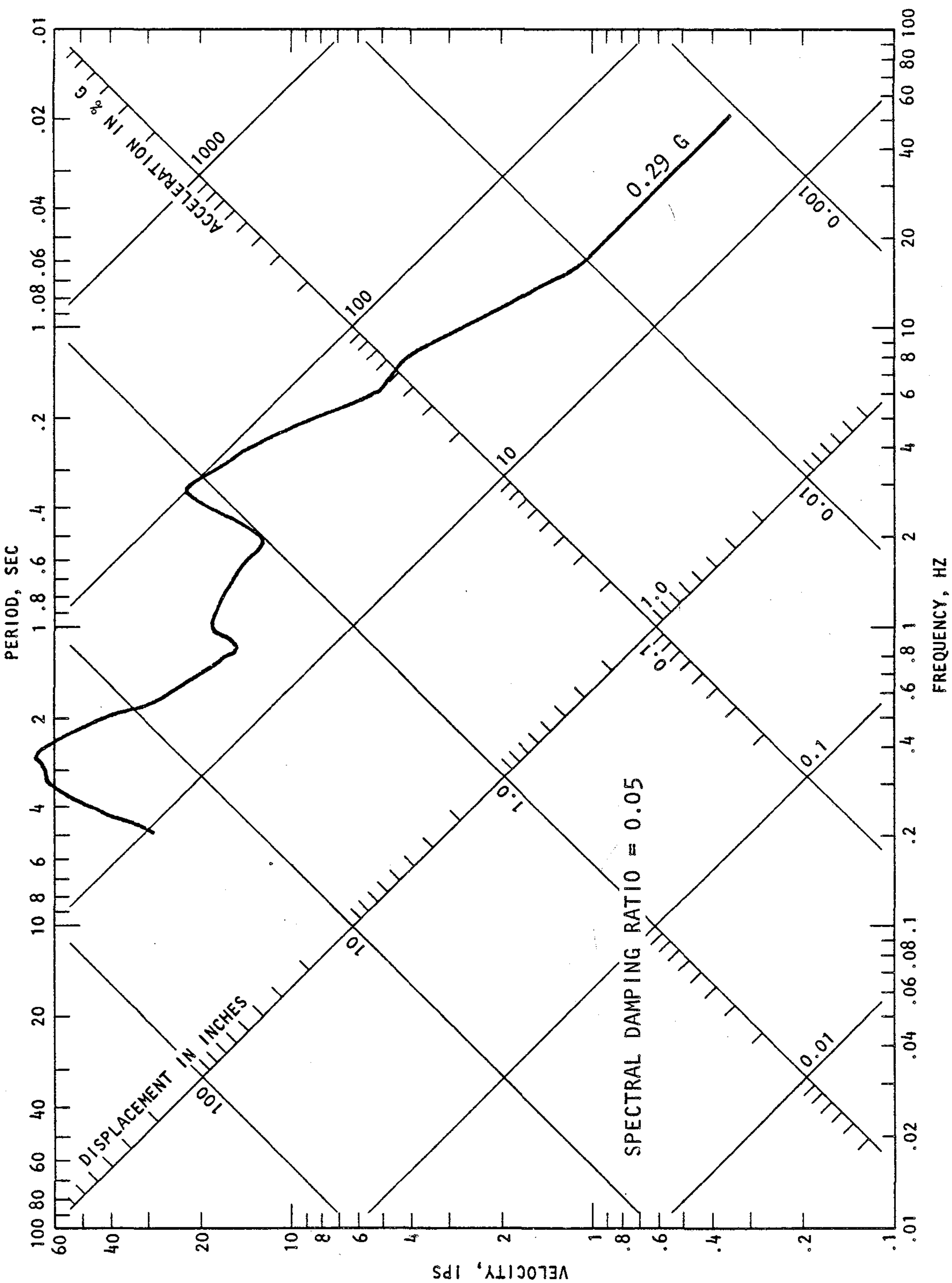

FIGURE 2-17. RESPONSE SPECTRUM FOR SCALED VERTICAL COMPONENT OF 1971 ORION RECORD

The response spectra for the scaled N00°W component of Orion and ATC design earthquake for Los Angeles are compared in Figure 2-16. Reasonable agreement of the two spectra is shown between 2 and 5 Hz. However, for frequencies above 5 Hz, the spectrum for the scaled Orion falls below the ATC spectrum. This drop is due to the effect of deep alluvium deposits that appear to attenuate some of the high-frequency content of the earthquake motions. For frequencies below 2 Hz, the scaled Orion spectrum is higher than the ATC spectrum due to the effect of the surface waves on the long period end of the spectrum.

The spectra from the scaled N00°W Orion and the two components of the scaled 1971 Castaic are compared in Figure 2-18. The three spectra compare well between frequencies of 3.5 Hz and 5.5 Hz. However, for frequencies above 5.5 Hz, the Castaic spectra are higher than the scaled Orion spectrum.

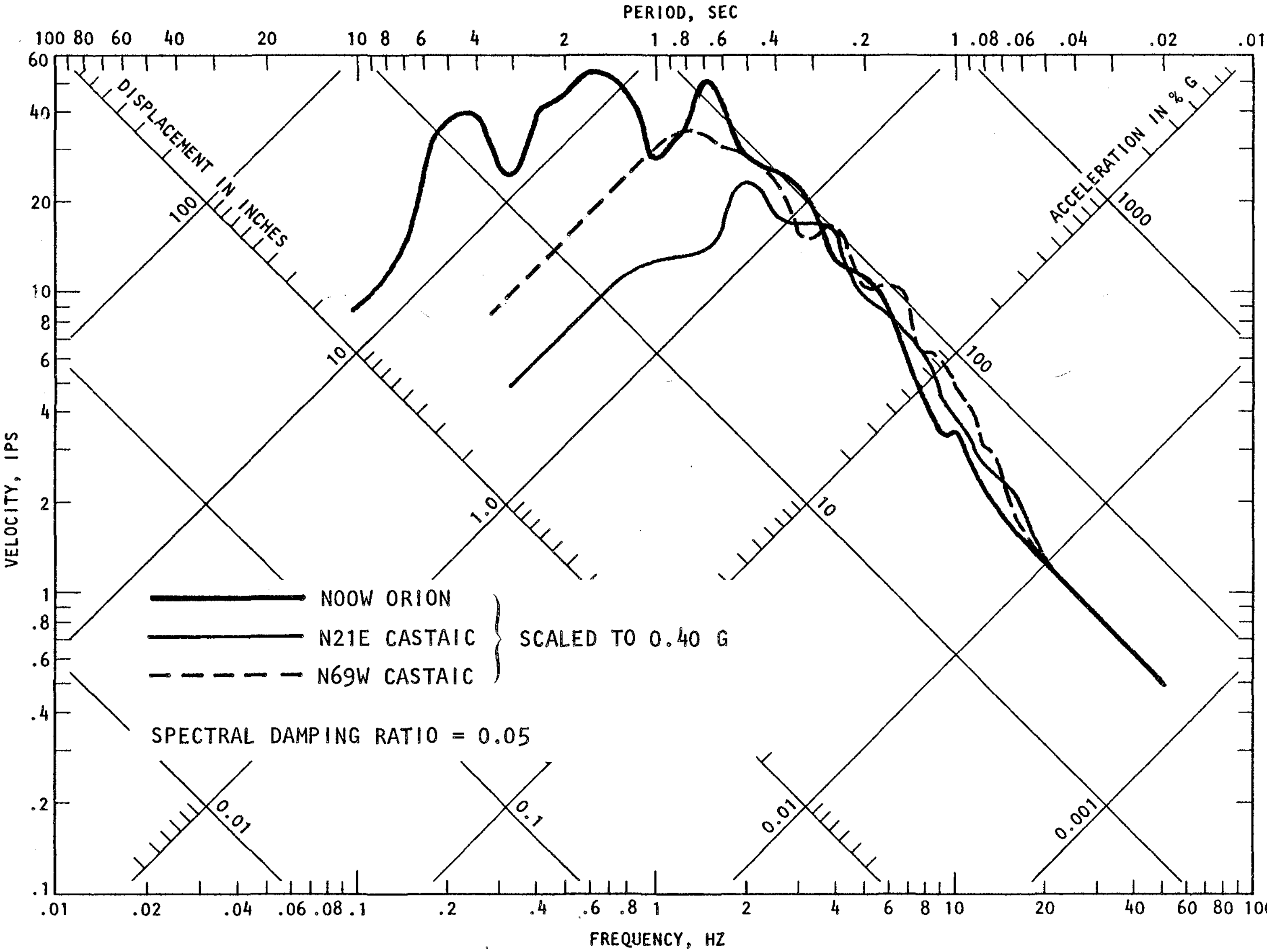

FIGURE 2-18. COMPARISON OF RESPONSE SPECTRA FOR 0.40 G SCALED COMPONENTS OF NOOW ORION — N21E CASTAIC AND N69W CASTAIC OF THE 1971 SAN FERNANDO EARTHQUAKE

SECTION 3

TWO-DIMENSIONAL SEISMIC ANALYSIS OF BUILDING 3

3.1 INTRODUCTION

This section provides the results of a two-dimensional finite element seismic analysis of the general medical and surgical building (Bldg. 3, Fig. 1-2). The six-story building has a reinforced concrete skeleton frame with a concrete panel wall faced with brick. This building was selected because it experienced considerable damage to the seismic (flexible) joints between building segments (Lew et al., 1971). The analysis estimates the relative displacements of Segments B1 and B2 of Building 3 at the expansion joints when subjected to the earthquake input developed in Section 2. These displacements are compared to the observed responses of these joints during the 1971 San Fernando earthquake. This comparison provides a tool for calibrating the earthquake input developed for the site in Section 2. The calibrated input will be used in Section 4 to evaluate the response of the reinforced brick masonry buildings at the site during the 1971 earthquake.

3.2 DESCRIPTION OF STRUCTURE

Figure 3-1 provides an elevation and typical floor plan of segments of Building 3: B1, B2, and part of Unit A. These are typical of the other two reinforced concrete structures at the hospital site.

Building 3B1 is 61.66 ft long and 37.25 ft wide, while Building 3B2 is approximately 135.25 ft long and 36.25 ft wide. All shear walls are wall bearing, supported on continuous wall footings. Interior columns are supported on isolated footings. The reinforced concrete walls are 12 in. wide at the basement and first floor levels. They are 10 in. at the second and third floor levels and 8.5 in. at the fourth and fifth floor levels.

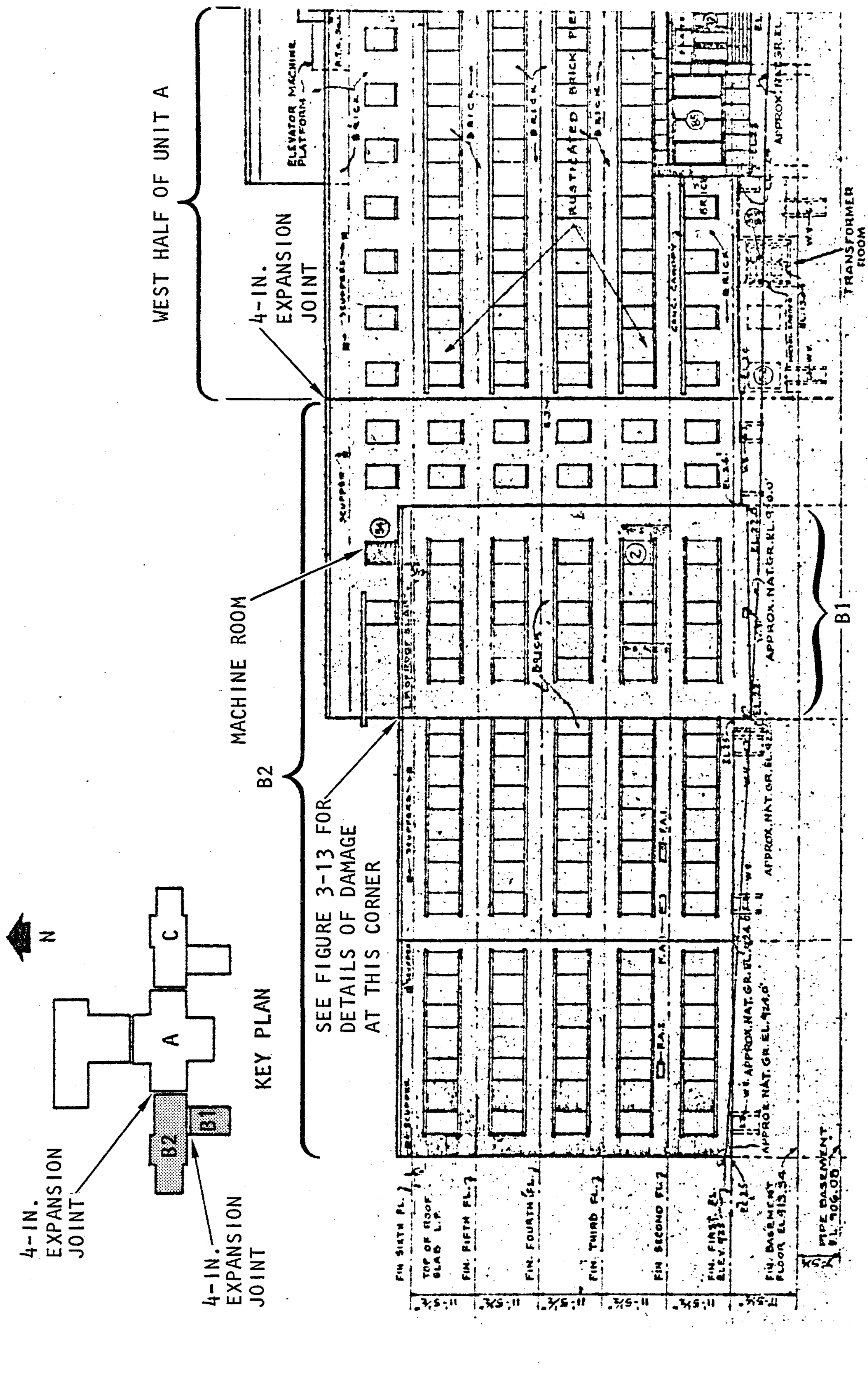

(a) Elevation (units A and B)

FIGURE 3-1. BUILDING 3

Reproduced from best available copy.

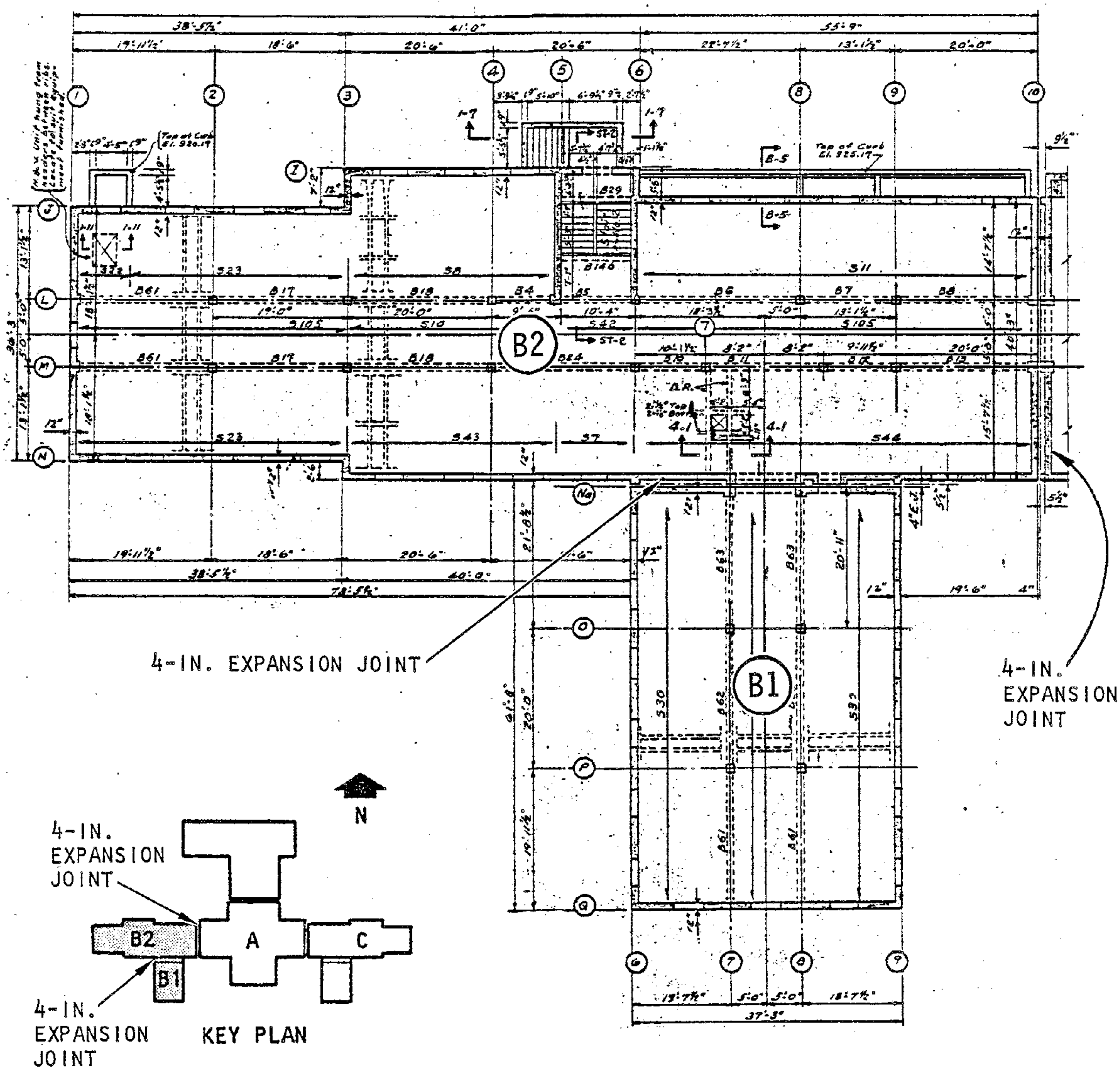

(b) First floor plan

FIGURE 3-1. (CONCLUDED)

All floor slabs are cast in place, reinforced concrete waffle type. All walls and slabs are constructed of Type C concrete with the following properties:

Maximum compressive strength	f'_c	=	3000 psi
Modulus of elasticity	E_c	=	3.16×10^6 psi
Modulus of rigidity	G	=	1.37×10^6 psi
Unit weight	w	=	145 lb/ft^3
Density	ρ	=	0.000217 lb-sec^2/in.^{4}

A characteristic feature of Part B of Building 3 is that both Segments B1 and B2 are rectangular and will behave like two separate shear walls when modeled in a N-S direction. The two segments are separated by a 4-in. flexible expansion joint.

3.3 MODELING PROCEDURE

The walls, slabs, and columns for a typical bay in Segments B1 and B2 were modeled using TRI/SAC code (AA, 1976). The two-dimensional finite element mesh is shown in Figure 3-2. The reinforced concrete walls are modeled as plane stress quadrilaterals. The weight of slabs and walls perpendicular to the plane of the model is lumped at the nodal points.

The soil spring elements simulate soil/structure interaction effects. Vertical springs included allow for both vertical and rocking motion of the building. However, no horizontal springs are included in the finite element model since both Buildings B1 and B2 have basements (buried), and the two buildings are assumed to have the same lateral motion at the base level. Appendix A gives calculations of the spring stiffness and finite element properties.

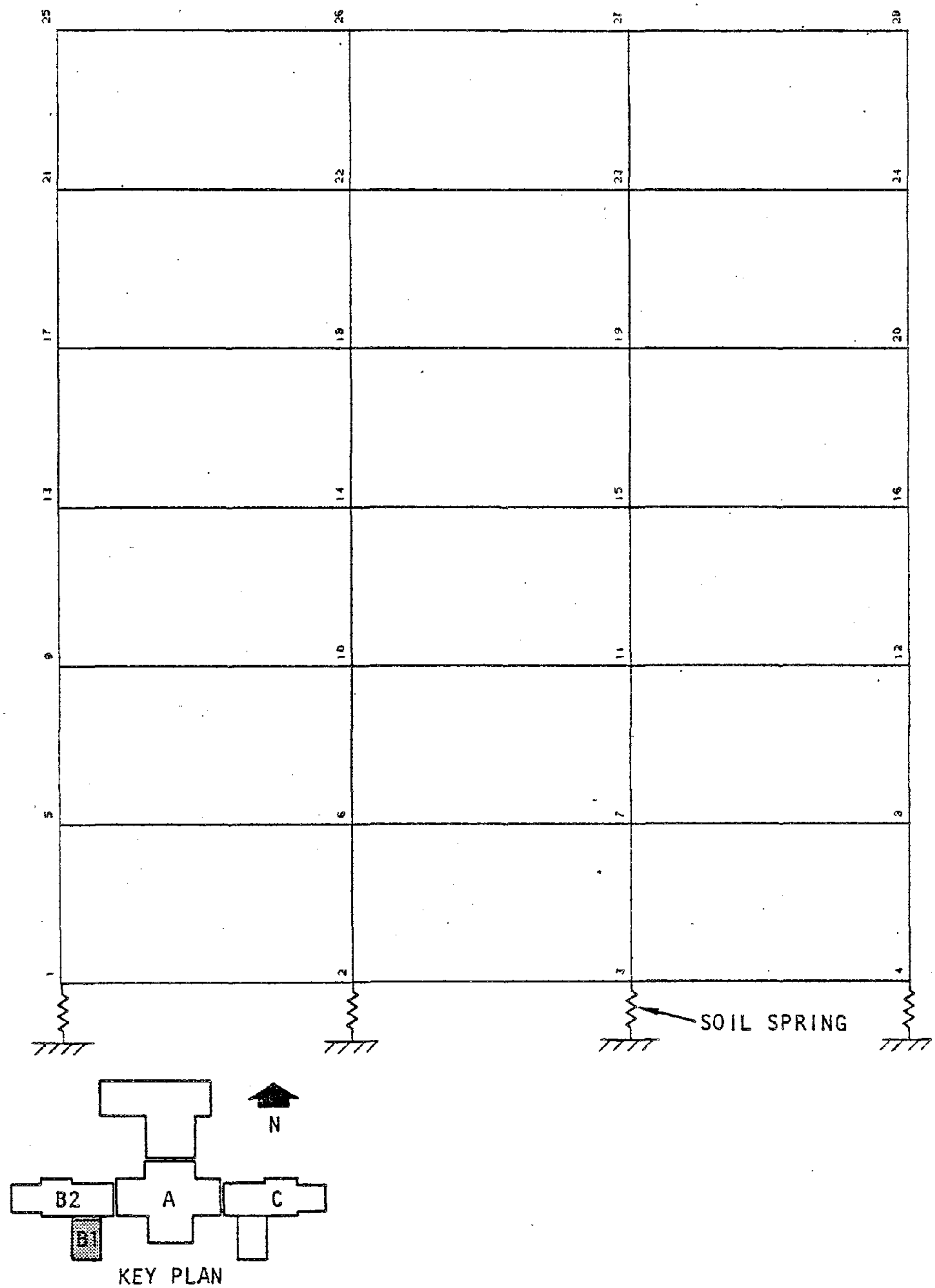

(a) Building 3B1

FIGURE 3-2. TWO-DIMENSIONAL FINITE ELEMENT MESH FOR TYPICAL TRANSVERSE SECTION

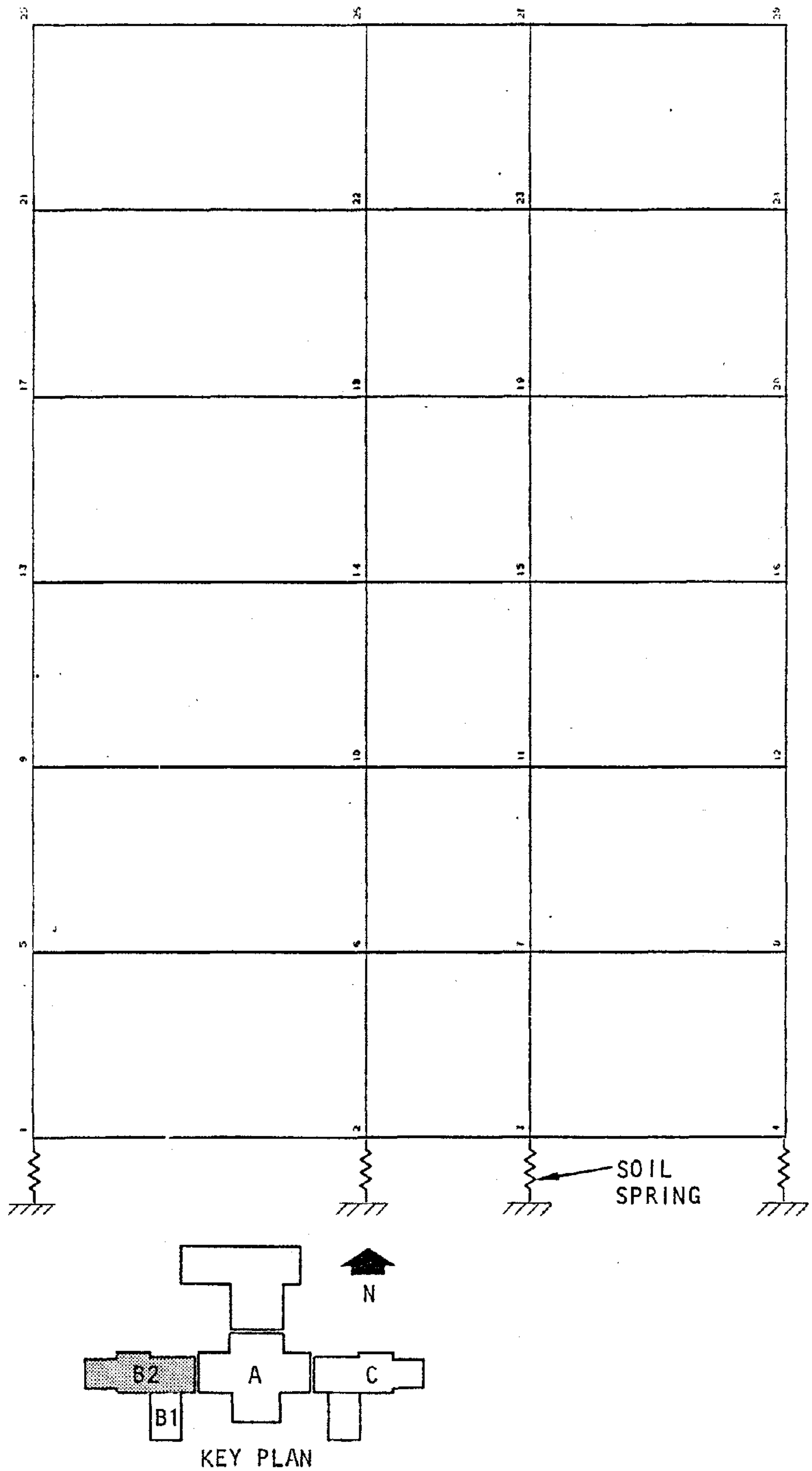

(b) Builidng 3B2

FIGURE 3-2. (CONCLUDED)

3.4 MODAL RESPONSE

To ensure an adequate computation of the response, the first six natural modes were included in the calculations. The first four significant frequencies and modes are described in Table 3-1. The corresponding mode shapes are shown in Figures 3-3 through 3-10.

It is important to note that even the first mode frequency of 3.2 Hz for Segment 3B2 is quite high compared to the first mode response of buildings of steel construction with comparable height. The fundamental frequency of Building 3B1 is higher than the fundamental frequency of Building 3B2 since it is modeled along the stronger direction. Thus, the typical segments of Building 3 are stiff and will experience much lower displacements than conventional steel structures when subjected to the same strong earthquake ground motion.

3.5 COMPUTED DISPLACEMENTS

Critical displacements were computed using the 0.40 g scaled 1971 Orion ground motions as input to the analysis. Since these calculations were performed using a two-dimensional model for budget limitations, the response was increased by a factor of 20%. This factor accounts, in an approximate manner, for the effect of the third component of earthquake motion (AA, 1973), which is not included in the two-dimensional model. The resulting displacements are shown in Figure 3-11, in which the 4-in. gap at the top between the two buildings has closed by an amount of 1.5 in.

3.6 OBSERVED DAMAGE TO BUILDING 3

Figure 3-12 shows typical wall cross sections at the roof of Buildings 3B1 and 3B2. Figure 3-13 shows damage to the flexible expansion joint at the corner of Building 3B1 adjacent to the machine room at the roof of Building 3B2. Examination of the details of this corner and other parts of Building 3 indicated the following:

a. The ATC coping (Wall Section 2-2) is offset by approximately 1.0 in. from the brick facing, resulting in a net expansion joint of only 3 in. at this corner.

b. The heavy gage metal flashing, covering the expansion joint at the roof, is embedded in the ATC cope at one end and in the brick facing at the other end. During the earthquake, this flashing exerted a tremendous pull on the ATC coping shown in Section 2-2, resulting in the cracks found in both the exterior and interior faces of the ATC coping (Fig. 3-13).

c. The flashing at the expansion joint appears to have been damaged by severe seismic cycles of tension and compression, as illustrated in Figure 3-14.

d. The permanent lateral displacement of the building was reported to be 0 in. at ground level to 1 in. at the sixth floor level (Brandow and Johnston, 1972(, as illustrated in Figure 3-15.

3.7 DISCUSSION OF RESULTS

The calculated frequencies and displacements for Building 3 are comparable to those obtained for similar buildings during past earthquakes. The results of the analyses indicate that the 0.40 g scaled 1971 Orion record provides a reasonable earthquake input for evaluating the response of the Sepulveda Hospital buildings during the 1971 San Fernando earthquake.

TABLE 3-1. CALCULATED FREQUENCIES AND MODE SHAPES FOR BUILDING 3B

(a) Building 3B1

Mode No.	Frequency Hz	Description
1	5.7	First shear mode with rocking of foundation
2	20.0	Second shear mode of building
3	24.9	Breathing mode
4	35.6	Combined shear and local deformations

(b) Building 3B2

Mode No.	Frequency Hz	Description
1	3.2	First shear mode with rocking of foundation
2	10.3	Second mode of building
3	16.6	Localized displacement
4	20.9	Vertical displacement mode

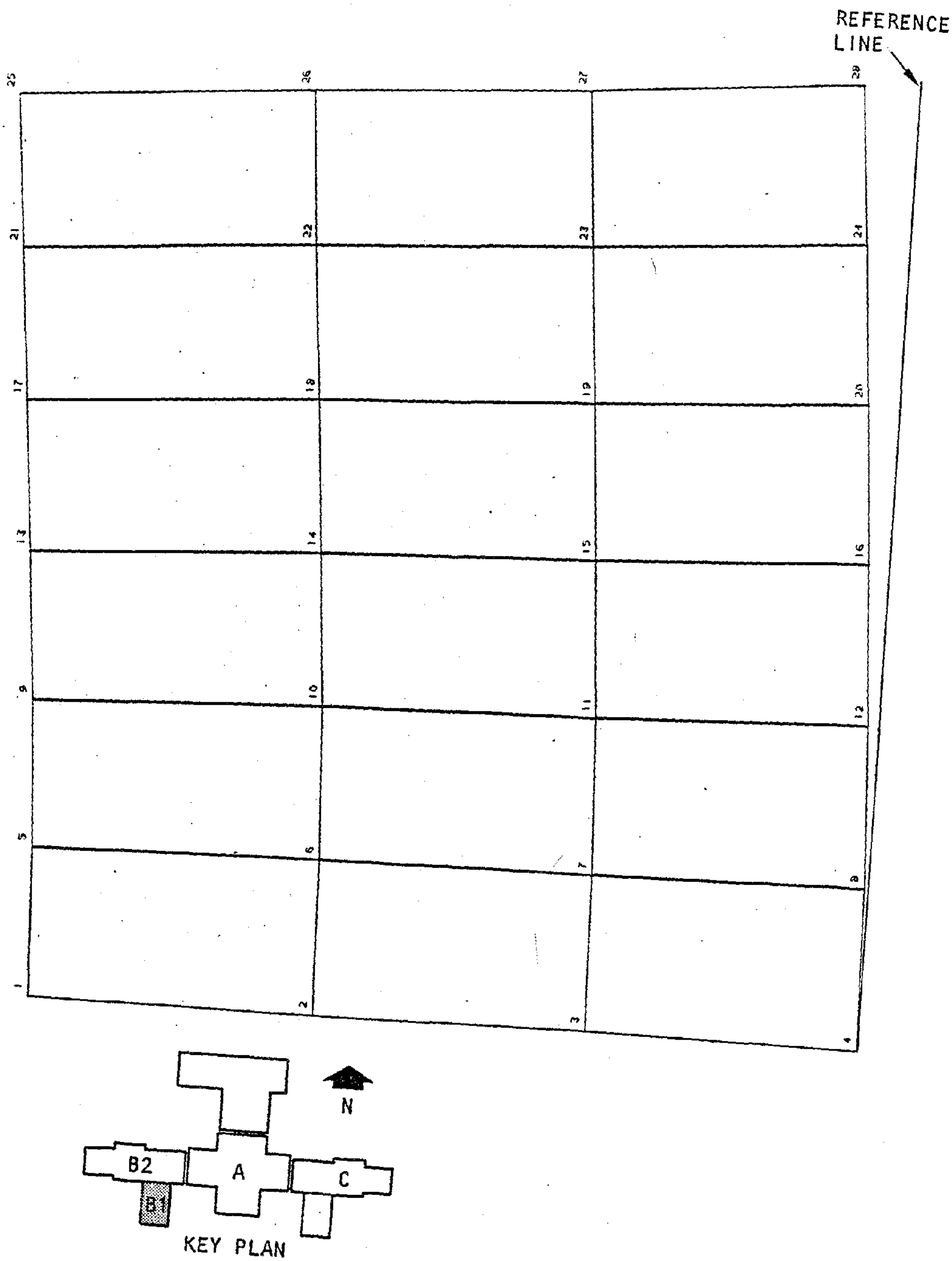

FIGURE 3-3. BUILDING 3B1: MODE 1

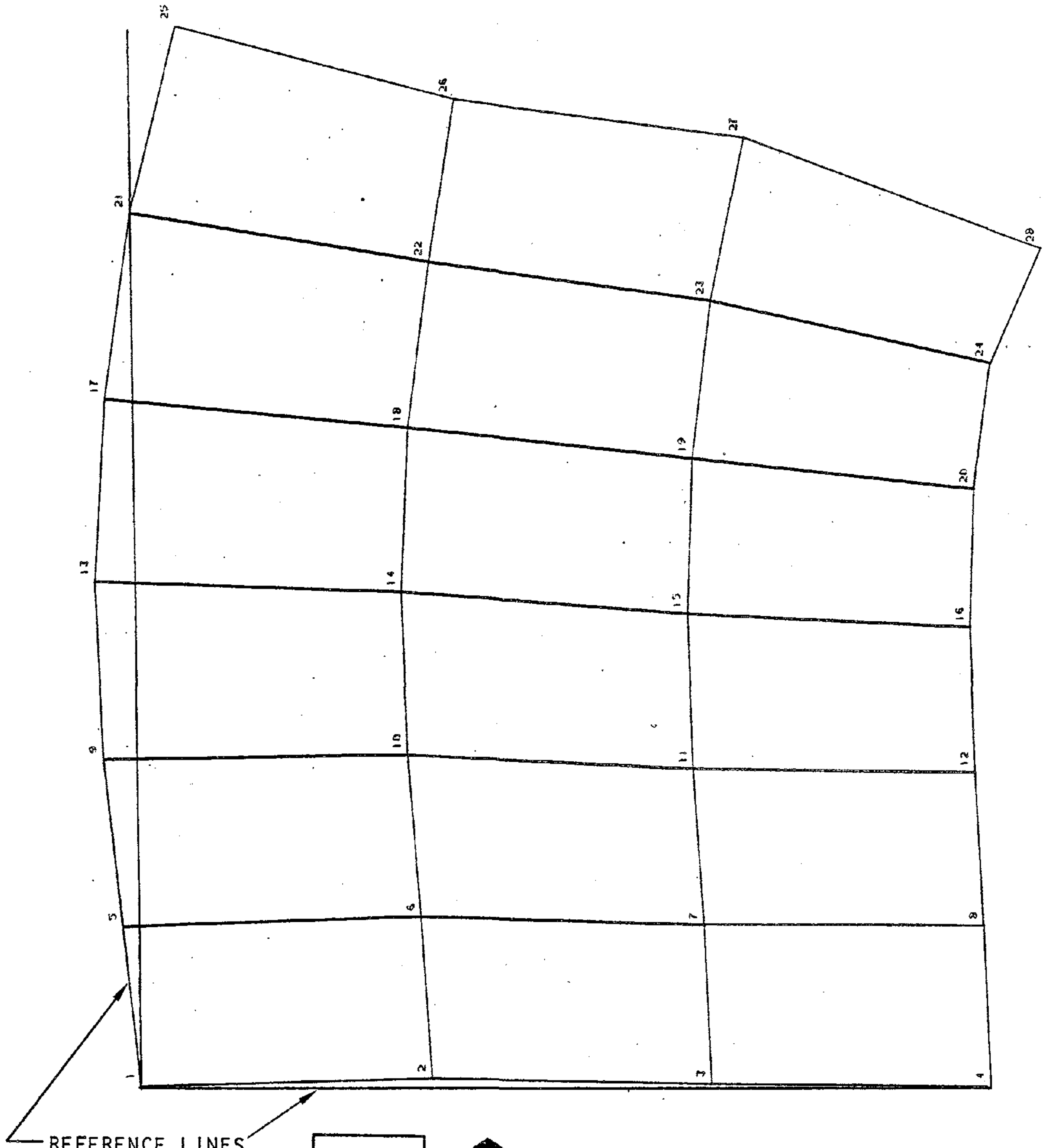

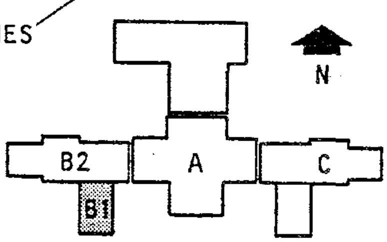

KEY PLAN

FIGURE 3-4. BUILDING 3B1: MODE 2

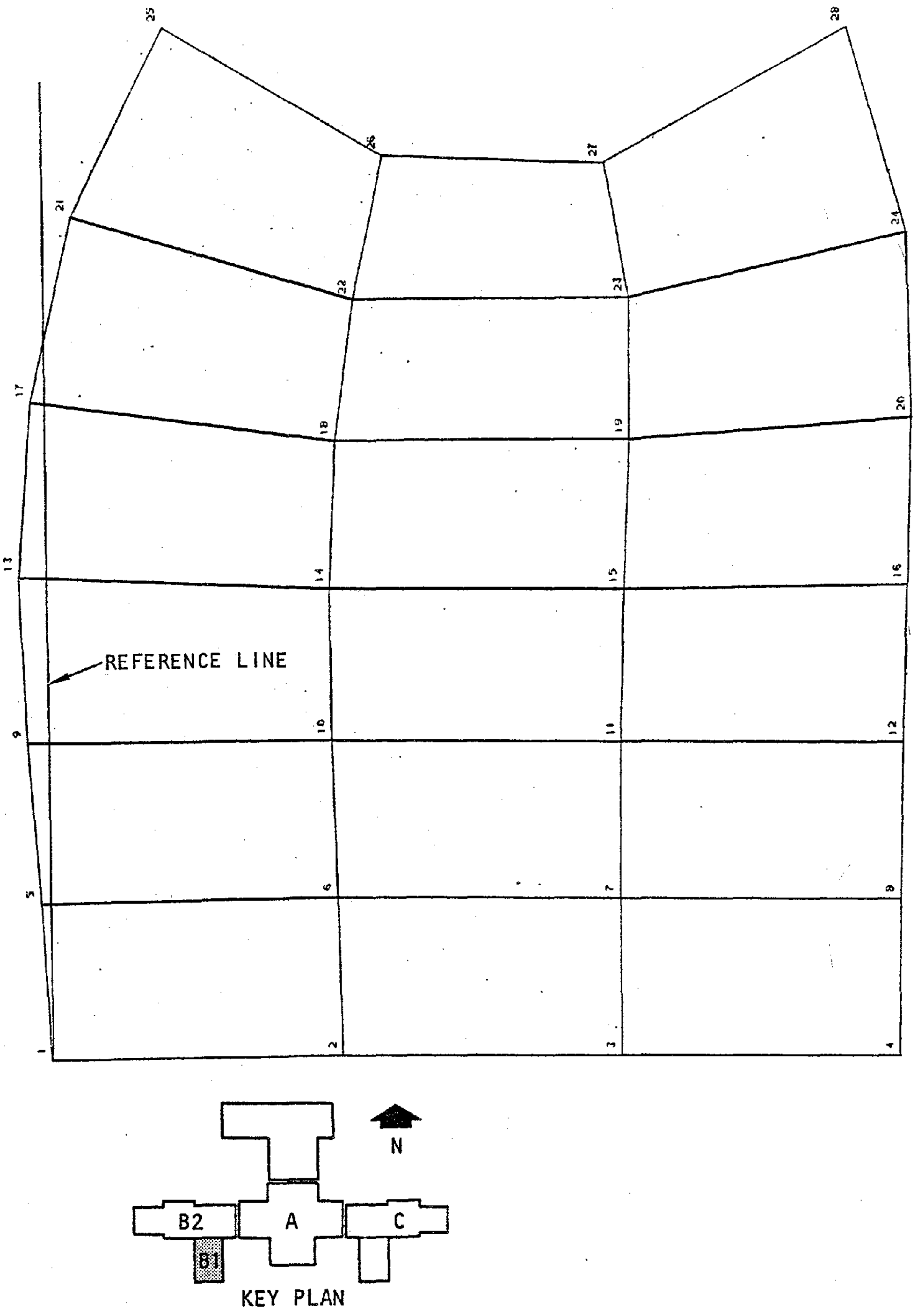

FIGURE 3-5. BUILDING 3B1: MODE 3

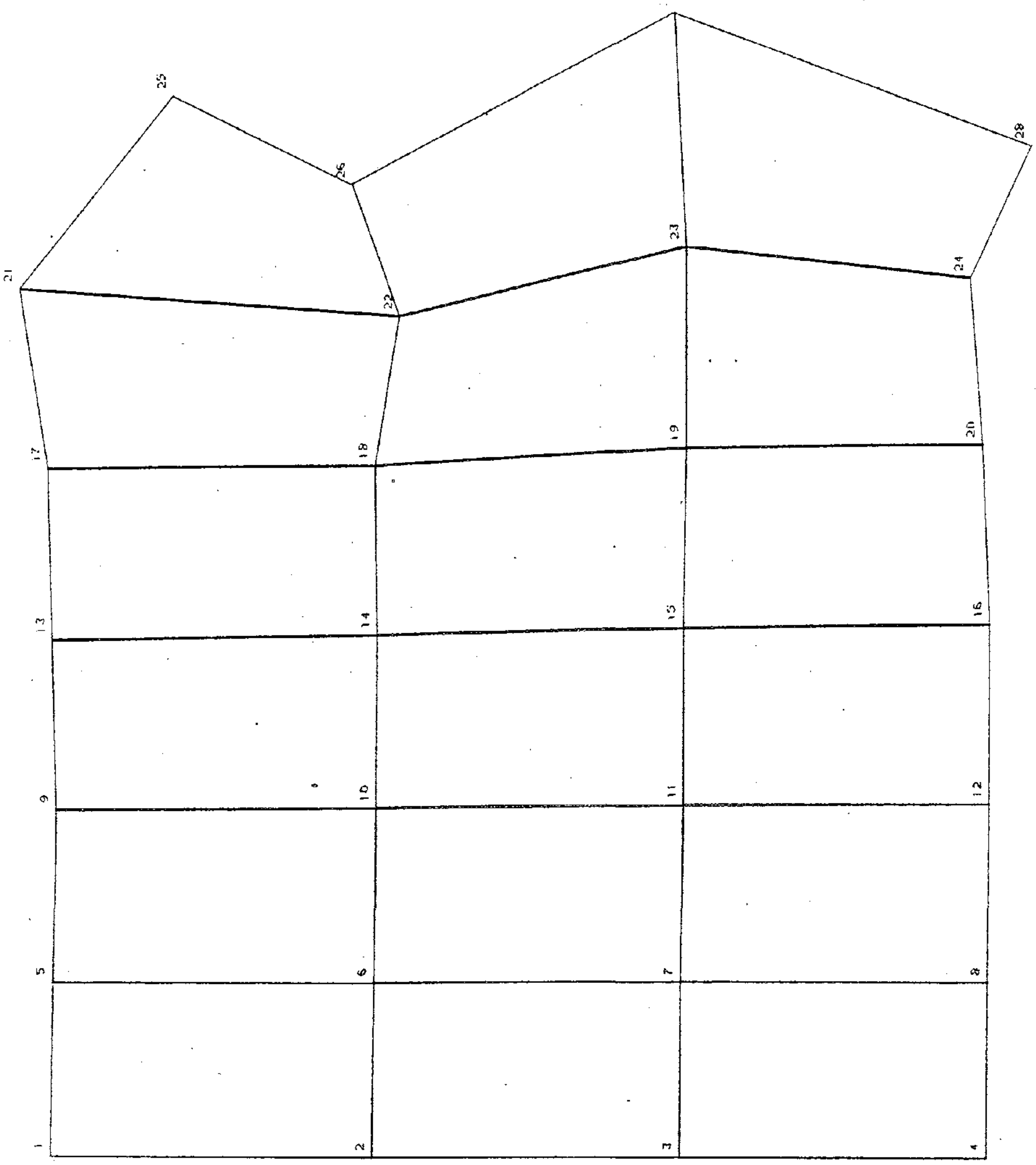

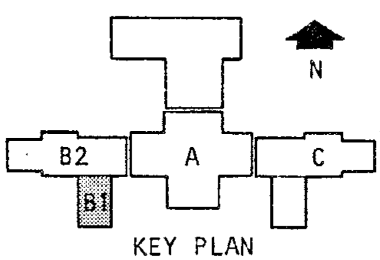

FIGURE 3-6. BUILDING 3B1: MODE 4

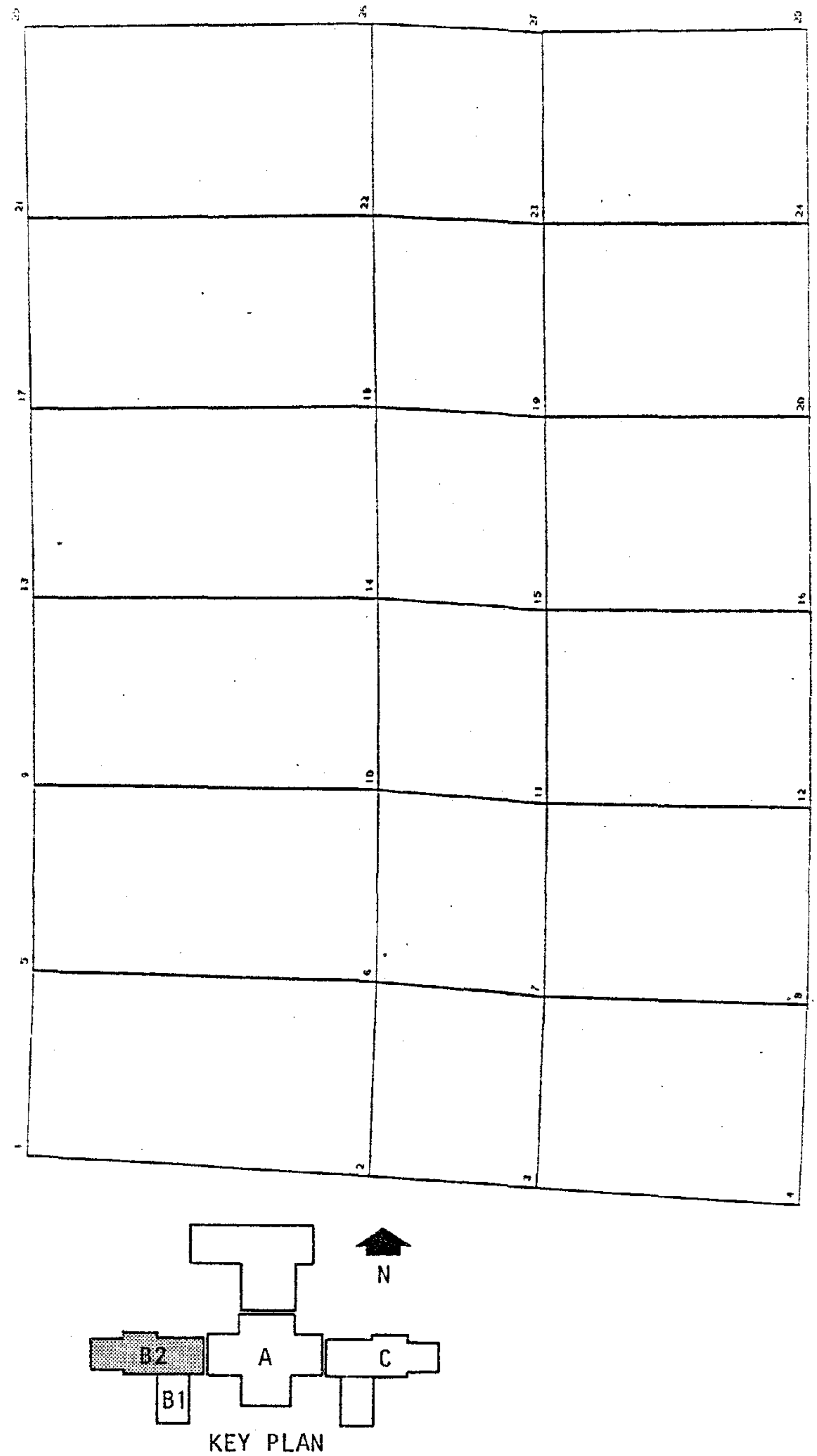

FIGURE 3-7. BUILDING 3B2: MODE 1

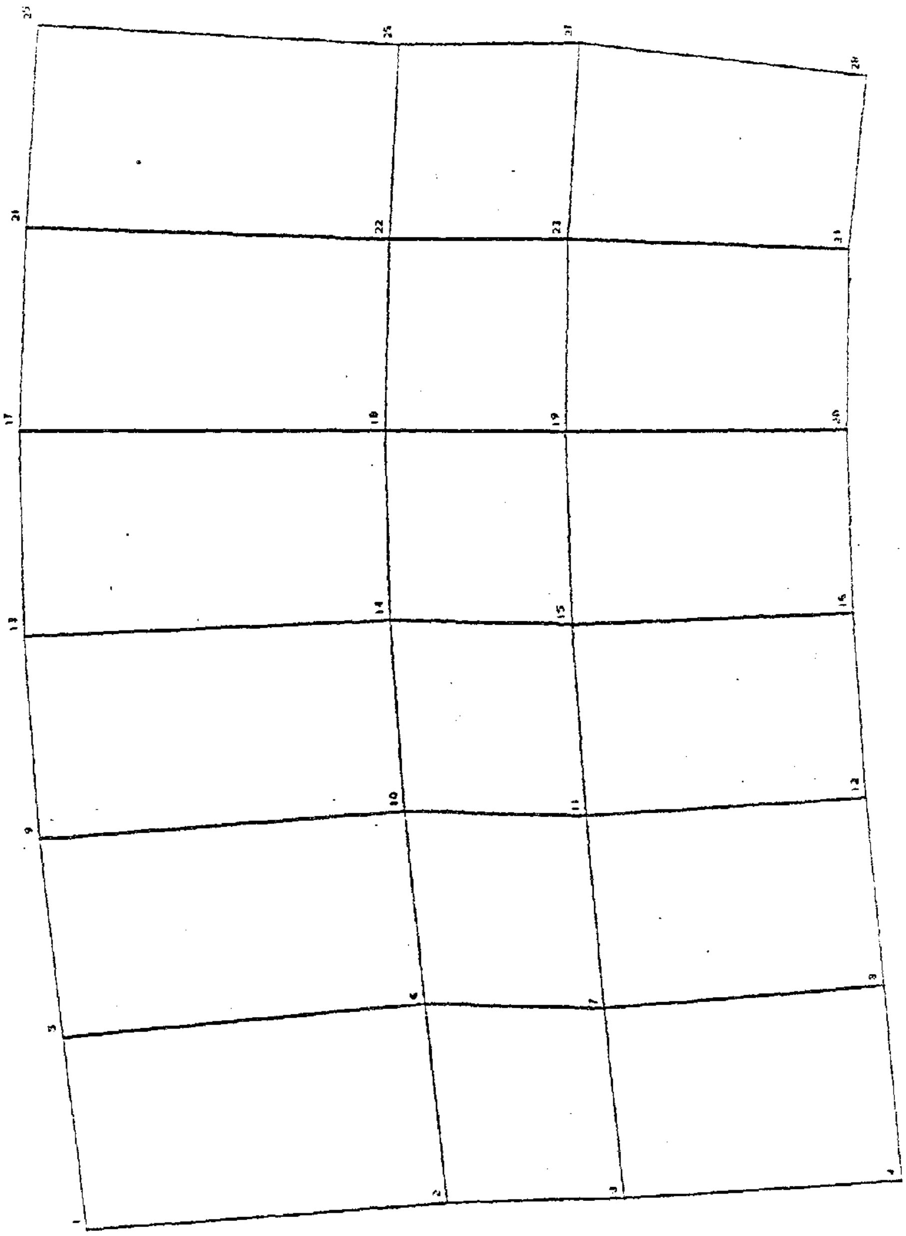

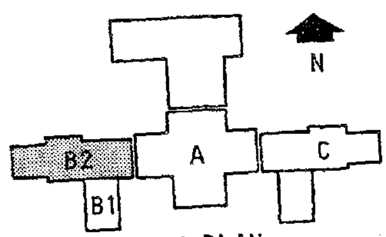

KEY PLAN

FIGURE 3-8. BUILDING 3B2: MODE 2

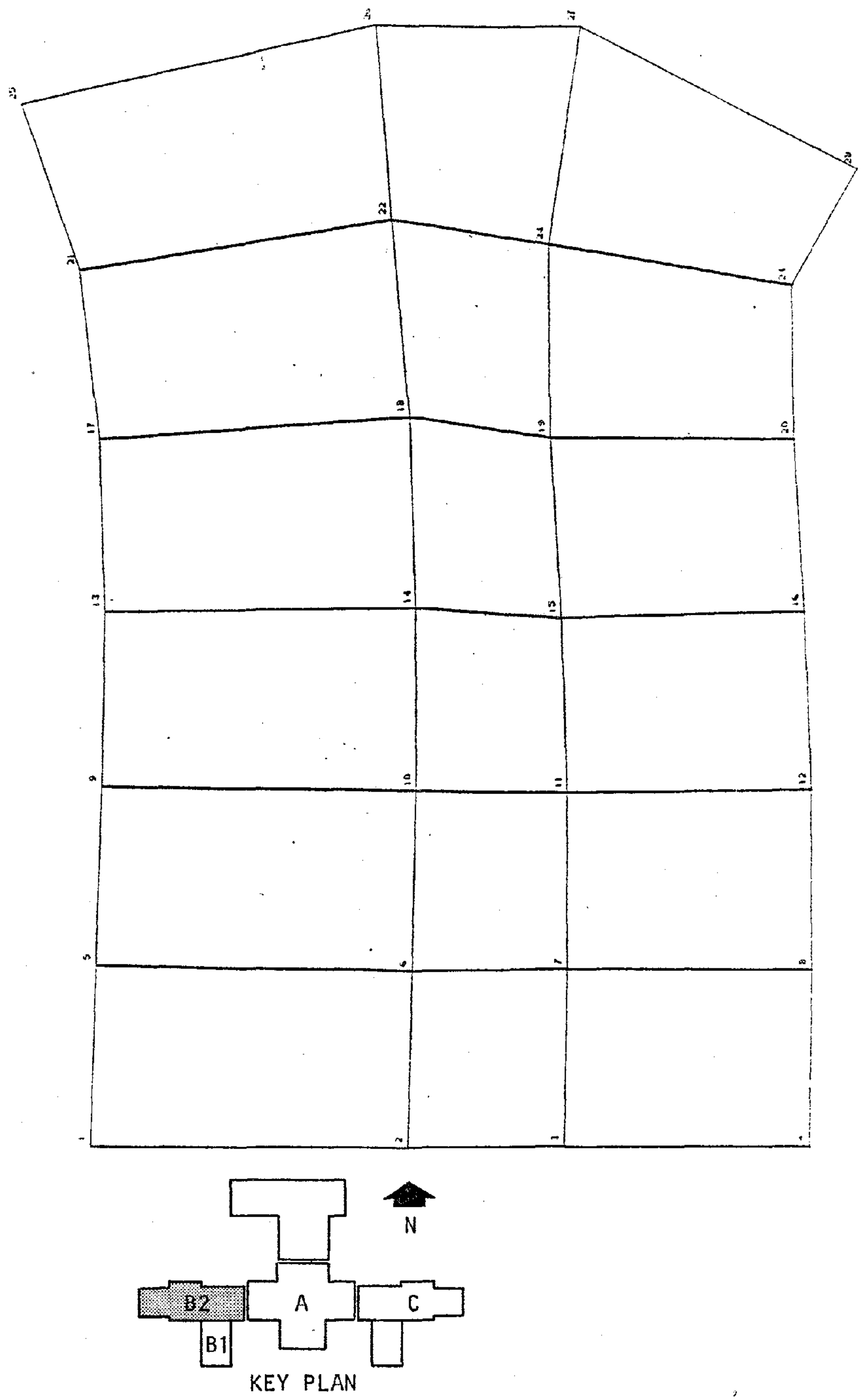

FIGURE 3-9. BUILDING 3B2: MODE 3

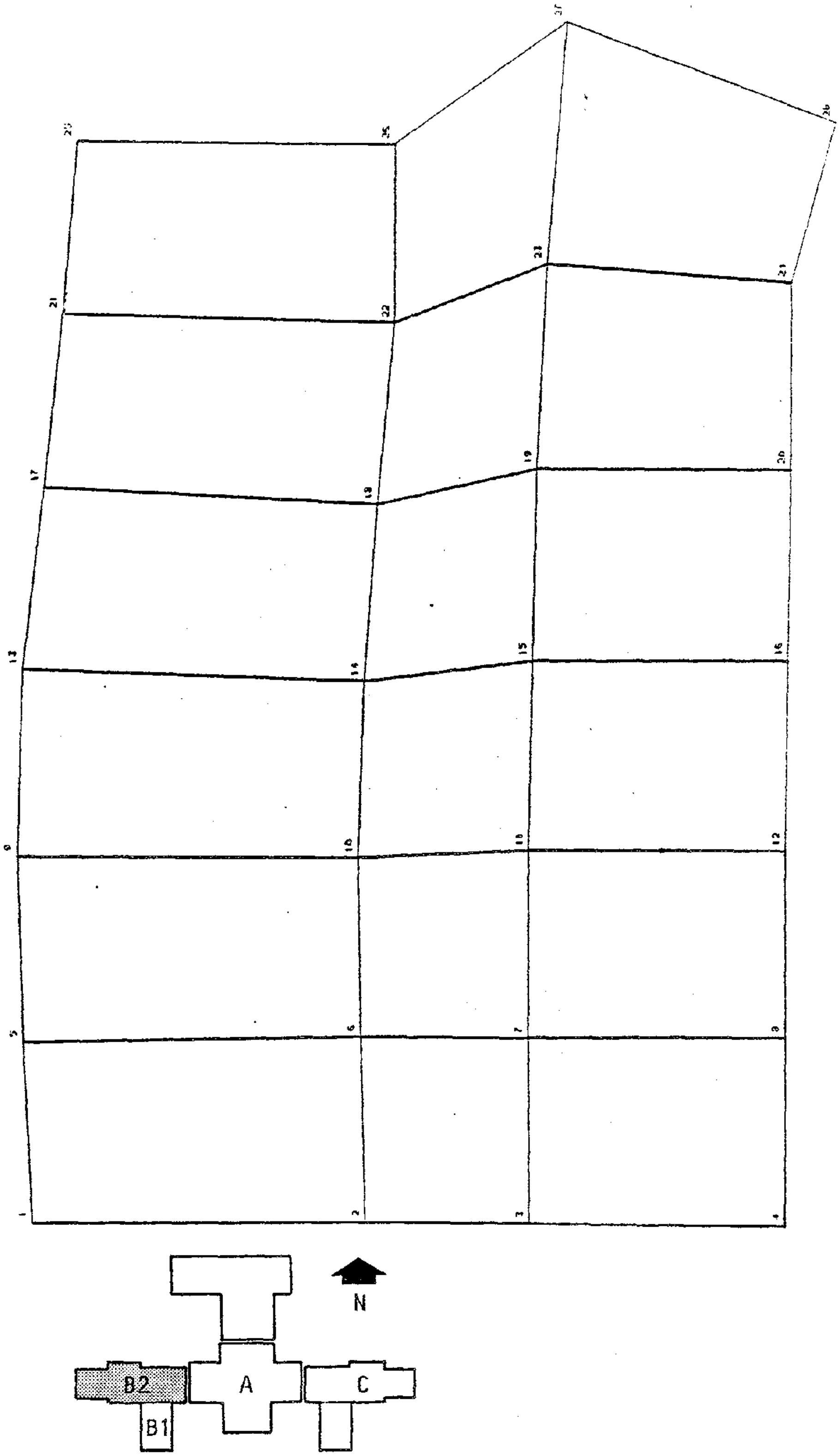

FIGURE 3-10. BUILDING 3B2: MODE 4

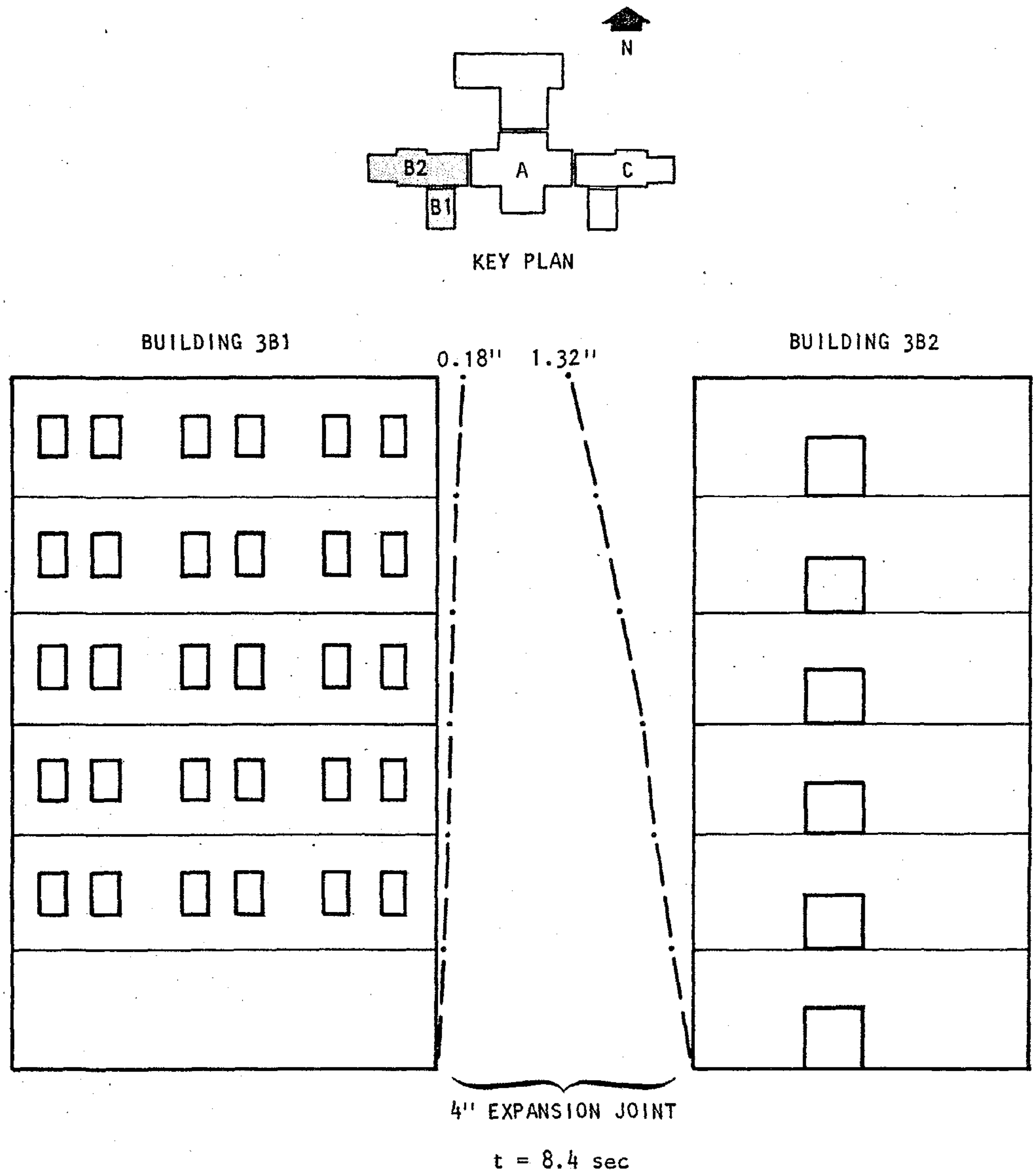

FIGURE 3-11. SCHEMATIC MAXIMUM RESPONSE FOR BUILDINGS 3B1 AND 3B2

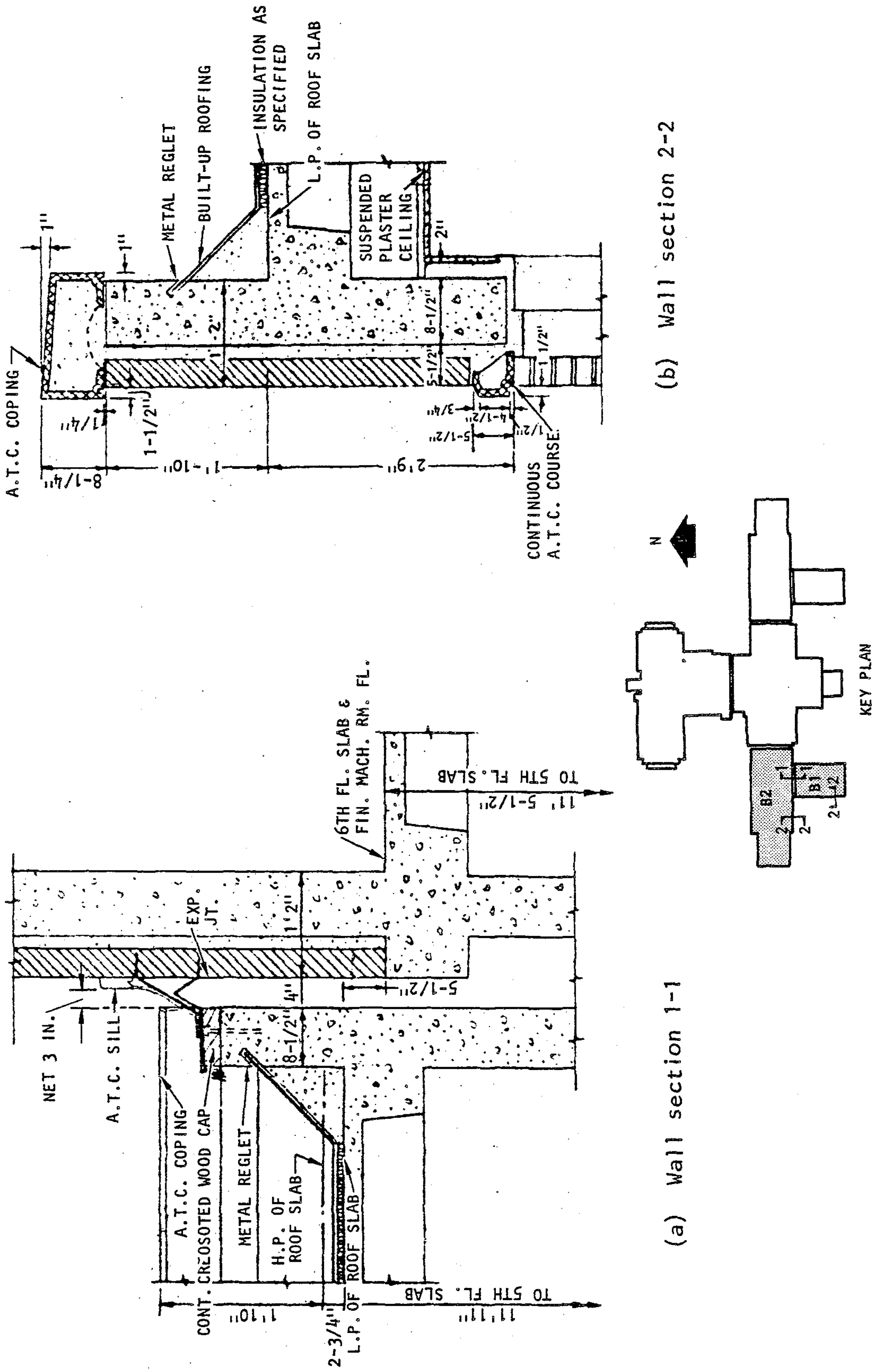

(b) Wall section 2-2

(a) Wall section 1-1

FIGURE 3-12. TYPICAL WALL SECTIONS

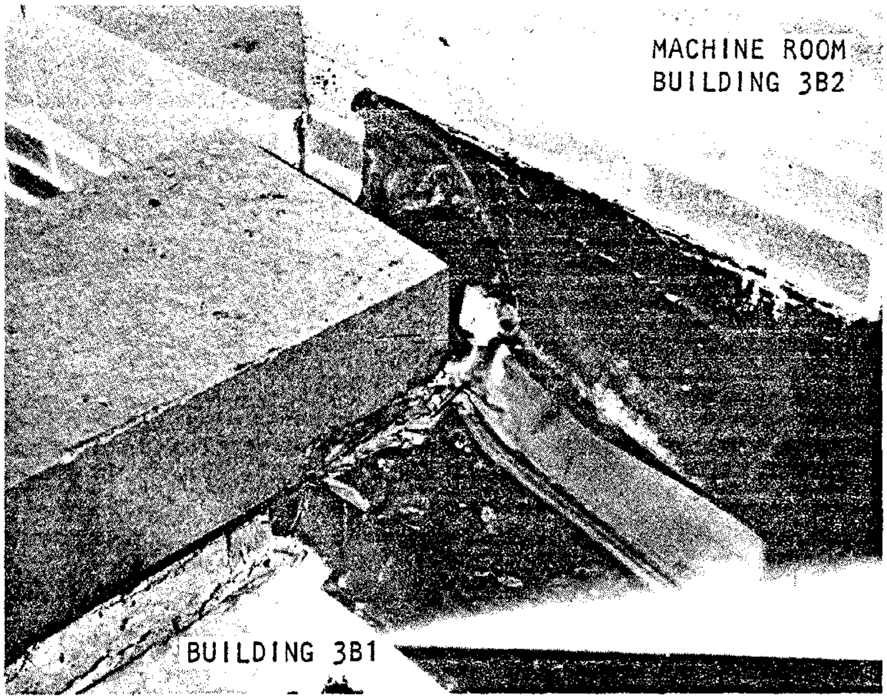

FIGURE 3-13. DAMAGE TO FLEXIBLE EXPANSION JOINT AT ROOF LEVEL (See Fig. 3-1a for location)

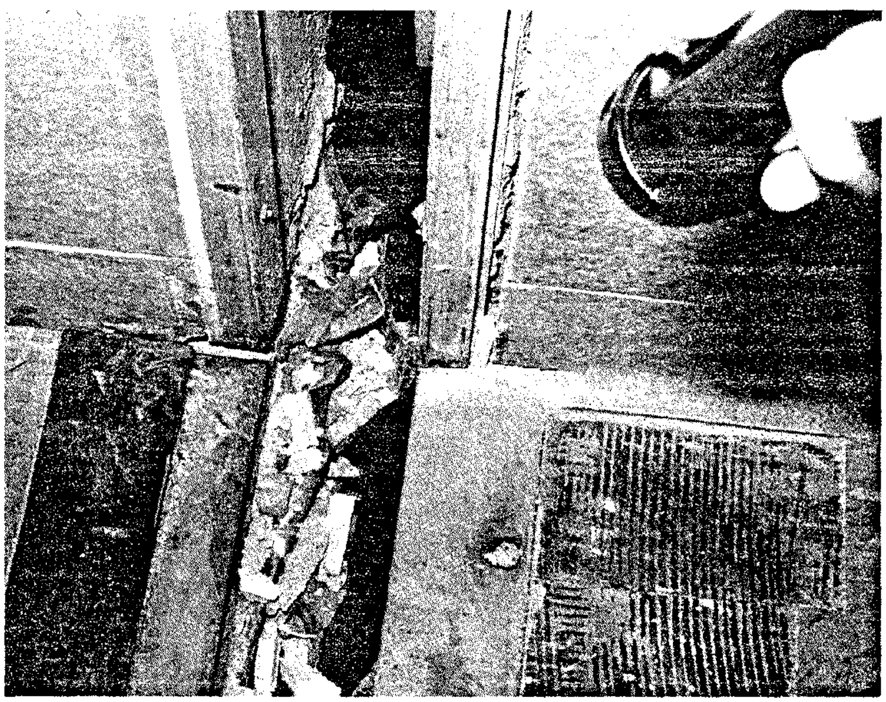

FIGURE 3-14. DAMAGE TO FLEXIBLE EXPANSION JOINT AT FIFTH FLOOR LEVEL OF BUILDING 3B

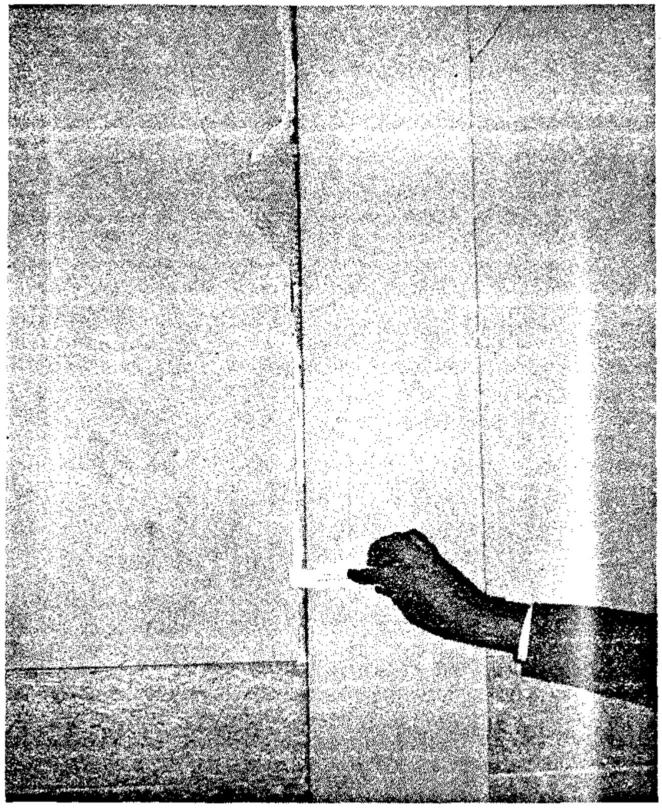

FIGURE 3-15. PERMANENT DISPLACEMENT OF APPROXIMATELY 1 INCH AT THE SIXTH FLOOR LEVEL OF BUILDING 3B

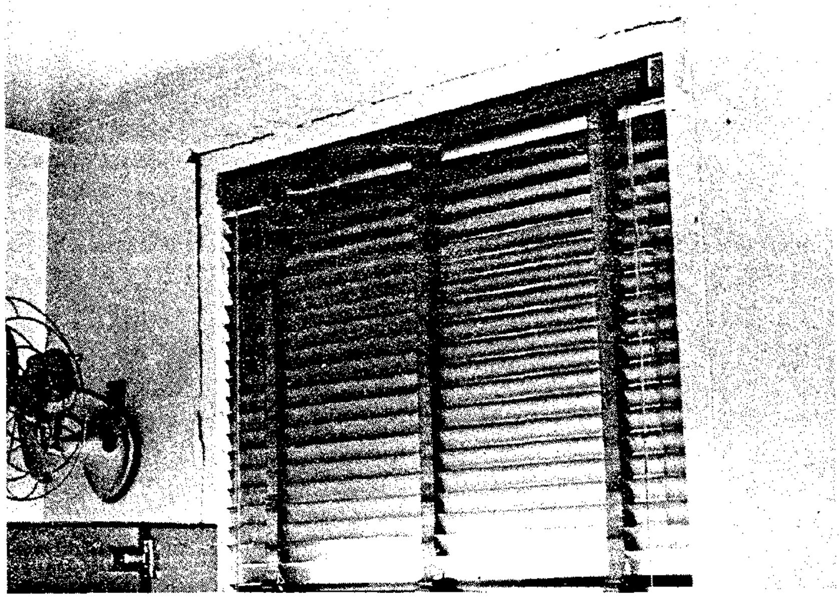

FIGURE 3-16. WINDOW JAMB IN SIXTH FLOOR JOLTED OUT OF PLACE BY STRONG SHAKING OF BUILDING 3

SECTION 4

SEISMIC ANALYSIS OF BOILER BUILDING

4.1 INTRODUCTION

Seismic analyses of the boiler building (Building 40) were made to estimate the stresses and response that the structure experienced during the 1971 San Fernando earthquake. The earthquake motion applied to this structure is the scaled Orion record, the same motion used in the analysis of Building 3 (see Section 3). This exercise provides additional evidence that the calibrated input motion established in Section 3 and then applied to the three-dimensional seismic analysis of Building 10 (in Section 5) reasonably reflects the site response during the 1971 earthquake. The following procedure was used:

1. Compute seismic stresses in the structure members where cracks were observed.

2. Assess the allowable strength of the structural material used.

3. Compare the allowables with the calculated stresses to check if the calibrated input motions of Section 3 can reproduce the damage pattern of the structure observed as a result of the 1971 earthquake (Figure 4-2).

Two seismic analyses were performed to compute the stresses in the structure: one using finite element approach and the other using simple hand calculations.

4.2 DESCRIPTION OF STRUCTURE

The boiler house, as shown in Figure 4-1, is a reinforced concrete structure with exterior brick walls on four sides. The main structural

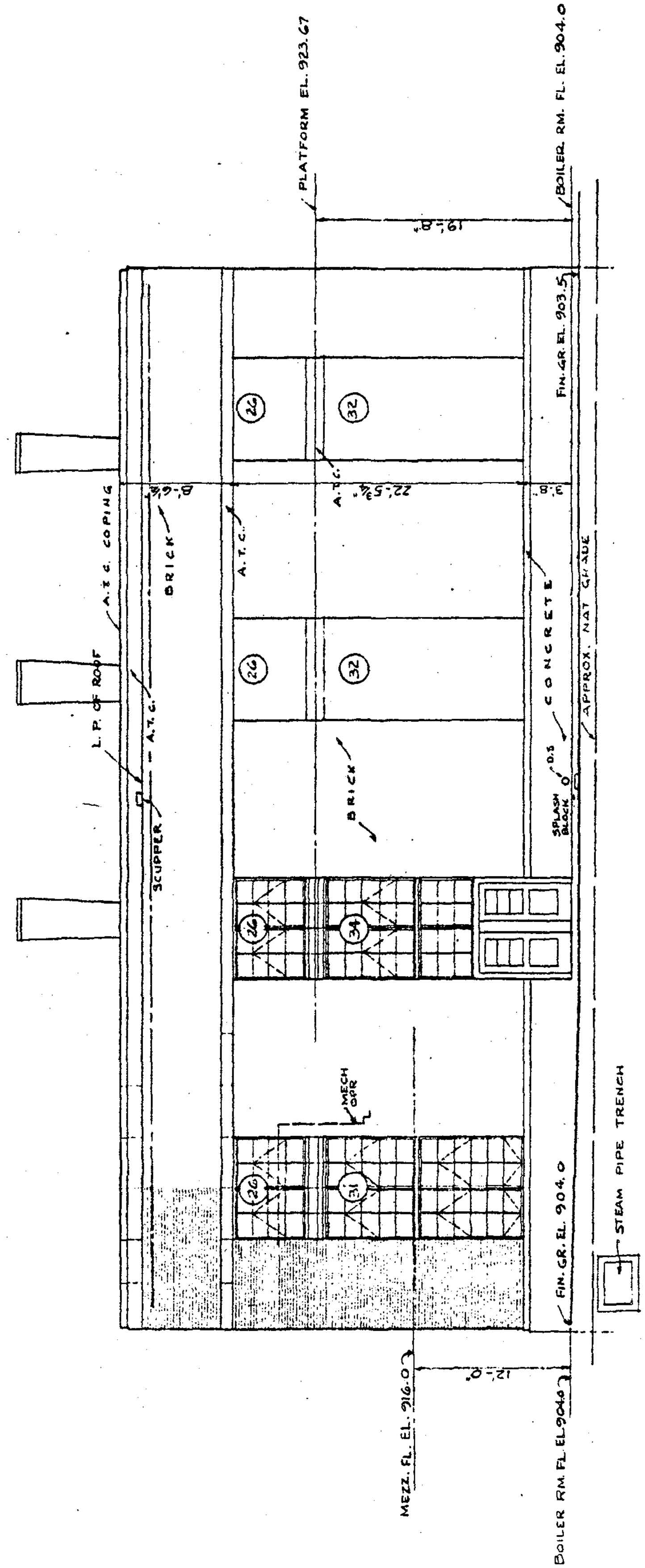

(a) South elevation

FIGURE 4-1. BOILER HOUSE

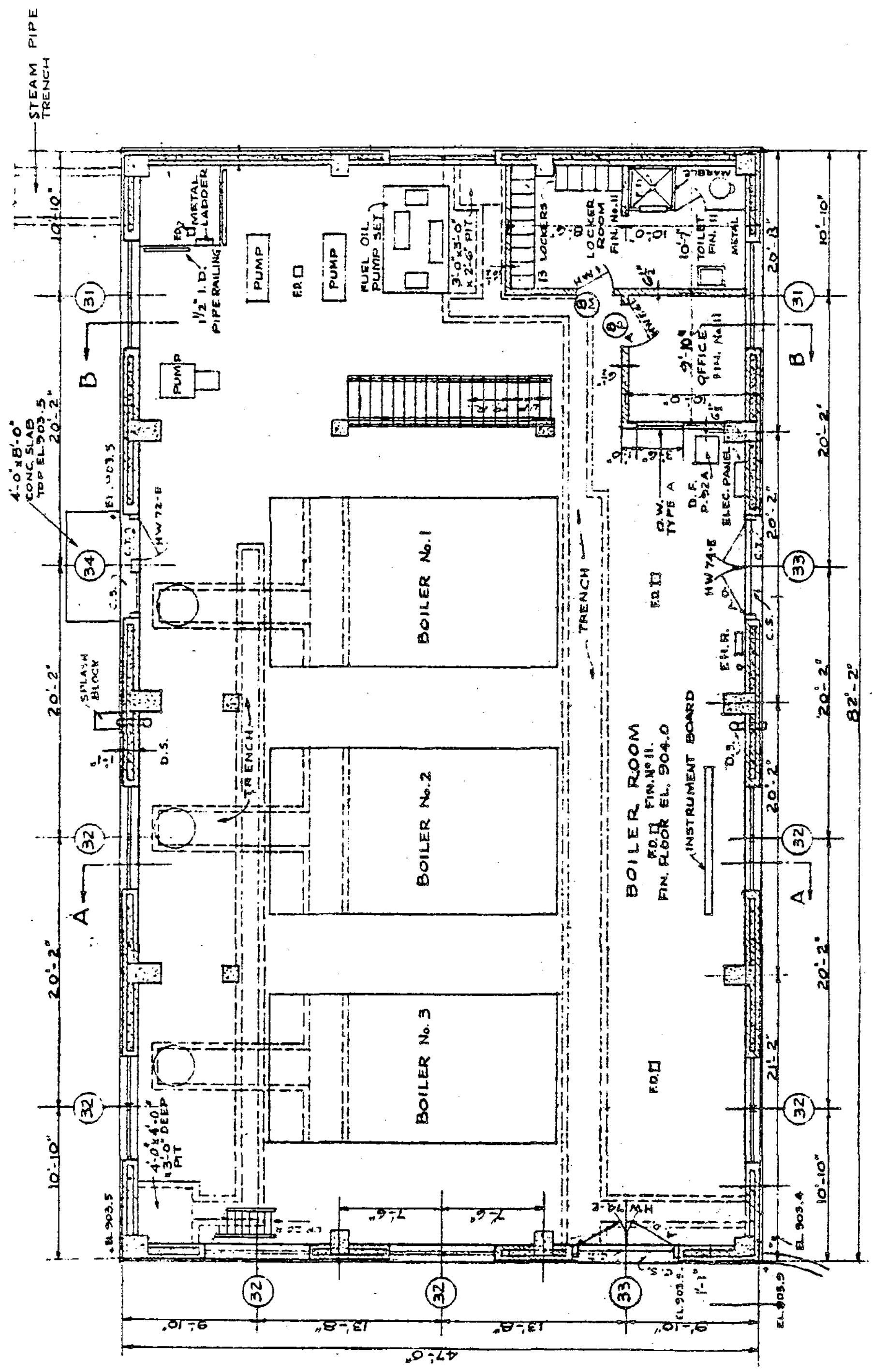

Reproduced from best available copy.

(b) Plan

FIGURE 4-1. (CONTINUED)

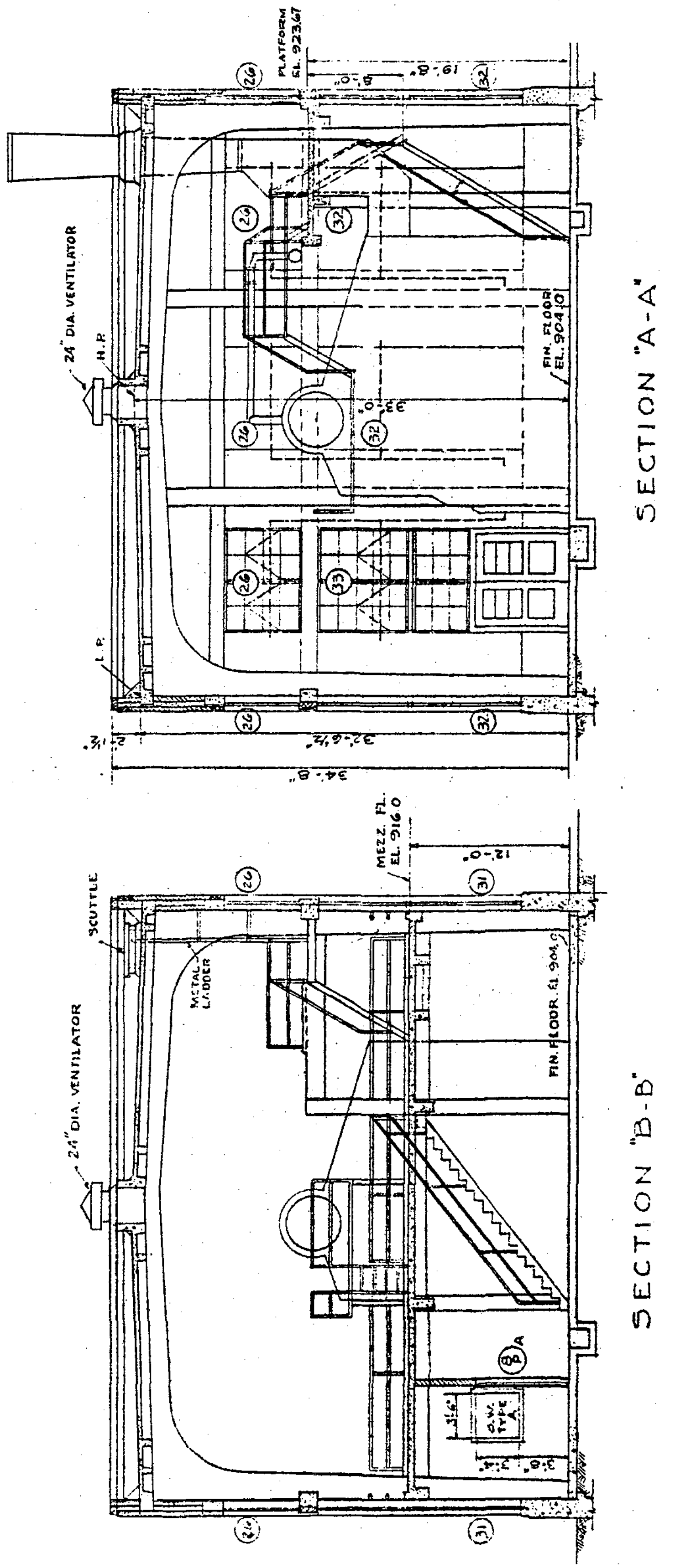

Reproduced from best available copy.

(c) Section

FIGURE 4-1. (CONCLUDED)

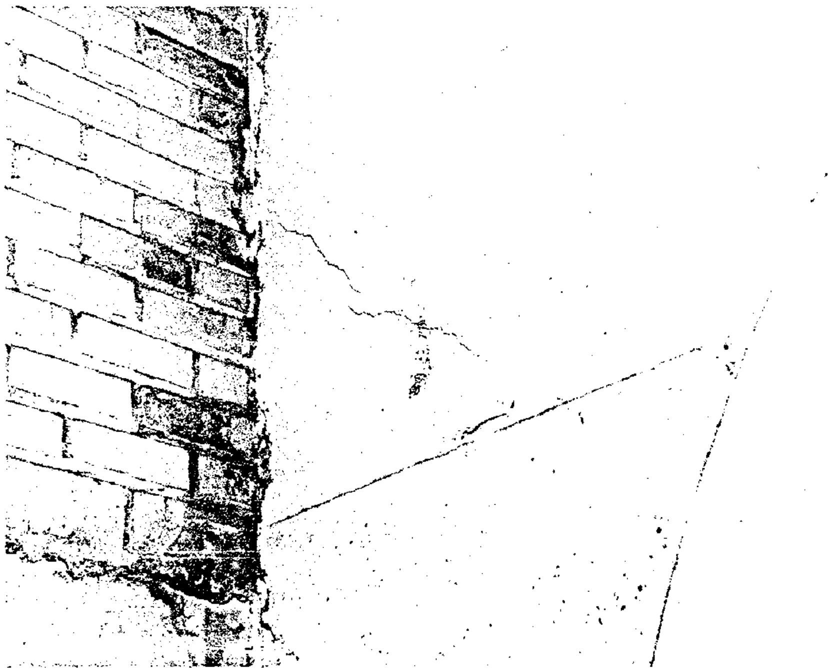

FIGURE 4-2. CRACK IN THE REINFORCED CONCRETE FRAMES SUPPORTING BOILER HOUSE ROOF (BUILDING 40)

elements of the building are the three reinforced concrete single bent frames which carry the roof load and seismic load in the north-south direction. The brick walls were designed to carry the seismic load in the east-west direction. The roof slabs, made of reinforced concrete of waffle construction, act as diaphragms under the earthquake motion. The concrete used for the construction is classified as Type B, with a strength f'_c = 2500 psi.

The building houses three large boilers which rest on their foundation. These boilers do not therefore induce any type of load to the building structure. A mezzanine and a platform, located on the west and south sides of the building respectively, are considered as part of the building structure. A building model that includes the mezzanine and platform was constructed for each of the finite element and hand calculation methods. In the following sections, the analytical model and results of each approach are discussed.

4.3 FINITE ELEMENT APPROACH

Since the main objective of this analysis is to examine the stress level in the reinforced concrete frame where the cracks were developed during the 1971 San Fernando earthquake, the single bent frame, where the cracks were observed, was analyzed using TRI/SAC computer code (AA, 1976). In Figure 4-3, a two-dimensional finite element mesh for the frame is shown. It contains 35 nodes and 34 beam elements. Each node has three degrees of freedom, i.e., two translational and one rotational. The boundary condition of the frame at foundations is idealized as a hinge. To reflect the rapid change in cross-sectional depth at the joints, the finite element mesh was carefully refined in these regions.

The particular frame bent for which the finite element model is constructed is the one located at the center of the building (Figs. 4-1 and 4-3). The masses lumped at the nodes are calculated based on the tributary area of the roof, mezzanine, and platform, plus the weight of the frame itself. No live load was considered in the mass calculation since the boilers and other equipment exert no force on the particular frame considered here.

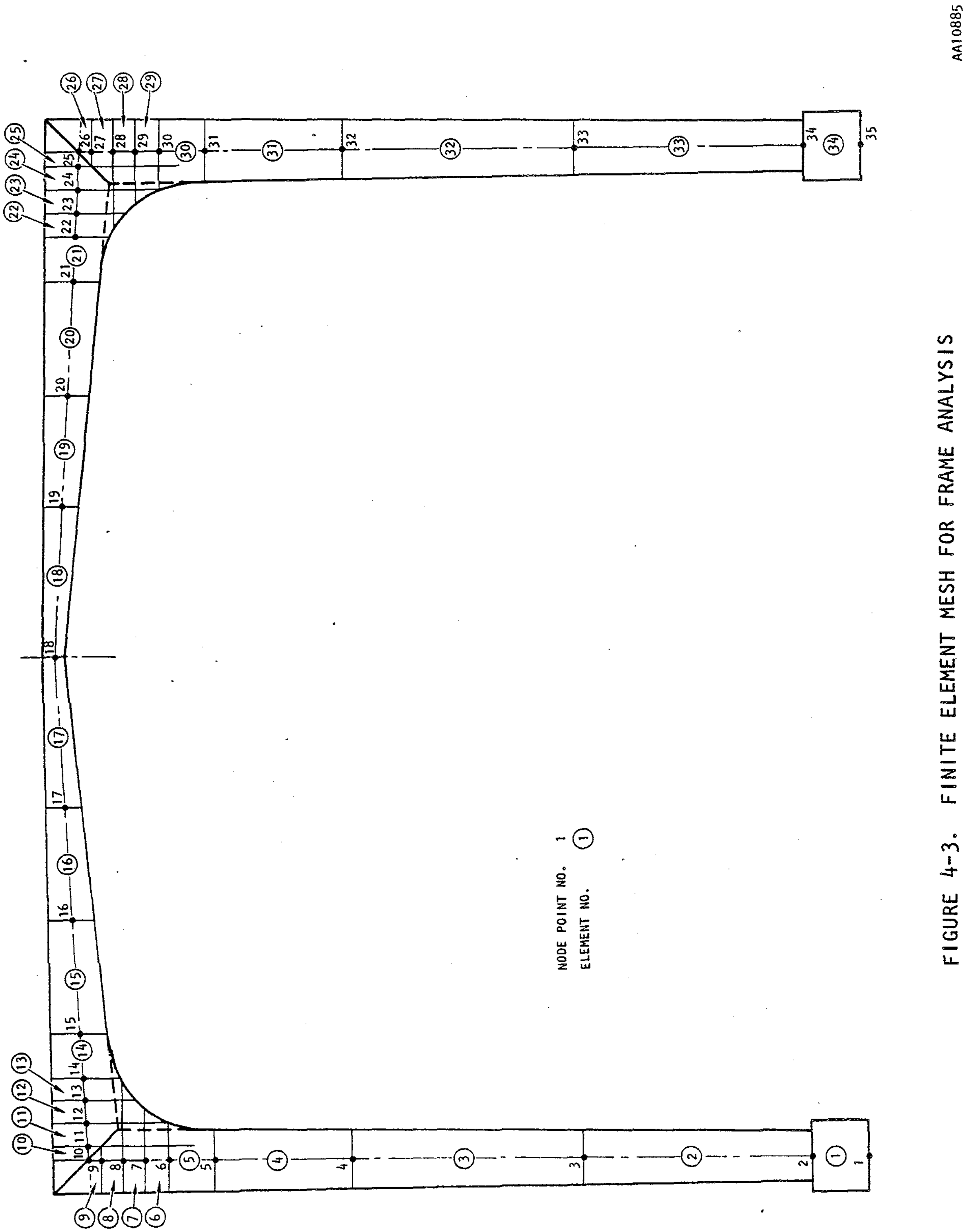

FIGURE 4-3. FINITE ELEMENT MESH FOR FRAME ANALYSIS

Mode extraction was performed for the frame model described above. Eight mode shapes and corresponding frequencies were obtained. The first four significant ones are listed and described in Table 4-1. The corresponding mode shapes are also shown in Figure 4-4.

It is noted that the first mode, which has a frequency of about 0.67 Hz, is associated with motion in the horizontal direction, while the second mode, about 3.3 Hz, is related to vertical motion. These two modes are the major participants in the structure response under earthquake motion. The other higher modes make only minor contributions to the responses.

The seismic-induced stresses were computed for the N00°W horizontal component and the vertical component of the scaled 1971 Orion ground motion. They were calculated by normal mode technique where all 8 modes of the structure were included. The length of the input motion used in the analysis was 25 seconds. The critical internal forces at and around the joint area are listed in Table 4-2. These are the maximum values in the entire 25 sec time period.

4.4 SIMPLE HAND CALCULATION

The purpose of this exercise is (1) to estimate the critical seismic stress in the frame structure by a simple approach and (2) to run a check on the result of finite element analysis. To perform such calculations, the same frame structure as described above was simplified into a single-degree-of-freedom system. A single mass was obtained by lumping all the masses within its tributary area. The spring constant of the system was calculated based on stiffness of the frame in the horizontal or vertical directions. The detailed computations of the mass and the spring constant are attached in Appendix B.

Figure 4-5 shows the single-degree-of-freedom system model for the structure and the associated frequency formula. By substituting the spring constant and mass of a specific type of motion into this equation, a frequency

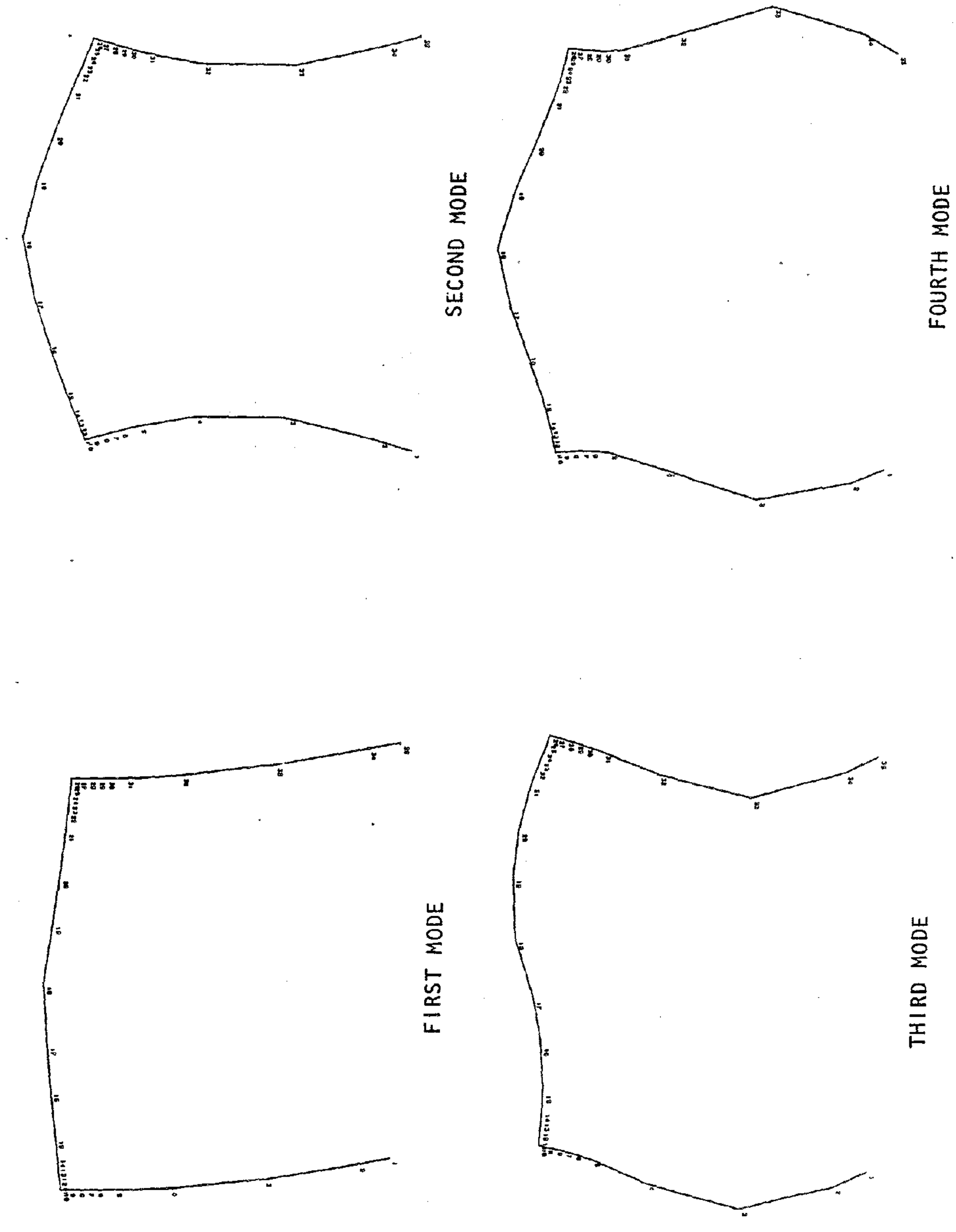

FIGURE 4-4. MODE SHAPES (BOILER HOUSE)

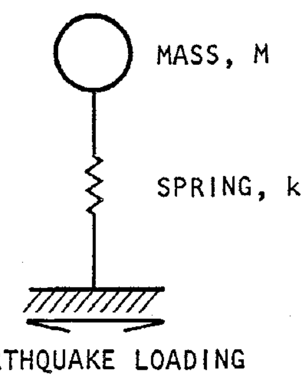

FREQUENCY, $f = \frac{1}{2\pi}\sqrt{\frac{k}{m}}$

SHEAR FORCE, S = MASS x ACCELERATION

$= M \times a$

FIGURE 4-5. SINGLE-DEGREE-OF-FREEDOM SYSTEM FOR HAND CALCULATION

TABLE 4-1. CALCULATED FREQUENCIES AND MODE SHAPES FOR BOILER HOUSE

Mode No.	Frequency, Hz	Description
1	0.67	Horizontal shear displacement
2	3.32	Vertical displacement, bending of beam
3	6.95	Horizontal displacement, bending of frame
4	8.95	Vertical displacement, bending and extension of columns

TABLE 4-2. SEISMIC FORCES AT JOINTS

Element No.	Node No.	Cross Sectional Area, in.^{2}	Axial Force, N kips	Shear V kips	Moment, M kip-in.
4	4	512	85.52	37.75	16,970
	5	512	85.52	37.75	19,540
5	5	544	84.99	32.81	19,540
	6	544	84.99	32.81	20,270
6	6	672	84.97	30.47	20,270
	7	672	84.97	30.47	20,610
7	7	832	84.96	28.74	20,610
	8	832	84.96	28.74	20,920
8	8	1248	84.94	26.89	20,920
	9	1248	84.94	26.89	21,230
9	9	1920	84.92	25.12	21,230
	10	1920	84.92	25.12	21,430
10	10	2278	30.30	82.23	32,430
	11	2278	30.30	82.23	20,790
11	11	1606	28.88	82.39	20,790
	12	1606	28.88	82.39	19,840
12	12	1158	27.56	82.46	19,800
	13	1158	27.56	82.46	18,880
13	13	902	27.08	82.32	18,880
	14	902	27.08	82.32	17,920
14	14	838	24.75	82.57	17,920
	15	838	24.75	82.57	15,990
15	15	774	21.17	82.57	15,999
	16	774	21.17	82.57	11,140

of 0.64 Hz and 3.1 Hz, corresponding to the horizontal and vertical displacement of the frame respectively, were obtained from the simple system, as compared with 0.67 Hz and 3.3 Hz from the finite element method. Having determined the two lowest frequencies of the structure, the spectrum method (Clough and Penzien, 1975) was applied to calculate the shear stresses. The input spectra used here are the scaled N00°W component of the 1971 Orion record shown in Figures 2-16 and 2-17. It should be pointed out here that this type of simple calculation ignores coupling effects and the resulting shear force is due to one component of motion only. The detailed calculation of the shear stress at the joint is presented in Appendix B. The results show a shear stress of 125 psi and 130 psi in the column and beam adjacent to the corner region respectively.

4.5 ALLOWABLE SHEAR STRESS OF CONCRETE

By examining the crack patterns as shown in Figures 4-6 and 4-7, it is evident that these cracks were caused by the diagonal tension. Since the diagonal tension is related to shear stress, the shear capacity of reinforced concrete in resisting diagonal tension was assessed based on the approach given by ACI Standard 318-71. Section 11.4.4 of this standard provides a formula to compute allowable shear stresses, ν_c, for members subjected to significant axial tension:

$$\nu_c = 2\left(1 + 0.002 \frac{N_u}{A_g}\right) \sqrt{f'_c} \qquad (4\text{-}1)$$

where

N_u = negative for tension

f'_c = compressive strength of concrete

A_g = gross area of the section

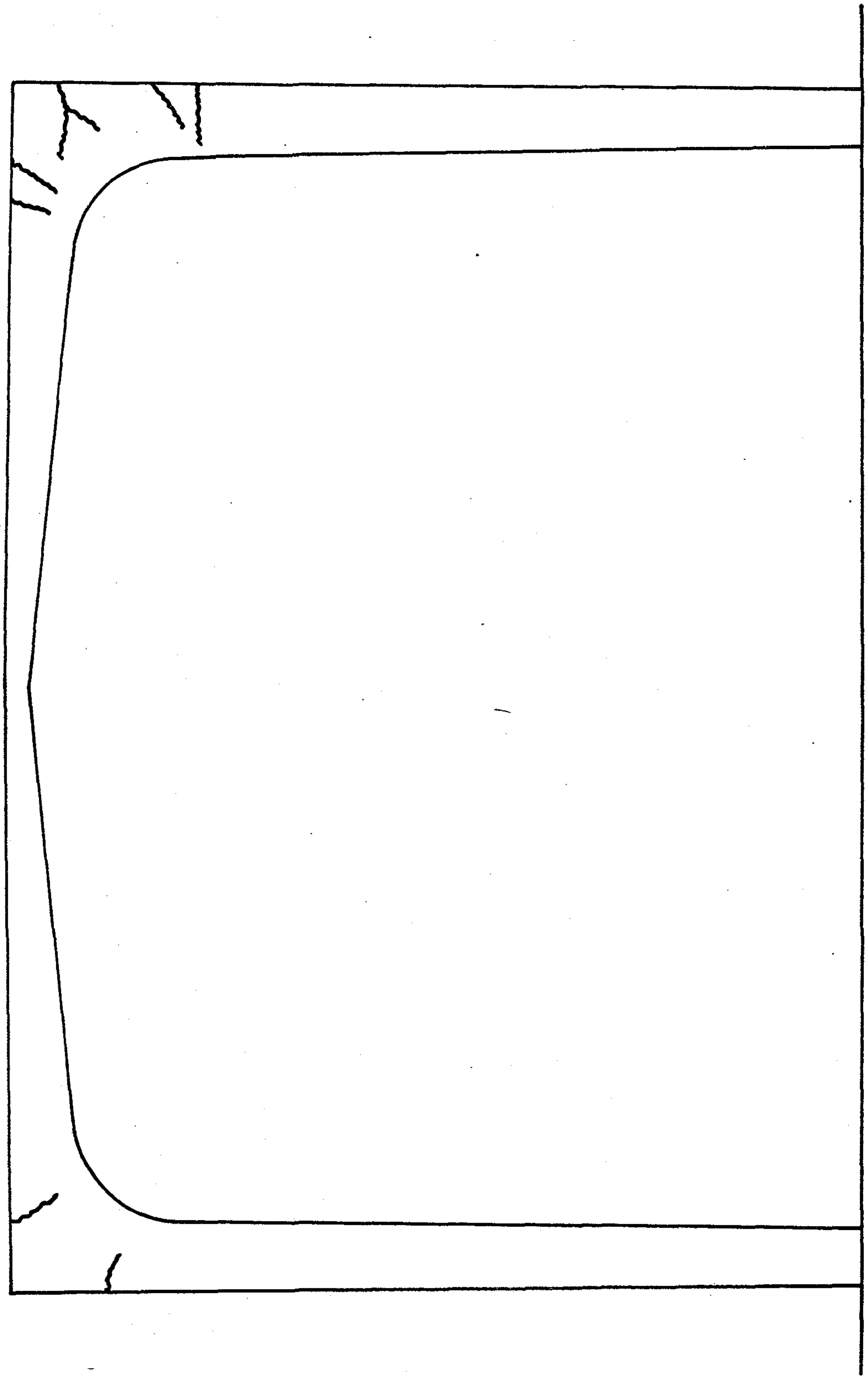

FIGURE 4-6. CRACK PATTERN OBSERVED IN BOILER HOUSE BUILDING AS A RESULT OF THE 1971 SAN FERNANDO EARTHQUAKE

TABLE 4-3. CRITICAL SHEAR STRESSES IN FRAME STRUCTURE

Location Where Stress is Calculated*	Finite Element Method, psi	Hand Calculations, psi	Allowable Stresses, psi
Column Section	84	125	82
Beam Section	160	130	94

*See figure below.

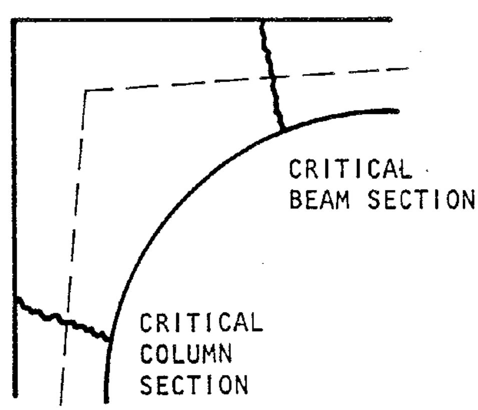

FIGURE 4-7. CRITICAL BEAM AND COLUMN SECTIONS

Using this equation, the allowable concrete shear can be computed. This shear does not take into account tension from diagonal cracks in the reinforced concrete. Detailed calculations to estimate the allowable stresses in the column and beam sections near the joint are given in Appendix B. The selection of this particular section was based on (1) the observation of crack locations in the frame and (2) the stress pattern computed by the finite element method. The allowable shear stress of concrete was found to be 82 psi and 94 psi for the column and beam sections respectively (Fig. 4-7). In Table 4-3, the critical shear stresses in the framed structure, obtained by both finite element analysis and hand calculations, are compared to the allowable stresses.

4.6 CONCLUSIONS

The analyses results indicate that the maximum shear stresses obtained by both finite element method and hand calculations at the critical beam and column sections did exceed the allowable stresses (Table 4-3). This result confirms the overstressed condition of the structure observed during the 1971 San Fernando earthquake. Such findings indicate that the calibrated input earthquake motions provided in Section 3 are a reasonable representation of the intensity of ground motion at the hospital site during the 1971 San Fernando earthquake.

SECTION 5

THREE-DIMENSIONAL SEISMIC ANALYSIS OF A TWO-STORY, REINFORCED, GROUTED BRICK MASONRY BUILDING

5.1 INTRODUCTION

The structure considered in this section is a two-story, reinforced, grouted brick masonry building with a reinforced concrete basement (Bldg. 10). The earthquake input motions, estimated in Section 2 and calibrated in Section 3 and 4, are applied as input to the analyses of Building 10. The middle segment (Unit A) of the building was analyzed first by a three-dimensional model. Critical response of shear wall elements was evaluated. A second analysis was conducted in which the building model was expanded to include the other two segments of the building. The second analysis assessed the effect of eliminating the expansion joints in the response of this building as a total unit.

5.2 DESCRIPTION OF THE STRUCTURE

Figure 5-1 provides an elevation of the building, while Figure 5-2 shows the second floor plan of Unit A of Building 10. All floor slabs are cast-in-place reinforced concrete. Basement walls are 12-in. reinforced concrete, while all walls constructed above basement level are of 13-1/2-in. reinforced grouted brick. All perimeter shear walls are wall-bearing, while interior columns are supported on isolated footings.

A characteristic feature of Segment A of Building 10 is that it is not symmetrical about the x-axis. Also, the central portion has additional rooms at the roof together with a pipe chase below the basement. Therefore, this segment has five levels in some portions.

Building 10A is 100 ft long and 97 ft wide. Buildings 10B and 10C are identical and are each divided into two parts; the first part is 176 ft 5-1/2 in. long by 76 ft 6 in. wide, while the second part is 43 ft 9 in. long and 82 ft 9 in. wide. Therefore, the total length of the three units when

Reproduced from best available copy.

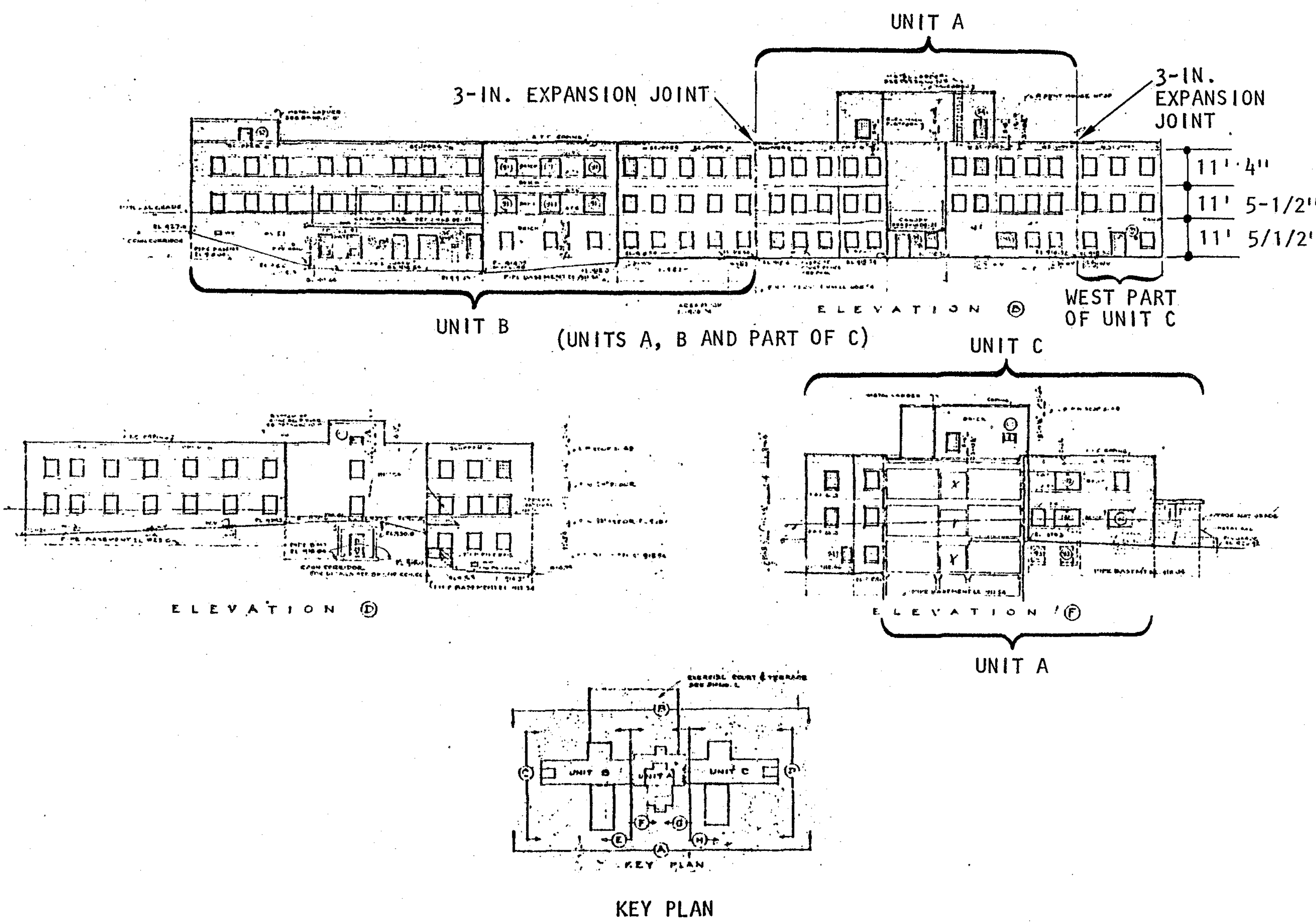

FIGURE 5-1. BUILDING 10: ELEVATION

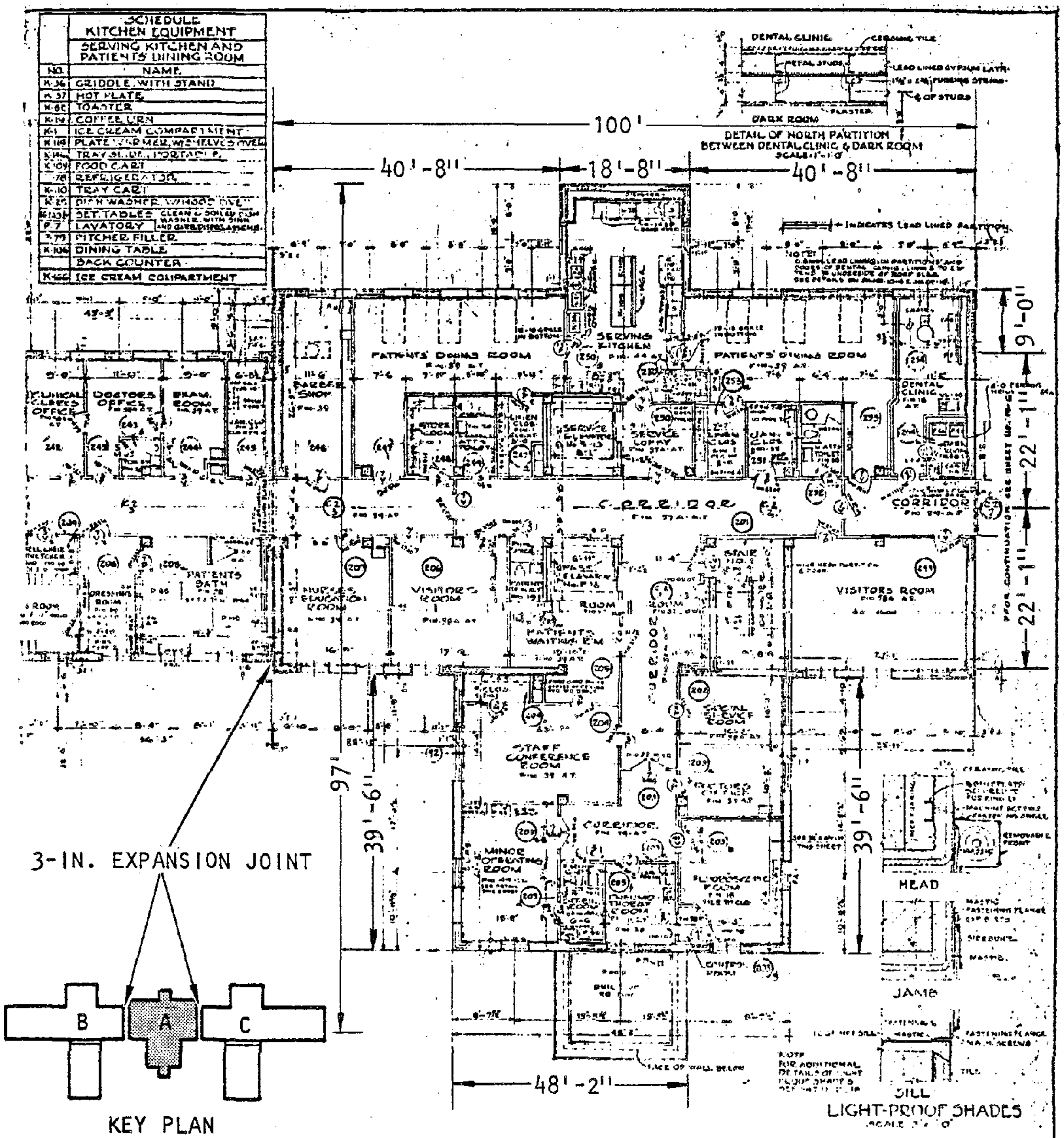

FIGURE 5-2. BUILDING 10: SECOND FLOOR PLAN — UNIT A

Reproduced from best available copy.

tied together is 452 ft 11 in. Flexible expansion joints separating various portions of Segments A, B, and C are 3 in. wide, in contrast to the 4 in. used in the six-story Building 3.

In the construction of the reinforced brick masonry walls of this hospital, steel reinforcement was tied in place, after which the brick in the outer tier, or wythe, was laid up for not more than three courses. In a 12-in. wall, the inner wythe was laid up one course, and the space between the wythes filled with grout in which the bricks in the center wythe are floated. Specifications provided that all bricks be laid with full head and bed joints (Guard, 1954). Figures 5-3 and 5-4 show details of piers and wall-to-beam connections. Basement walls are 12-in. reinforced concrete, while all walls constructed above basement are constructed of 13-1/2-in. reinforced moderate weathering brick of mortar type M with the following properties:

Compressive strength of brick	2500 psi
Compressive strength of masonry prism	1500 psi
Minimum steel ratio	0.0024
Designed according to 1951 Los Angeles City code	

5.3 MODELING PROCEDURE

This structure was modeled using TRI/SAC code (AA, 1976). Shear walls and floor slabs were modeled by plate elements, while columns were modeled by beam elements. In all, the model utilized 225 plate elements and 159 beam elements and has 202 nodal points (Fig. 5-5).

The most critical stresses due to earthquake motions should occur near the ground floor level. Therefore, the reinforced brick shear wall elements of the first floor, which is located directly above the reinforced concrete basement, are expected to experience the highest stresses in masonry in this building. Additional data on the model are given in Appendix B.

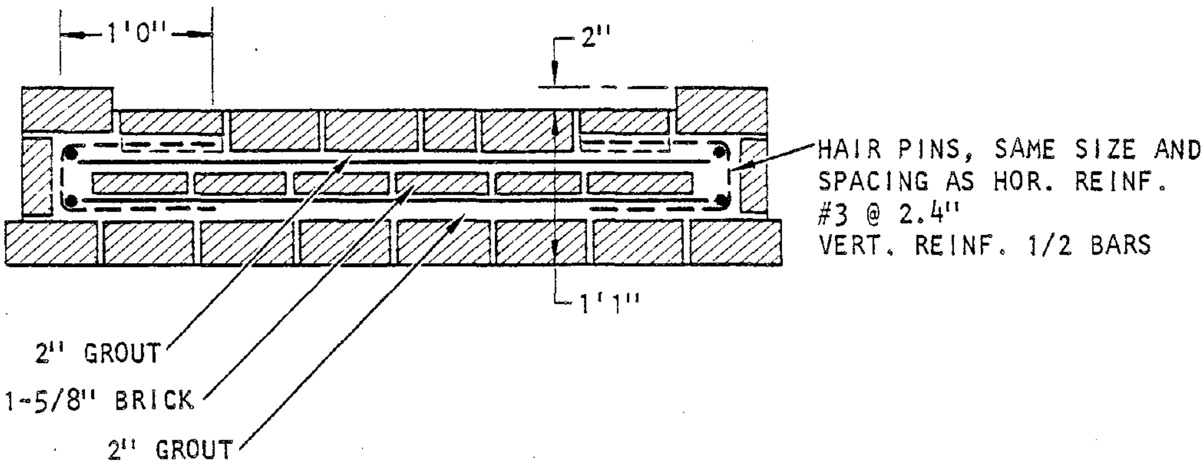

FIGURE 5-3. PIER SECTION SHOWING TYPICAL DETAIL AT JAMBS FOR 13" BRICK WALLS

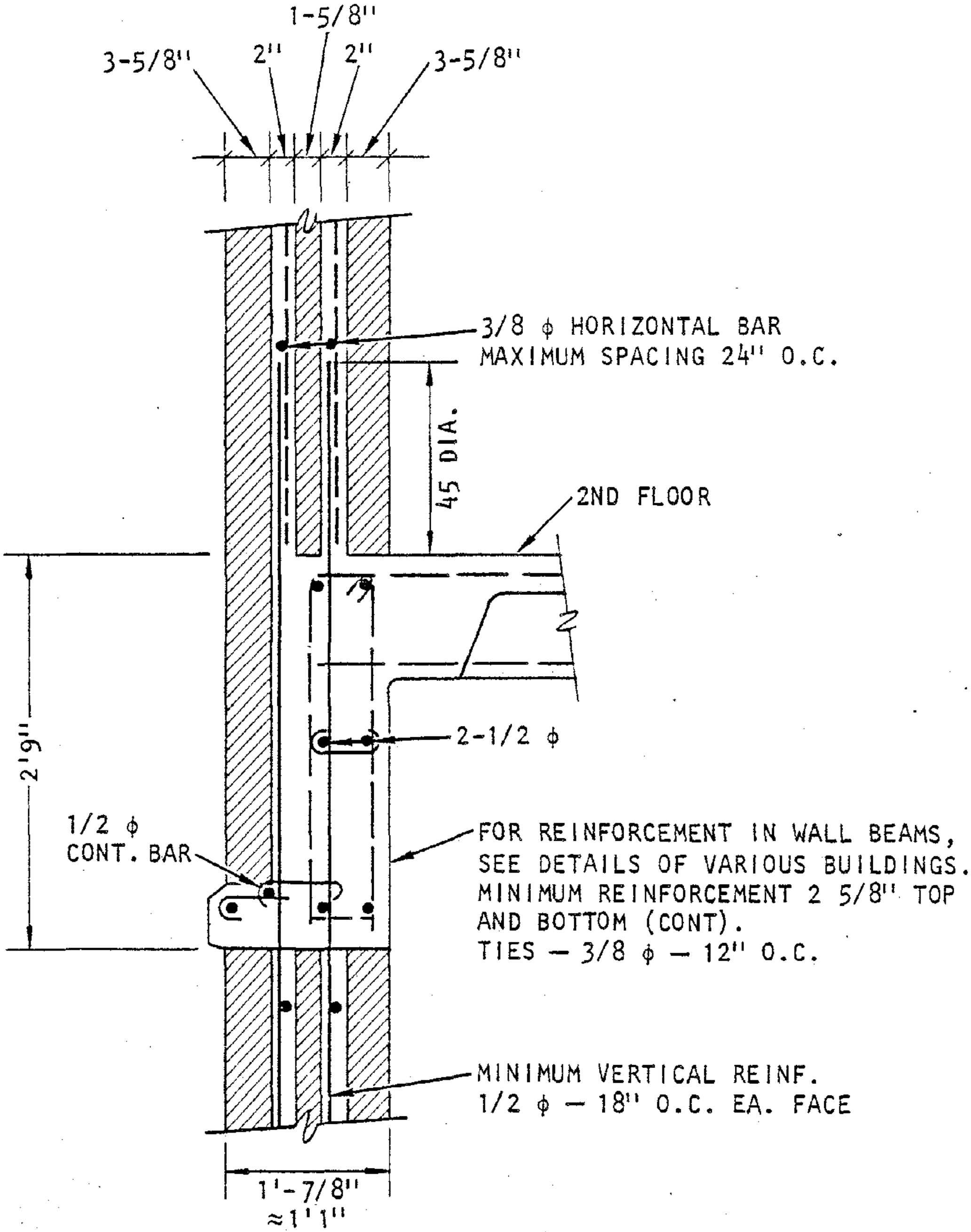

FIGURE 5-4. TYPICAL DETAIL OF WALL-BEAM (AS BUILT, 1954)

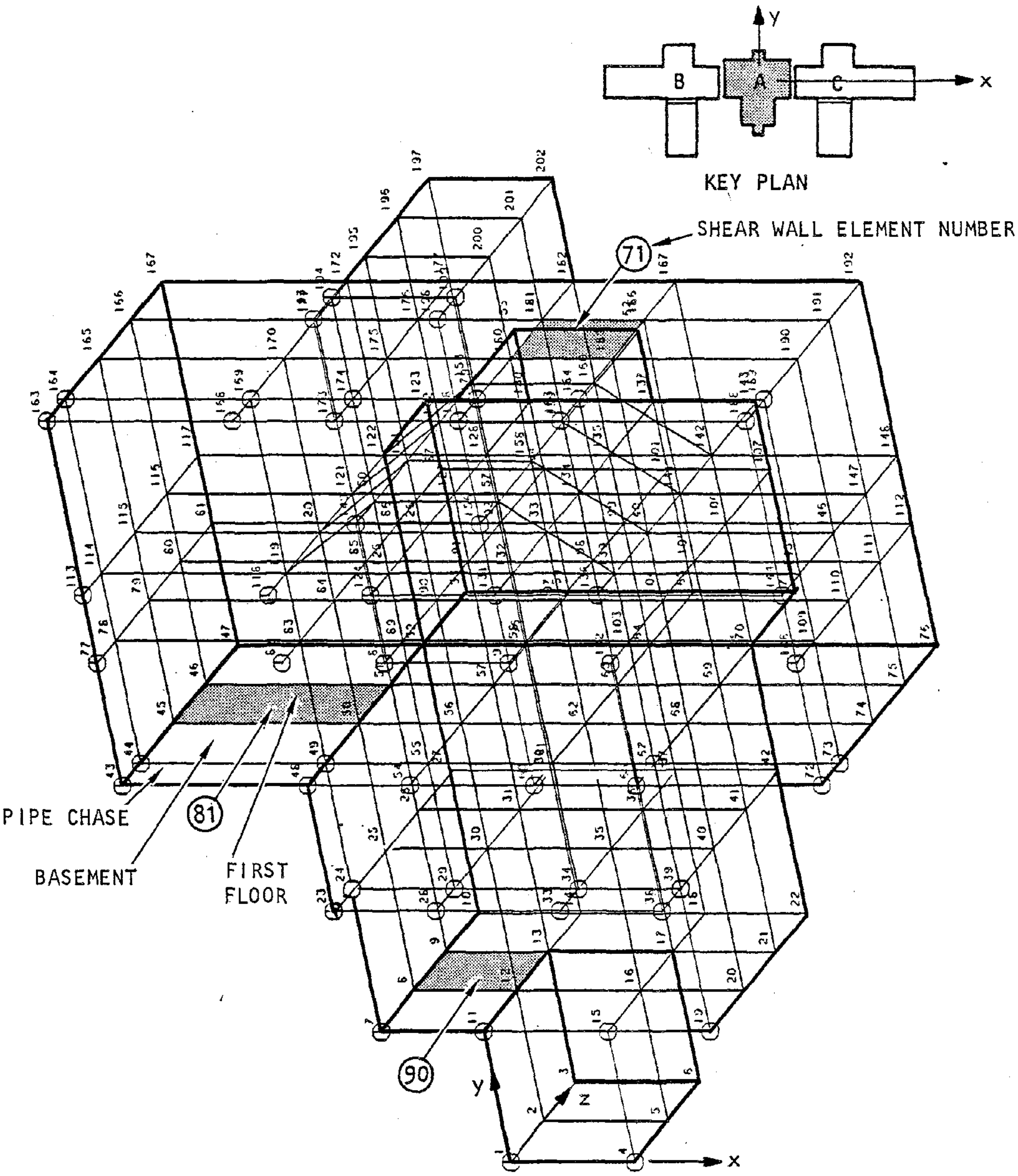

FIGURE 5-5. BUILDING 10A: FINITE ELEMENT MESH

A second model of Building 10 is shown in Figure 5-6. This model includes Segment A, which is shown in Figure 5-5, in addition to Segments B and C, which are assumed to be tied to Segment A. This model represents the condition of Building 10 without expansion joints. Segment A is represented by the same refined mesh shown in Figure 5-5. However, Segments B and C are presented by a smaller number of elements and nodal points. This simplification was dictated by the need to stay within storage capacity of the computer and to reduce the cost of running a three-dimensional finite-element model, while preserving the same refinement for Segment A to compare responses under both conditions. The combined model of Building 10 comprises 353 plate elements, 183 beam elements, and 314 nodal points.

5.4 MODAL RESPONSE

The first 10 natural mode shapes and frequencies of response of Buildings 10A and 10 were included in the calculations. The first three significant frequencies and modes are described in Table 5-1. The corresponding mode shapes are shown in Figures 5-7 through 5-12.

It is significant to note that the first natural mode of Segment A was in the x-direction. A frequency of 9.0 Hz is associated with this mode. However, when Segments A, B, and C were tied together, the overall weaker direction switched to the y-axis direction. Since the three segments, when tied together, comprise a very long building in the x-direction, the average stiffness of the assemblage in the direction of the x-axis was lower than the stiffness of Unit A in the direction of the y-axis. Therefore, the fundamental frequency of the assemblage was 7.3 Hz as compared to the 9 Hz calculated for Segment A.

5.5 COMPUTED STRESSES

Critical stress conditions were computed for the three components of the scaled 1971 Orion ground motions. High stresses were calculated for some elements of Building 10A model. However, as illustrated in Section 7, these stresses were not great enough to cause major cracks in the structure (Table 5-2). The stresses resulting from analysis using the second model of Building 10, where Segments A, B, and C are tied together, indicate a considerable stress increase in some elements (Table 5-2). These results are evaluated in more detail in Section 7.

TABLE 5-1. CALCULATED FREQUENCIES AND MODE SHAPES FOR BUILDING 10

Mode No.	Frequency, Hz	Description
1	9.0	First mode in X direction
2	12.0	Displacements in N-S and E-W directions; complex deformation pattern
3	14.0	First mode in Y direction

(a) Frequency of Building 10A (with Expansion Joints — segment A only)

Mode No.	Frequency, Hz	Description
1	7.3	First mode in Y direction
2	8.3	Twisting mode of building
3	10.5	First mode in X direction

(b) Frequency of Building 10 (segments A, B and C tied together)

TABLE 5-2. COMPARISON OF STRESSES IN BUILDING 10 WITH AND WITHOUT EXPANSION JOINTS

El. No.	σ_y					σ_x		S_{xy}		Principal Stresses			
	Dead Load	Seismic		Total						σ_1†		σ_2†	
		1	2	1	2	1	2	1	2	1	2	1	2
71	31.2	4.9	17.4	36.1	48.6	2.6	7.0	84.9	109.4	146.7	190.2	-110.6	-141.6
81	27.5	19.2	1	46.7	28.5	4.5	19.9	94.0	141.6	166.3	227.6	-119.6	-199.1
90	30.0	5.9	19.8	35.9	49.8	3.8	8.4	81.3	115.4	141.2	199.8	-105.3	-150.0

(-) Sign denotes tension

* Stresses are in psi

1 Building with expansion joints (existing configuration)

2 Building without expansion joints (Parts A, B, and C tied together)

† $\sigma_{1,2} = \frac{\sigma_y}{2} \pm \sqrt{\left(\frac{\sigma_y}{2}\right)^2 + \left(1.5\ S_{xy}\right)^2}$

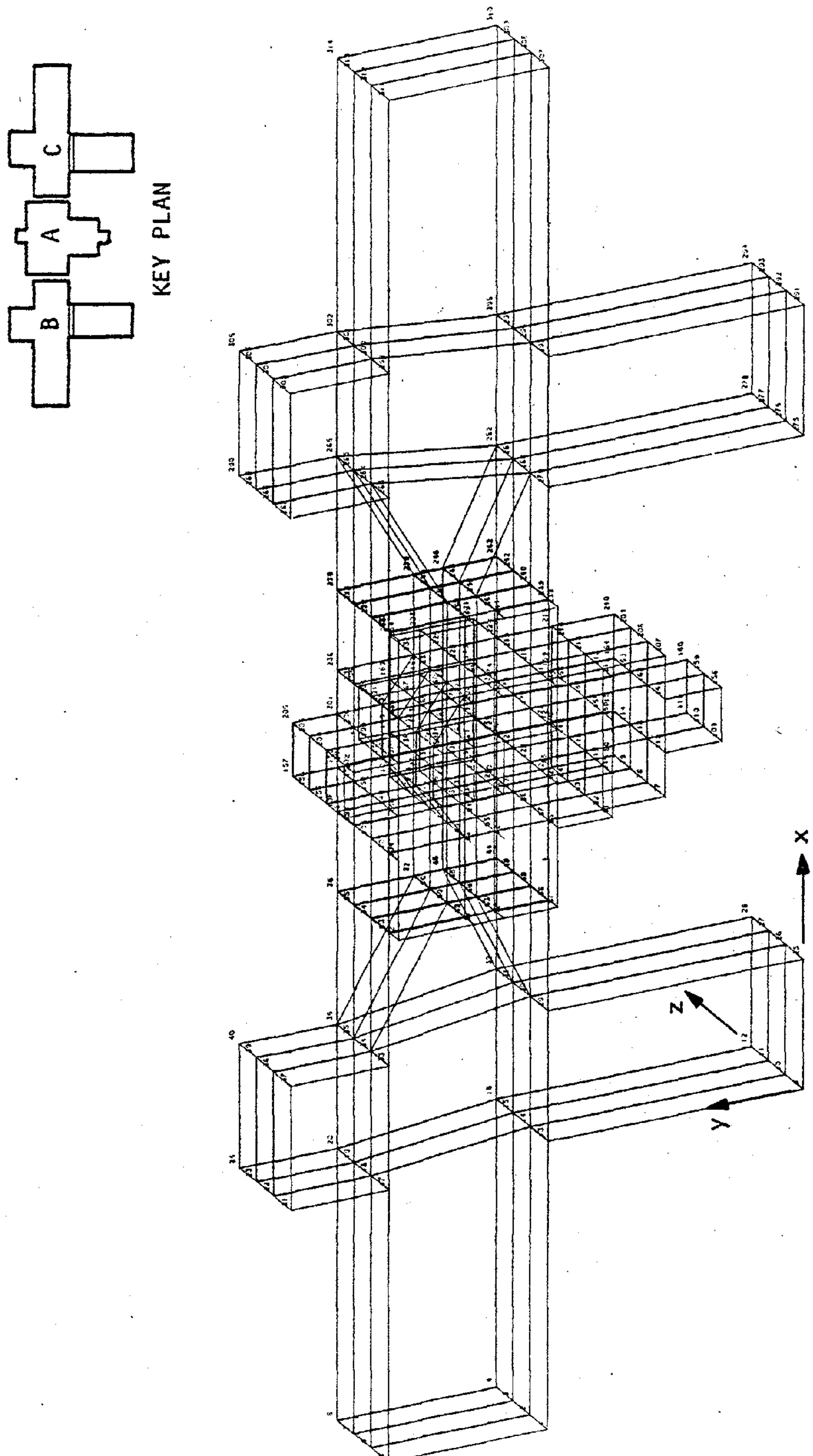

FIGURE 5-6. FINITE ELEMENT MODEL BUILDING 10 SEGMENTS A, B AND C TIED

Reproduced from best available copy.

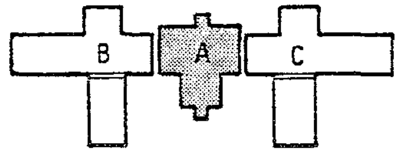

KEY PLAN

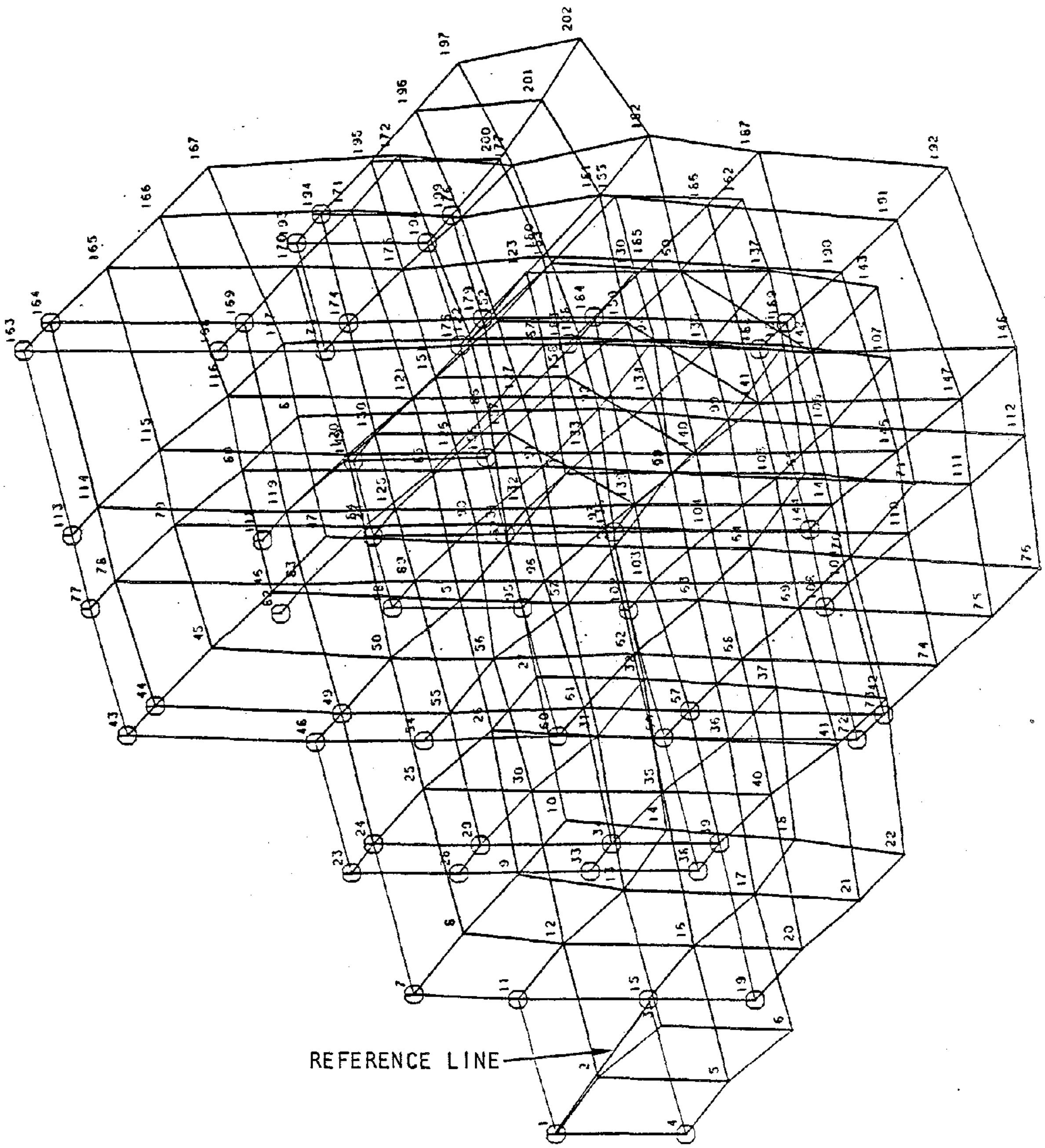

FIGURE 5-7. BUILDING 10A: MODE 1

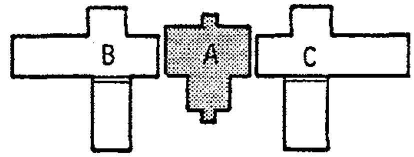

KEY PLAN

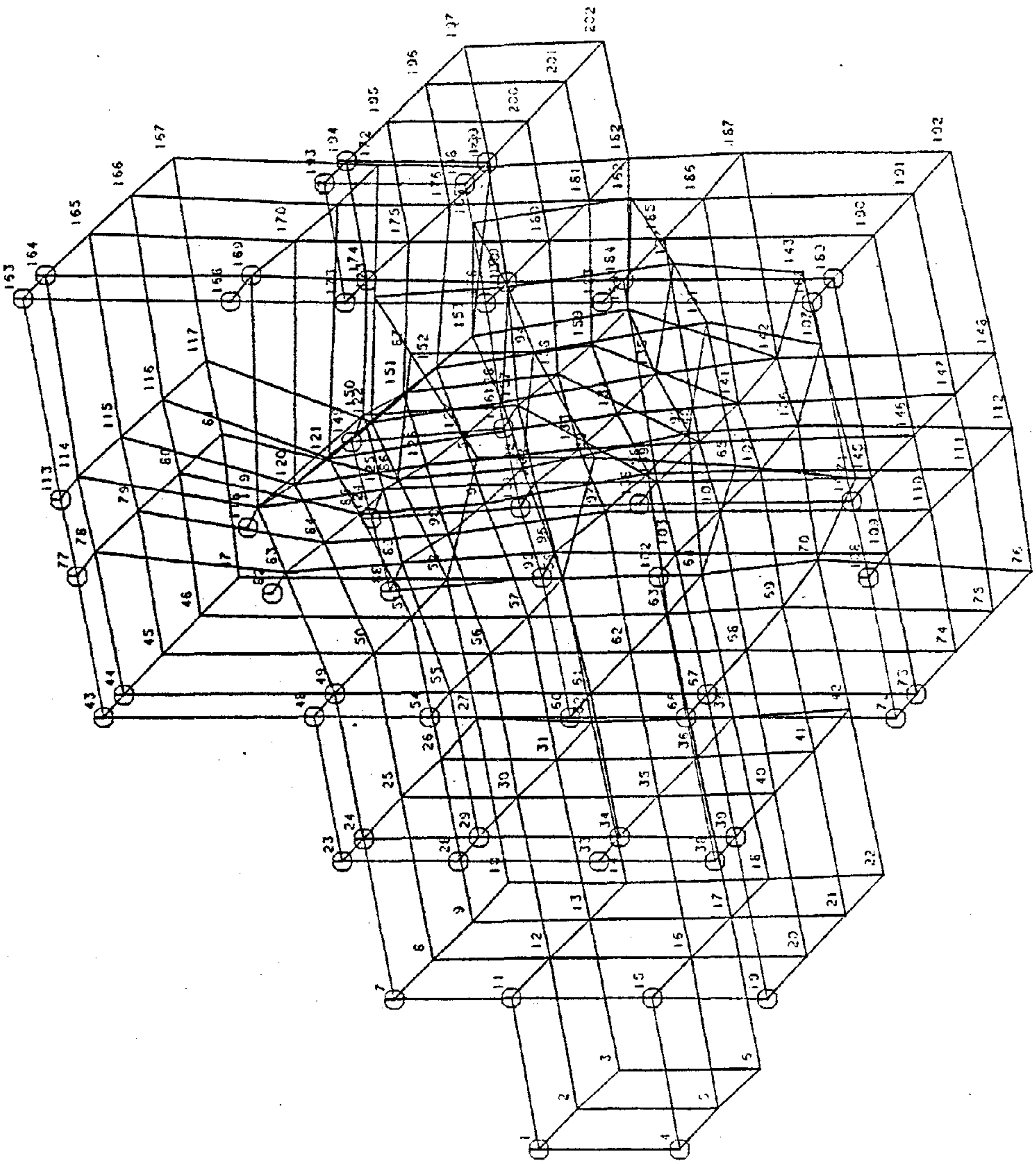

FIGURE 5-8. BUILDING 10A: MODE 2

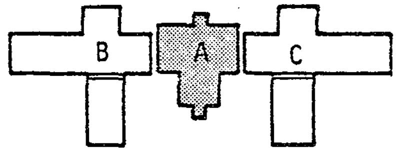

KEY PLAN

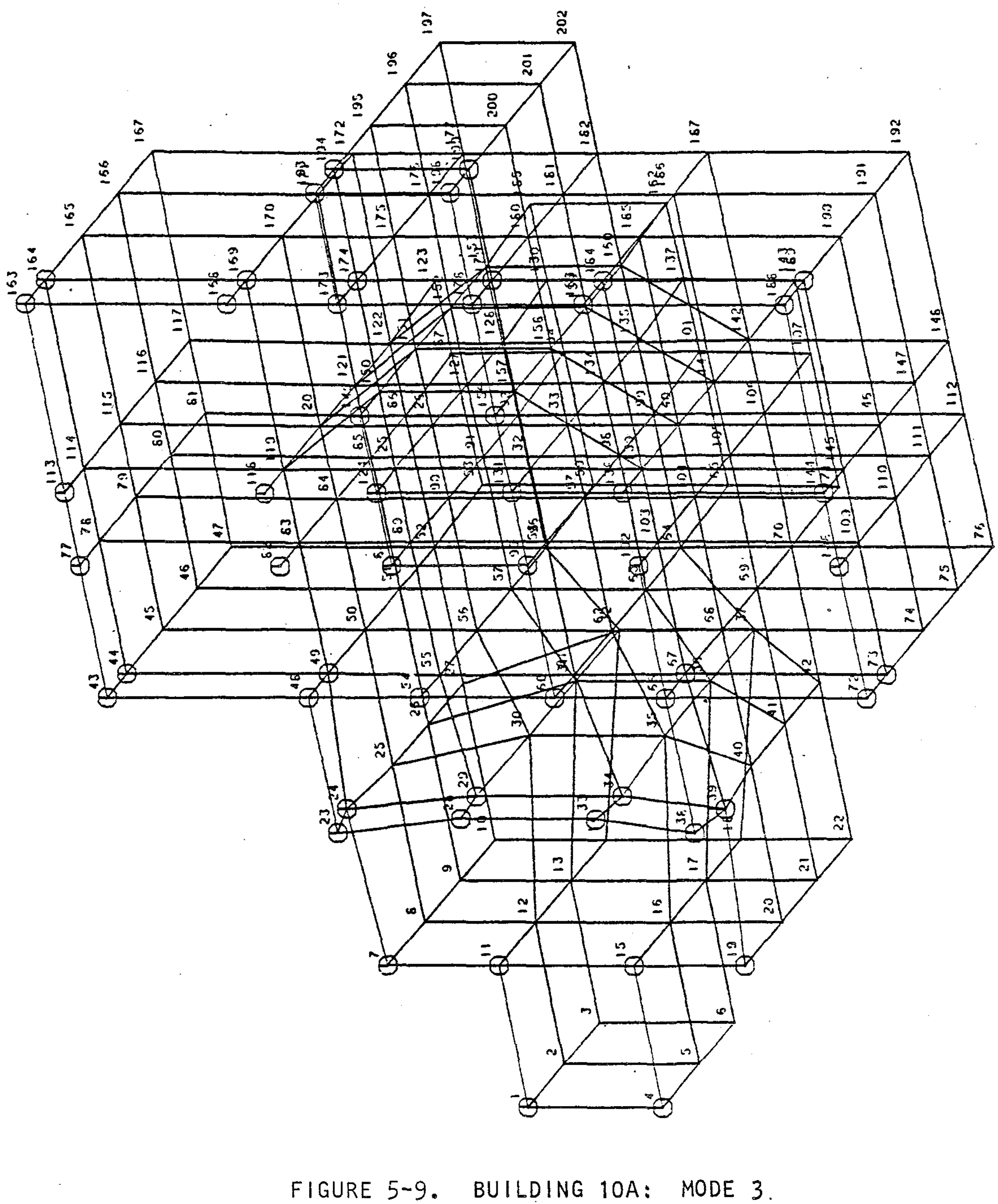

FIGURE 5-9. BUILDING 10A: MODE 3.

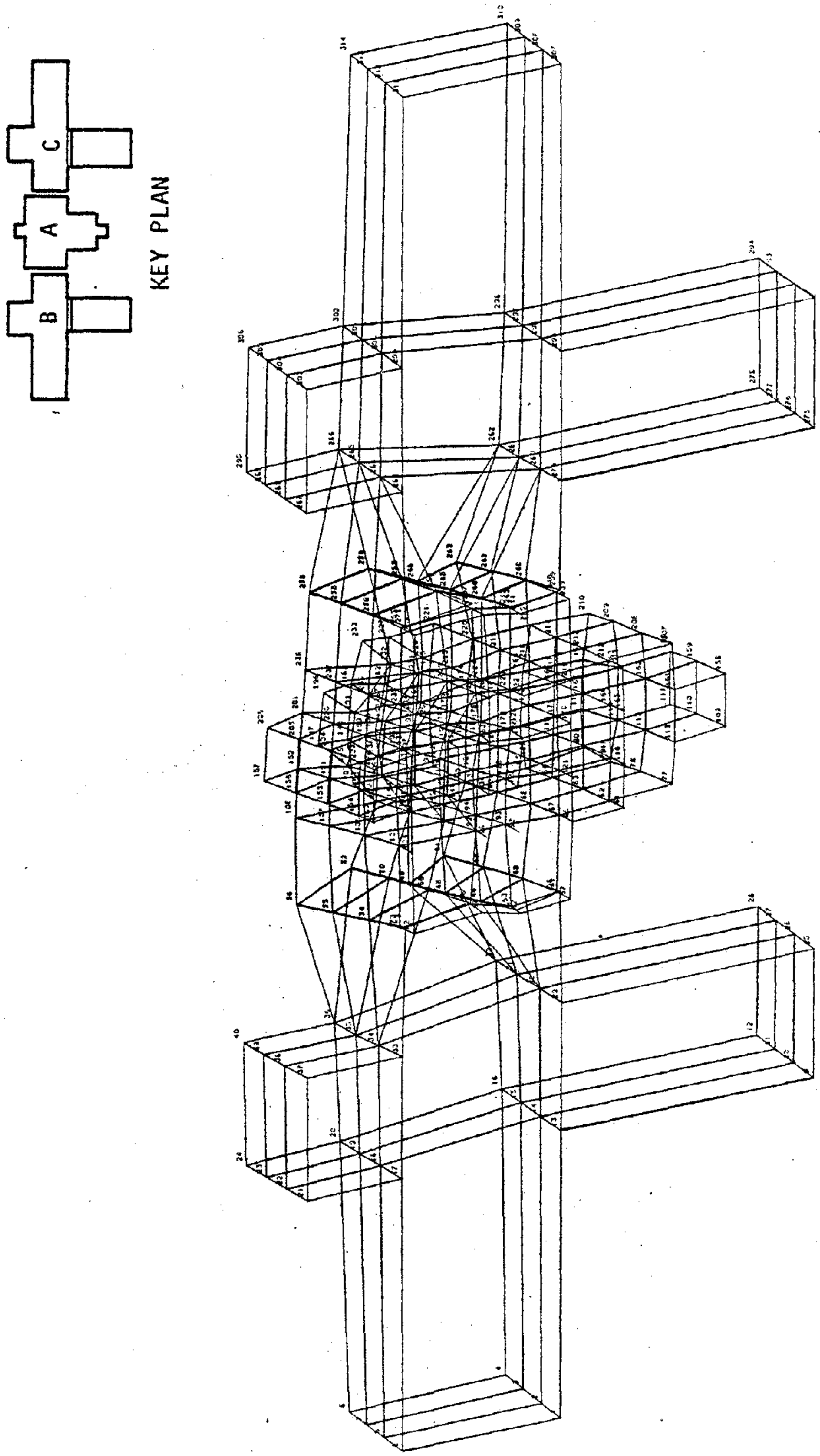

FIGURE 5-10. BUILDING 10: MODE 1

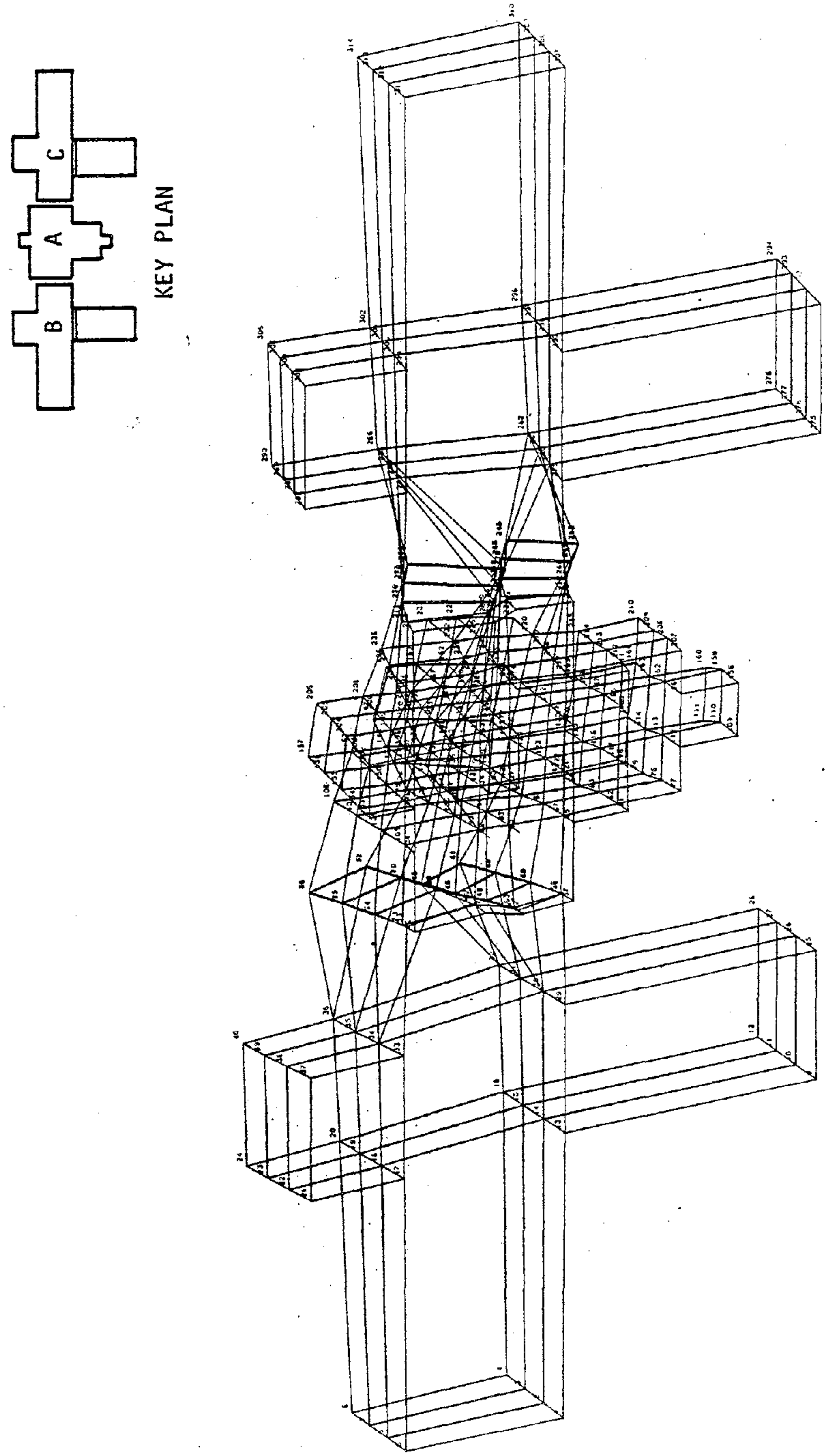

FIGURE 5-11. BUILDING 10: MODE 2

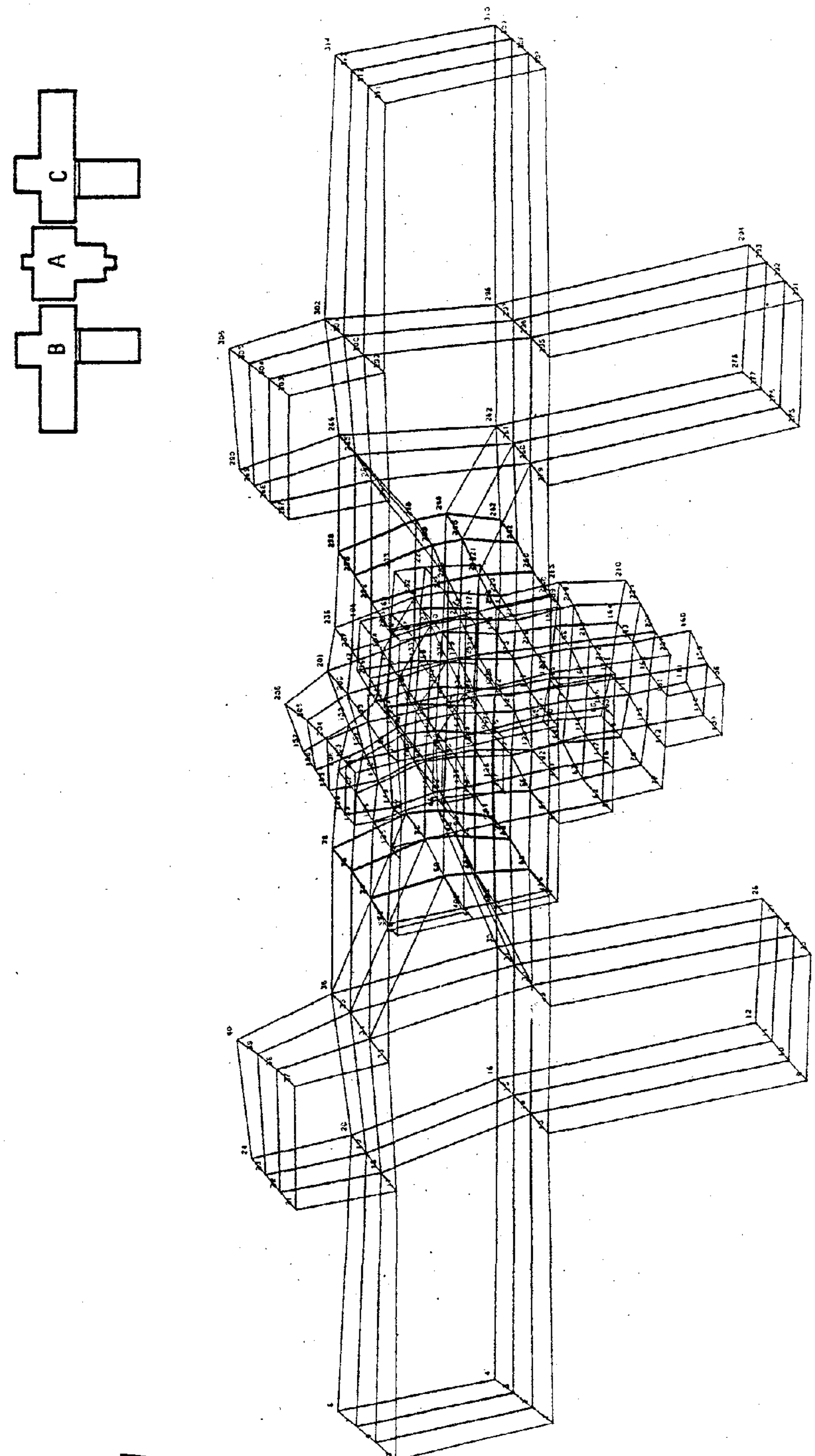

FIGURE 5-12. BUILDING 10: MODE 3

Reproduced from
best available copy.

SECTION 6

BEHAVIOR OF BRICK MASONRY WALLS UNDER SEISMIC LOADING

6.1 INTRODUCTION

Brick masonry walls considered in this report are of multistory construction and must function in both shear and bending. One of the important requirements of the study is to provide a failure criteria for such walls when subjected to seismic loads.

In contrast to the large number of tests on the compressive strength and behavior of concrete masonry walls and prisms, little is presently known about the behavior of joints under combined shear and compressive normal stress distribution. Available experimental data are restricted entirely to initial joint failure (first cracking, or load decrease) in unreinforced, ungrouted, hollow concrete masonry. Most data concern compressive normal stress distributions rather than tensile. Little is known about postcracking or postelastic behavior of joints.

A representative cross section of the current literature on joint behavior is given by Young et al. (1972), Self (1974), Balachandra (1974), Hedstrom (1966). In an effort to supplement the existing literature on joint behavior, wall panels, and piers, two major experimental studies were initiated (Hegemier, 1975; Mayes and Clough, 1975) in conjunction with the masonry program at the University of California, San Diego (UCSD) and University of California, Berkeley (UCB) campuses. In these studies, joint planes were subjected to constant levels of (average) normal stress and either static or dynamic (average) shear stress. Behavior of concrete masonry under biaxial stresses was also studied at UCSD, while piers were studied at UCB. Selected portions of these studies are presented herein. This section is concluded by providing recommendations for shear and biaxial failure criteria for evaluation of the earthquake response of the Sepulveda Hospital.

6.2 STRENGTH OF BRICK JOINTS UNDER COMBINED COMPRESSION AND SHEAR

In the case of brick, the classical joint tests are the couplet tests of Benjamin and Williams (1958). Their test setup and findings are illustrated in Figures 6-1 and 6-2. The tests showed little or no influence of brick and mortar compressive strengths on the couplet bond strengths in tension and shear.

Shear strength of mortar joints is greatly affected by the normal stress acting on the joint. Tests indicate that a nearly Coulomb type of behavior occurs at failure in mortar and concrete materials. The curves in Figure 6-2 were compiled from the results of tests using these loading arrangements. An average Coulomb relationship for the strength of the mortar joint is given in Figure 6-2 as follows:

$$S_{xy} = R + 1.1\ \sigma_y \qquad (6\text{-}1)$$

where

- S_{xy} = Shearing resistance of the mortar joint (psi)
- R = Shearing resistance of the mortar joint for zero normal stress (psi)
- σ_y = Normal stress acting on the joint; compressive stress taken as positive (psi)

An average value for R of about 230 is indicated in Figure 6-2. In this equation, S_{xy} is the maximum shearing stress developed on the section and should be multiplied by two-thirds to obtain the average stress on the joint.

Test results shown in Figure 6-2, as well as other tests on concrete and mortar materials, indicate that the failure envelope is nonlinear, particularly in the low normal stress range. Therefore, careful examination of data plotted indicates that Equation 6-1 with $R = 230$ is only applicable when the normal stress is compressive and is greater than about 60 psi.

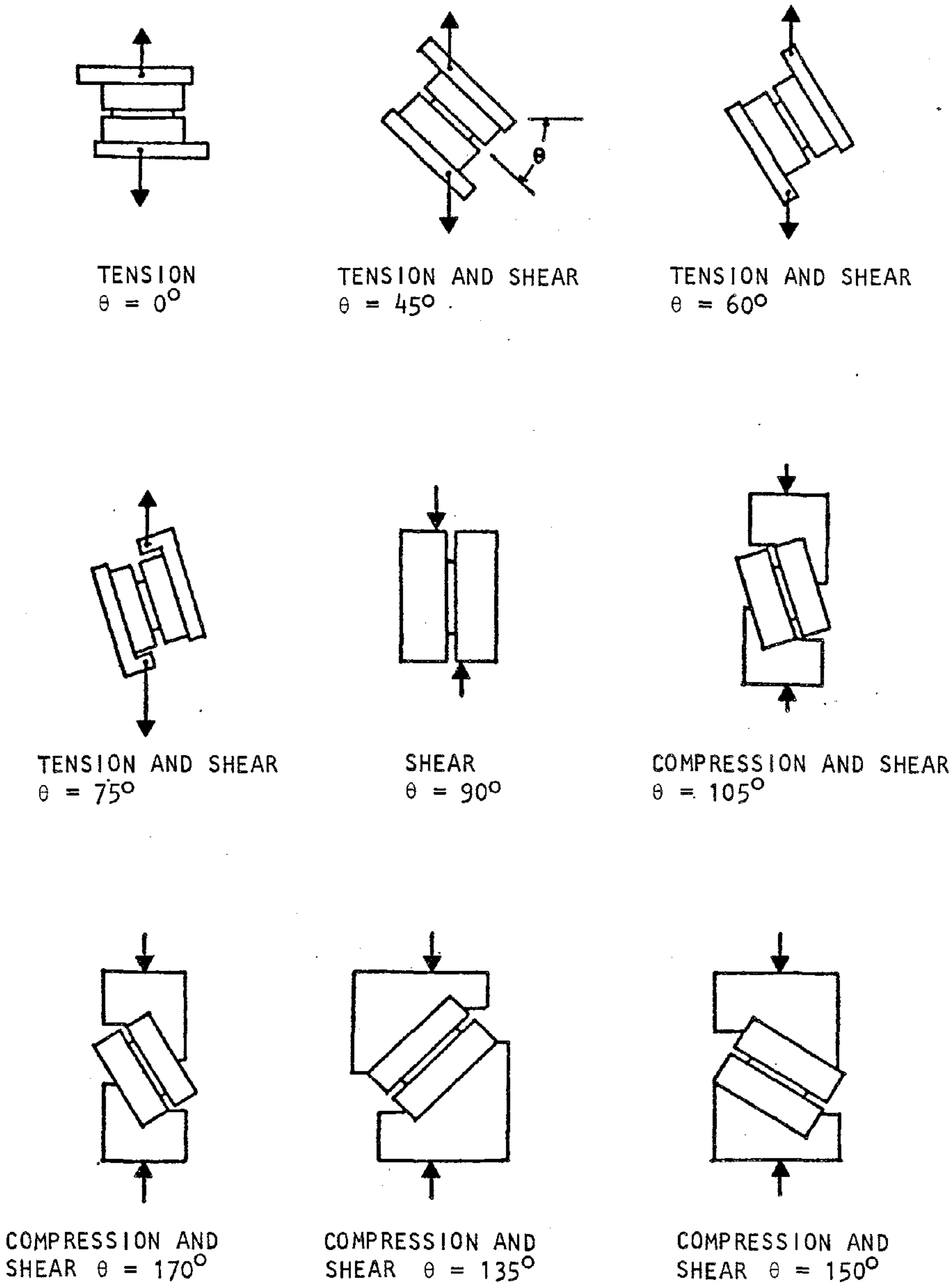

FIGURE 6-1. ARRANGEMENTS FOR COMBINED STRESS TESTS OF MORTAR JOINT (Benjamin and Williams, 1958)

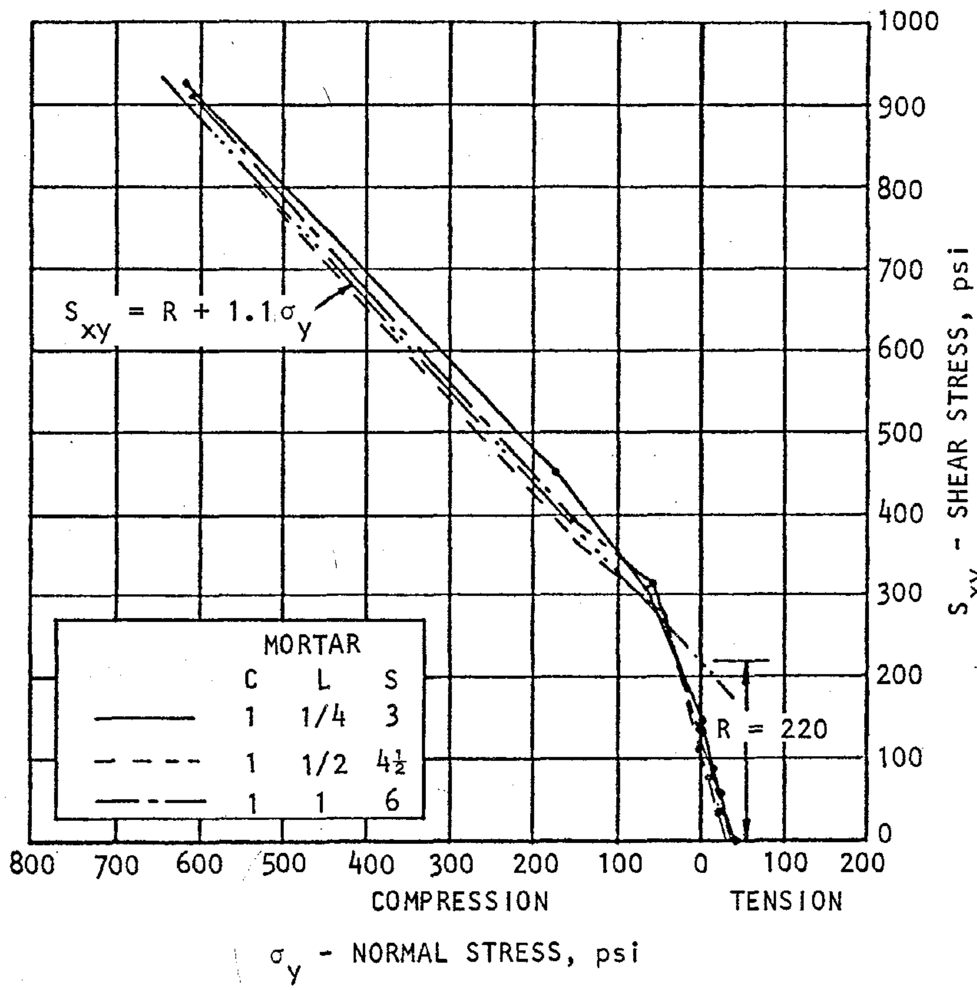

FIGURE 6-2. COMBINED STRESS COUPLET STRENGTH CURVES (Benjamin and Williams, 1958)

Haller (1969), adopting the test setup shown in Figure 6-3, arrived at an empirical relation for normal quality masonry consisting of cored brick and cement-lime-sand and mortar. The Haller formula, when approximated to a linear relation, results in the following formula:

$$S_{xy} = 50 + 0.88\ \sigma_y \quad \text{for} \quad \sigma_y < 200 \text{ psi compression} \tag{6-2}$$

where σ_y and S_{xy} are in psi. For special quality brick, Haller's relationship can be approximated to the following formula:

$$S_{xy} = 160 + 1.0\ \sigma_y \tag{6-3}$$

Equations 6-1, 6-2, and 6-3 are plotted to the same scale in Figure 6-4.

Yorulmaz and Sozen (1967) tested masonry specimens of model bricks of the type shown in Figure 6-5. A line fitting these tests would follow the equation

$$S_{xy} = 150 + 0.46\ \sigma_y \tag{6-4}$$

This equation is plotted in Figure 6-4.

Experimental studies at the University of California, San Diego on concrete block masonry included joint planes that were subjected to constant levels of (average) normal stress and (average) shear stress (Hegemier et al., 1978). Test specimens in the joint test series consisted of triplets, i.e., three blocks and two interfaces. Typical specimens are illustrated schematically in Figures 6-6 and 6-7. The complete test series included: (1) ungrouted bed joints, (2) grouted bed joints, (3) grouted bed joints with steel, (4) head joints, and (5) combination of head and bed joints with and without steel.

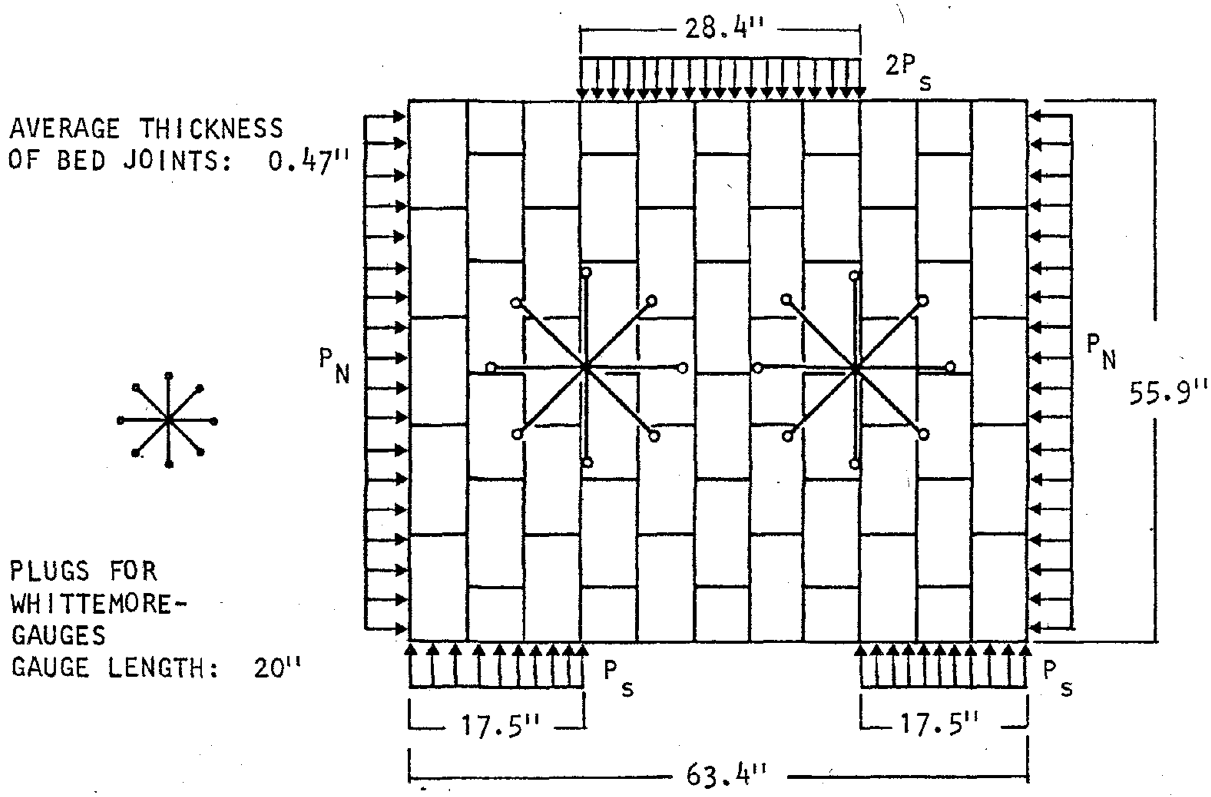

FIGURE 6-3. TEST SPECIMEN ADOPTED BY HALLER (1969)

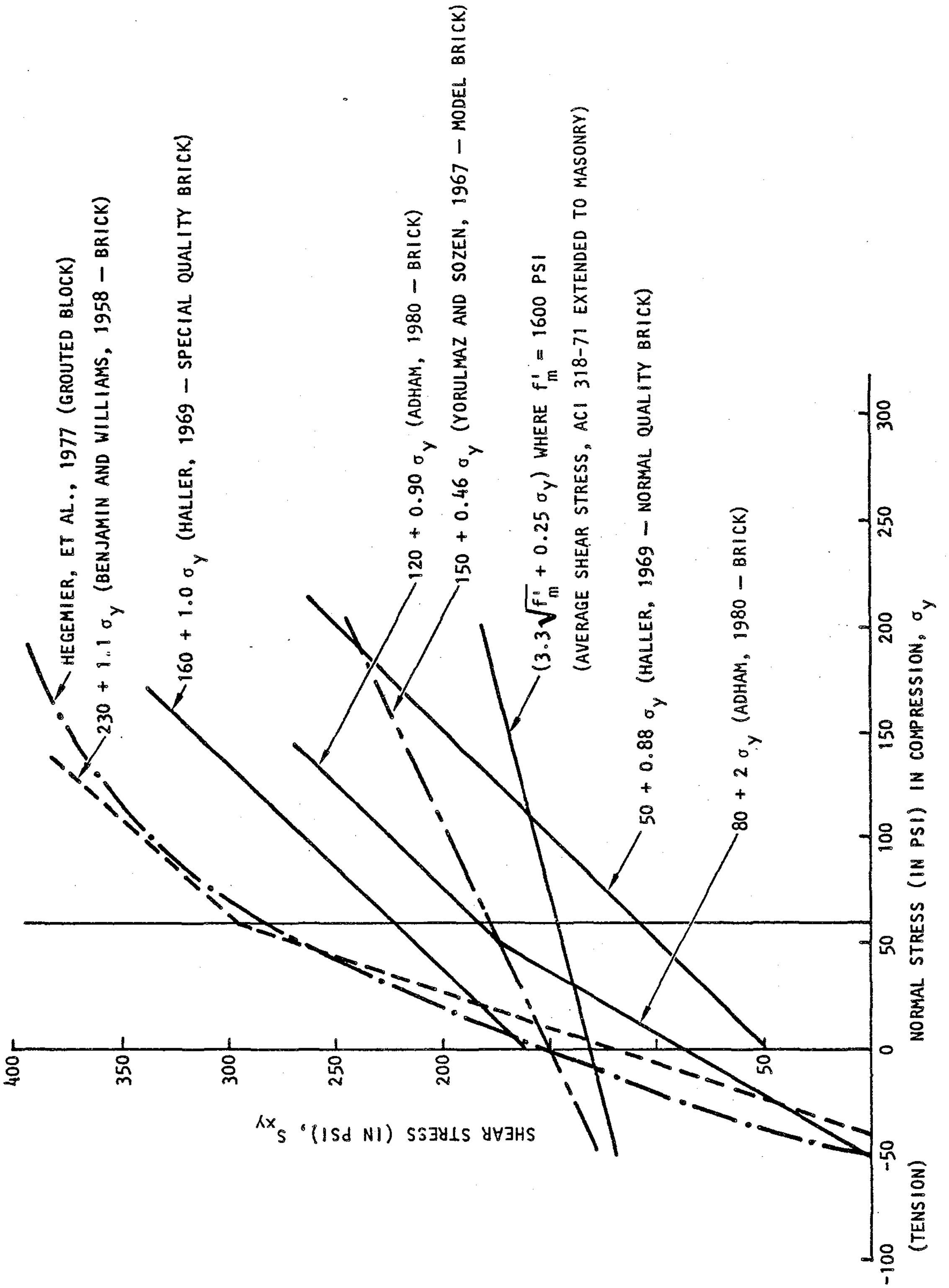

FIGURE 6-4. EFFECT OF NORMAL STRESS ON CRITICAL SHEAR STRESS

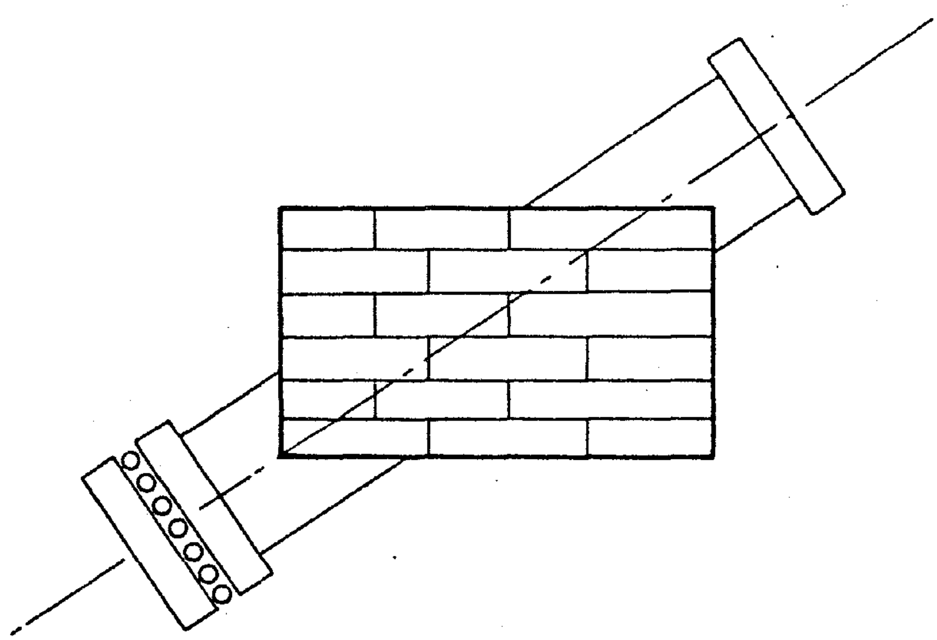

FIGURE 6-5. TYPE OF TEST SPECIMENS USED BY YORULMAZ AND SOZEN, 1967

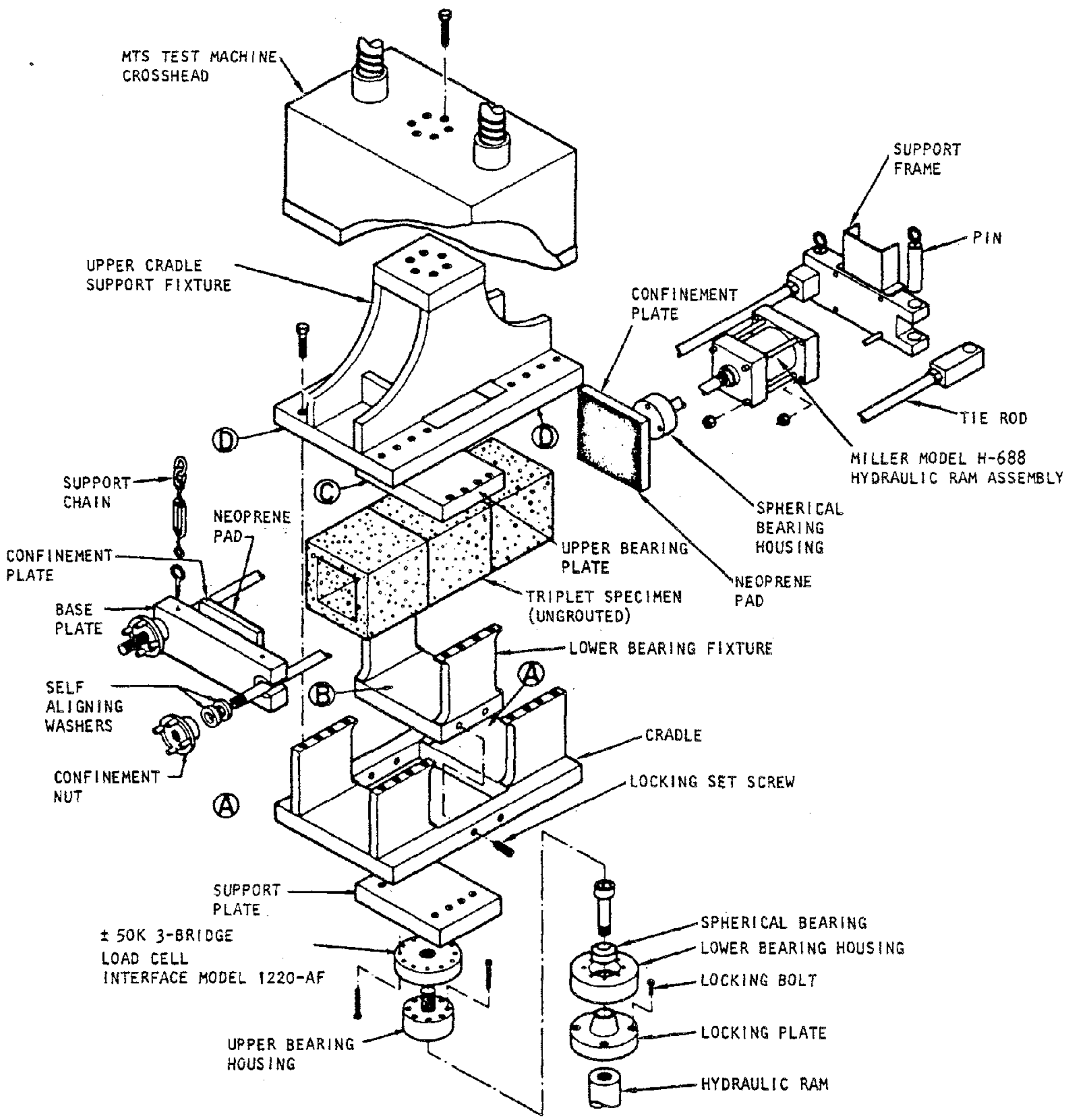

FIGURE 6-6. EXPLODED ISOMETRIC VIEW OF THE CYCLIC TRIPLET — TEST FIXTURE (Hegemier et al., 1987)

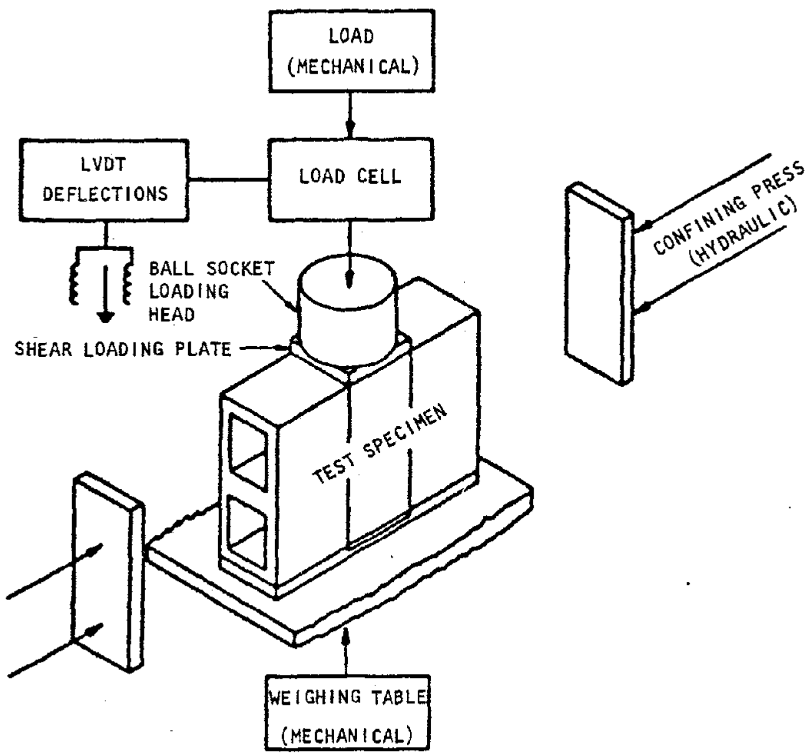

FIGURE 6-7. MECHANICAL SCHEMATIC — MONOTONIC TRIPLET TEST (Hegemier et al., 1978)

Figures 6-8 and 6-9 exemplify typical behavior of head joints and grouted and ungrouted bed joints. The following basic characteristic of such joints is noted: joint fracture strength increased monotonically with precompression up to a block-failure transition (the maximum shear stress vs. normal stress as shown in Figs. 6-8 and 6-9). For grouted bed joints, the solid curve shown in Figure 6-8 represents a parabolic, least-square fit of the data for $\sigma_y \geq 0$ and linear fit for $\sigma_y \leq 0$. Data on grouted joints were selected for comparison with data on brick and are replotted in Figure 6-4 for comparison.

6.3 RECOMMENDED FRACTURE CRITERION BASED ON INTERACTION OF SHEAR AND NORMAL STRESSES

Figure 6-4 provides comparison of data provided by different investigators. It is of interest to note that the ACI 318-71 formula for average critical shear stress as a function of normal stress can be extended to masonry by substituting compressive strength of masonry at 28 days, f'_m, for specified compression strength of concrete, f'_c. This formula was plotted in Figure 6-4 for f'_m of 1600 psi, which is the value assigned to brick masonry construction at the Sepulveda Hospital.

Analysis of data plotted in Figure 6-4 indicates that an average relationship can be derived from the above results. This relationship can be simplified to a piece-wise linear formula as follows:

$$S_{xy} = 80 + 2\sigma_y \qquad \text{for} \quad \sigma_y \leq 50 \qquad (6\text{-}5a)$$

$$S_{xy} = 120 + 0.9\,\sigma_y \qquad \text{for} \quad \sigma_y > 50 \qquad (6\text{-}5b)$$

The factor 0.9 in Equation 6-5b was recommended by Hegemier et al. (1978). This formula will be used in this study to check the performance of brick masonry shear walls of Building 10 during the 1971 San Fernando earthquake.

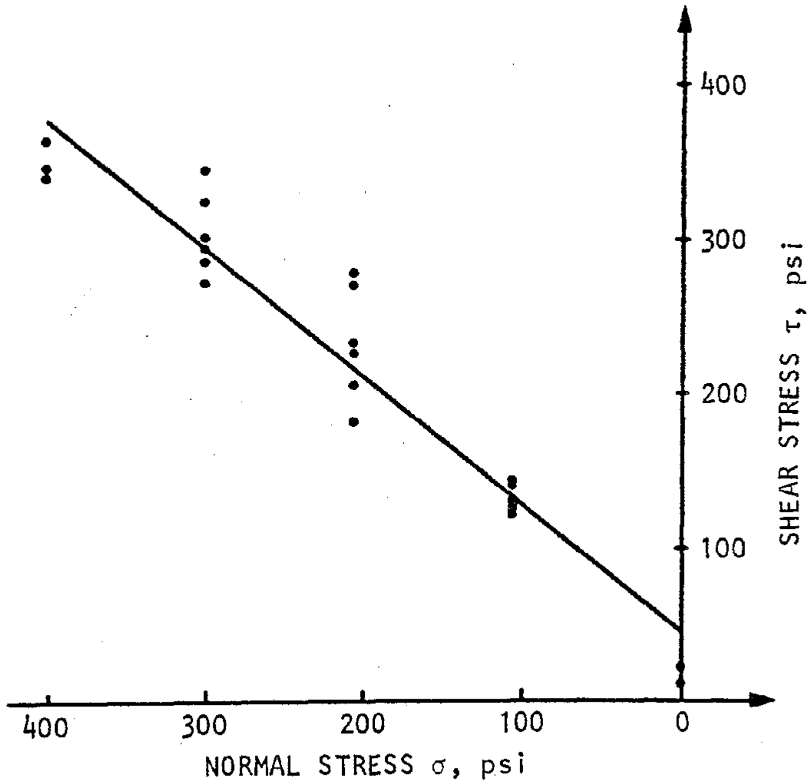

FIGURE 6-8. FAILURE ENVELOPE FOR HEAD JOINTS — HALF-BLOCK TRIPLETS (Hegemier et al., 1978)

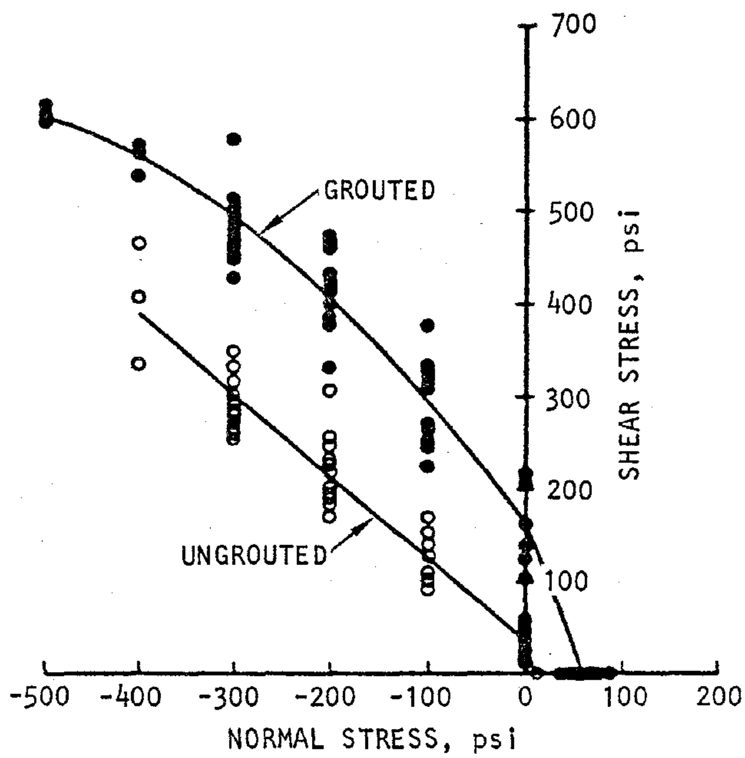

FIGURE 6-9. FAILURE ENVELOPE FOR BED JOINTS — HALF-BLOCK TRIPLETS (Hegemier et al., 1978)

6.4 FAILURE CRITERION FOR BRICK MASONRY UNDER BIAXIAL STRESSES

Biaxial panel tests conducted by Hegemier et al. (1978) represent a critical step in the continuum modeling process. A schematic of the biaxial test procedure is shown in Figure 6-10. Experimental data revealed weak dependence of strength on the layup angle θ, i.e., the masonry under consideration is approximately isotropic. Initial macrocracking stress surface was not significantly influenced by steel/masonry area ratios of 0.00176 or less. The Von Mises yield criterion is used for failure in compression, and the maximum tensile stress theory is adopted for cracking due to tension. Hegemier et al. (1978) assumed the failure criteria shown in Figure 6-10. This curve results from the intersection of the Von Mises cylinder in principal stress space with (σ_1, σ_2) principal stress plane. The material is assumed elastic and isotropic before the yield curve is reached.

The maximum tensile stress f'_t was found by Hegemier et al. (1978) to be approximately 0.095 f'_m. However, for simplicity, a factor of 0.10 was used. A similar factor was used by Adham et al. (1975) to study biaxial behavior of concrete. The criterion illustrated in Figure 6-10 will be used to assess the biaxial state of stress of shear walls of Building 10.

6.5 DAMAGE MODEL FOR QUALITATIVE ANALYSIS OF MASONRY BUILDINGS

Failure patterns of unreinforced masonry buildings that were damaged severely by the San Fernando earthquake are quite repetitive, with variations mainly in degree (Abel, 1973). These patterns are similar to those observed in all past moderate to severe earthquakes affecting this kind of construction and are valuable tools for qualitative estimates of performance of reinforced masonry buildings. These following patterns are used in Section 7 to provide

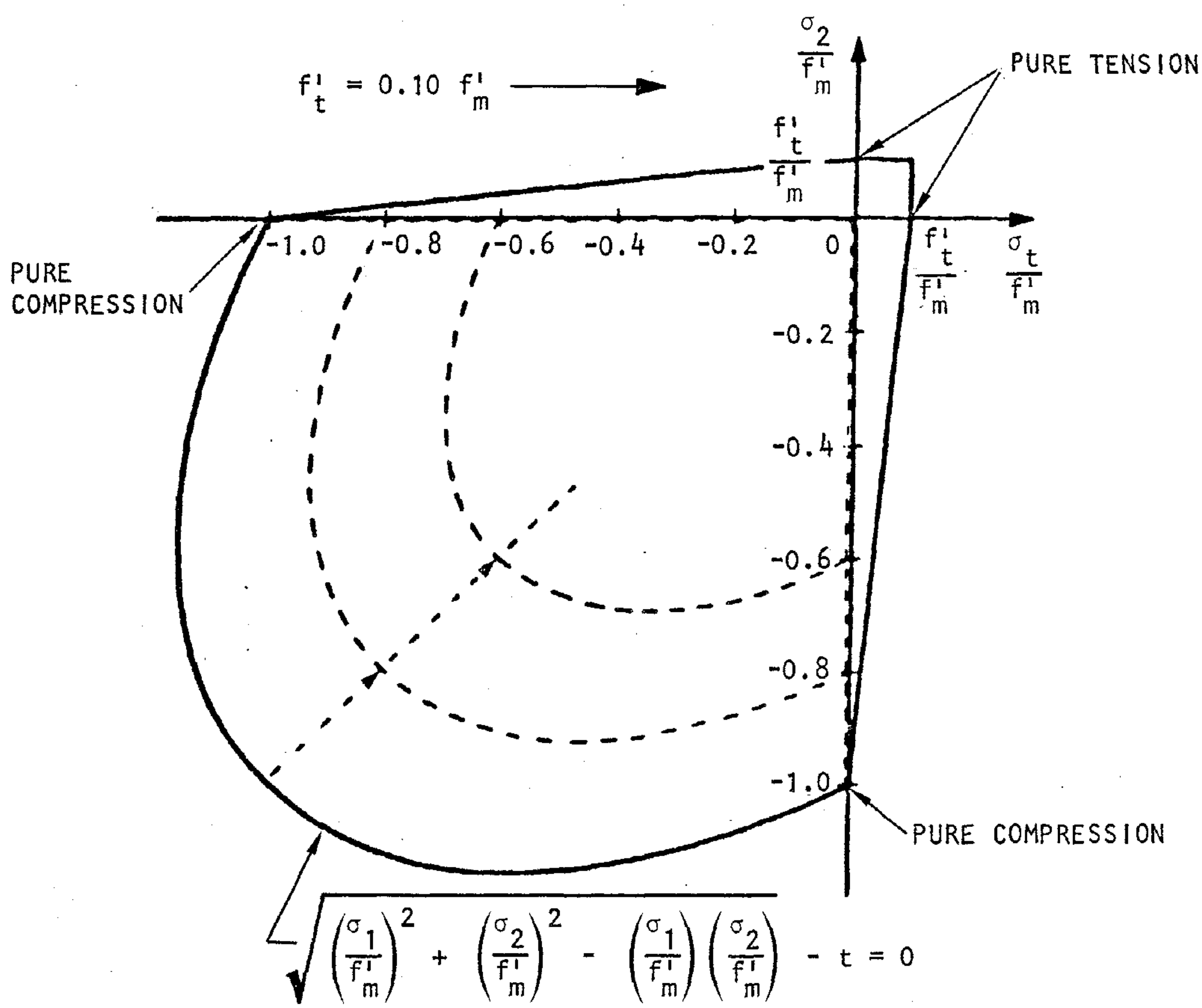

FIGURE 6-10. BIAXIAL FAILURE CRITERIA FOR BRICK MASONRY (Adapted from Adham et al., 1975 and Arya and Hegemier, 1978)

qualitative assessment of the response of the Sepulveda Hospital buildings during the San Fernando earthquake:

a. Typically, the wall moved in both the transverse (perpendicular to wall) and the longitudinal directions, with the former indicated by movement away from the building and the latter by diagonal cracks emanating from corners of window and wall openings. These cracks, which indicate diagonal tension failure, were not consistent in orientation, indicating reversals in direction of the inertial forces.

b. In some cases where openings were localized in one portion of the wall, more severe cracks were located in the more solid portion of the wall, indicating that prior to failure, shear was distributed to the resisting elements in proportion to their stiffness. However, where cracking was at all severe, it was general and throughout the wall area.

c. In the direction perpendicular to the wall, the wall was usually left with a residual movement away from the building, in some cases as much as 2 to 3 in. In those cases of great movement, portions of wall fell out completely, while in other cases, only portions of parapet fell.

d. Typically, there were vertical or inclined tension cracks at the ends where the side wall abutted the end wall, and it is presumed that these cracks were induced by movement of the end wall away from the building.

e. There is some occasional small movement of the side wall away from the floor. Such movement at the roof was concealed and could not be verified, except where major movement and failure had occurred.

f. In several buildings a vertical crack appeared at midlength of the side wall, originating below the ceiling and extending up through the parapet. The extreme result of this type of failure was loss of a portion of parapet or parapet plus wall. It is difficult to ascertain if principal movement in these instances was due to inertial force of the wall itself or to the loads that the deflected roof and floor imposed on the wall. The vertical crack could have been a tension chord failure in which the roof sheathing and walls act as a horizontal load due to the inertial force of the side walls and roof.

It is, perhaps, more likely that the parapet was buffeted inward and outward and, by being stopped short by the roof framing on an inward swing, cracked on this line and subsequently fell. Probably the effects of tension flange cracking and bending failure supplemented each other to produce the more severe failures of side walls.

g. Transverse movement caused pier cracks. The patterns of these cracks are used in Section 7 to provide qualitative assessment of the response of the Sepulveda Hospital buildings during the San Fernando earthquake.

SECTION 7

EVALUATION OF PERFORMANCE OF BRICK MASONRY BUILDINGS AT THE SEPULVEDA HOSPITAL DURING THE 1971 SAN FERNANDO EARTHQUAKE

7.1 INTRODUCTION

Evaluation of the performance of a masonry structure during an earthquake is one of the difficult tasks that a structural engineer faces today. The problem is compounded by lack of data on the performance of masonry structural components during an earthquake. This performance may vary greatly depending on workmanship, damping characteristics, anisotropy of reinforced brick masonry elements, and interaction with other structural components. Therefore, a simplified performance criteria is used to provide a quantitative assessment of building components. In addition, a damage model is used to provide a qualitative assessment of building behavior including flexural connections and construction details.

The performance criteria for assessment of hospital buildings requires examining strength characteristics as follows:

a. Shear strength of shear wall elements
b. Tensile strength
c. Flexural strength
d. Strength of wall-to-floor connections

7.2 SHEAR STRENGTH

7.2.1 PERFORMANCE CRITERIA

Fracture is assumed to depend on maximum shear stress developed in the shear wall panel. Critical shear stress is evaluated based on available information on material properties. Figure 6-4 illustrates the fracture criterion for normal quality brick developed for this study in Section 6.

The expected performance of Building 10 is expressed by the ratio B, which is defined as follows:

$$B = \frac{\text{critical shear stress}}{\text{calculated shear stress}} \qquad (7\text{-}1)$$

A value of B greater than 1.0 indicates that the panel would perform adequately, while a value significantly less than 1.0 would postulate failure of that particular panel.

7.2.2 ASSESSMENT OF STRESSES BASED ON CRITICAL SHEAR STRESS CRITERIA

Table 7-1 lists elements that have critical stresses in Segment A of Building 10. The critical shear stresses are calculated from the state of stress for each element by Equations 6-5 (a,b) and are given in Table 7-1. Performance factors for critical Elements 71, 81, and 90 are 1.8, 1.85, and 1.87, respectively. These factors are larger than 1, indicating that the building had a considerable resistance against failure by this mode from forces generated by the San Fernando earthquake.

7.3 TENSILE STRENGTH

7.3.1 PERFORMANCE CRITERIA

Fracture is assumed to initiate when tensile stresses exceed maximum allowable tensile stresses in a biaxial state of stress. The criteria for interaction between principal tensile stresses σ_2 and the principal compressive stress σ_1 are given in Figure 6-9. The maximum tensile stress is assumed to occur at the center of the panel and is calculated by means of Mohr's circle to be

$$\sigma_{1,2} = \frac{\sigma_y}{2} \pm \sqrt{\left(\frac{\sigma_y}{2}\right)^2 + (1.5\ S_{xy})^2} \qquad (7\text{-}2)$$

TABLE 7-1. ASSESSMENT OF CRITICAL STRESSES IN BUILDING 10A

Element No.	σ_y			σ_x	s_{xy} (1)	Critical Shear Stress Failure Criteria		Biaxial Failure Criteria		
	Dead Load	Seismic Load	Total			Critical Shear Stress* (2)	Performance Factor (2)/(1)	Principal Stresses σ_1†	Principal Stresses σ_2†	Performance Factor‡
71	31.2	4.9	36.1	2.6	84.9	152.0	1.8	146.7	-110.6	1.3
81	17.5	19.2	46.7	4.5	94.0	173.4	1.85	166.3	-119.6	1.2
90	30.0	5.9	35.9	3.8	81.3	151.8	1.87	141.2	-105.3	1.35

Stress in psi at 12.52 seconds

(+) Sign denotes compression

* Critical shear stress

$$s_{cr} = 80 + 2\sigma_y \qquad 0 \le \sigma \le 50 \text{ psi}$$

$$s_{cr} = 120 + 0.90\,\sigma_y \qquad 50 \le \sigma \le 400 \text{ psi}$$

† $$\sigma_{1,2} = \frac{\sigma_y}{2} \pm \sqrt{\left(\frac{\sigma_y}{2}\right)^2 + \left(1.5\, s_{xy}\right)^2}$$

$$x = \frac{\sigma_1}{f'_m} + \frac{\sigma_2}{0.1\, f'_m}$$

‡ Performance factor $= \frac{1}{x}$

where σ_2 is the maximum tensile principal stress and σ_y and $1.5\ S_{xy}$ represent the normal and shear stress on a horizontal section at the middle of the plate. The critical factor x is calculated from the interaction formula

$$x = \frac{\sigma_1}{f'_m} + \frac{\sigma_2}{0.1\ f'_m} \tag{7-3}$$

The performance factor B is calculated from the relationship

$$B = \frac{1}{x} \tag{7-4}$$

7.3.2 ASSESSMENT OF RESPONSE BASED ON BIAXIAL FAILURE CRITERION

Table 7-1 gives performance factors in Segment A of Building 10, using biaxial failure criteria. These factors range from 1.2 to 1.35 indicating that the shear panels have performed adequately during the 1971 San Fernando earthquake. However, the range of these factors is considerably less than the range of 1.8 to 1.87 obtained from the critical shear stress failure criteria. In addition, the lowest performance factor of 1.2 given for Element 81 indicates only a 20% safety margin over the factor of 1.0 that would postulate failure of that particular panel.

7.4 FLEXURAL STRENGTH

Failure is assumed when the flexural capacity of an element is exceeded. Flexural capacity of an element in this study is determined by using concrete failure criteria, except that f'_c is replaced by f'_m for masonry.

Analysis results of Building 10A indicate that flexural moments M_{xx} and M_{yy}, shown in Figure 7-1, are very small and would not create significant stresses.

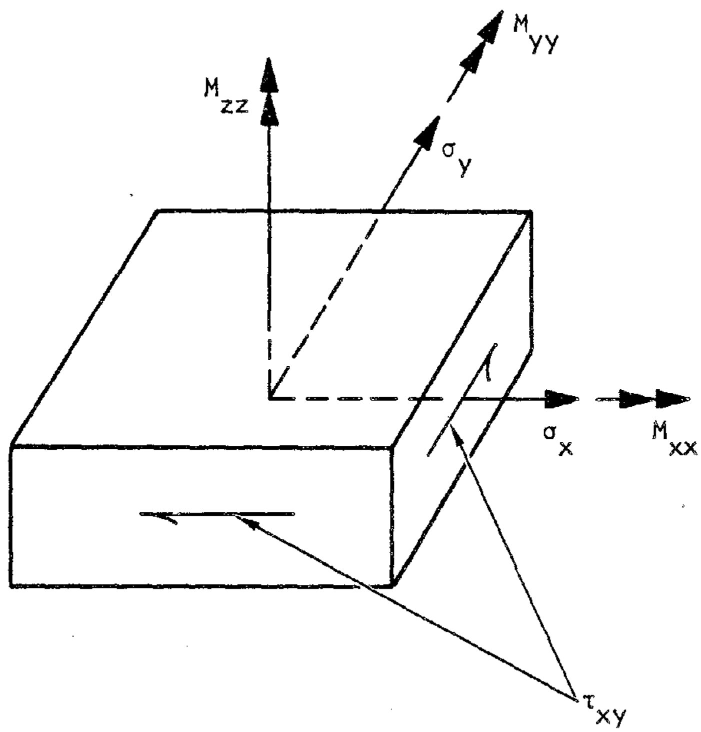

FIGURE 7-1. PLATE ELEMENT MOMENTS AND STRESSES
(POSITIVE DIRECTIONS SHOWN)

7.5 STRENGTH OF WALL-TO-FLOOR CONNECTIONS

Connections are usually the most important structural consideration with regard to seismic forces. If connections hold together and make the structure perform as a total system, there is an excellent chance for the structure to survive even great earthquakes.

Details of reinforcing bar size and spacing are dependent on engineering requirements and must be satisfactory to transmit the forces due to lateral and vertical loads. The elements must be sufficiently tied together to cause them to act as a unit.

7.5.1 PERFORMANCE CRITERION

Wall-to-floor connection must transmit the following forces (Figure 7-2):

a. Vertical load (including vertical resultants of lateral load)
b. Horizontal shear due to lateral load
c. Shear in the plane of the floors
d. Bending stress in the plane of the floors
e. Tie forces
f. Transverse bending due to floor loadings
g. Shear due to floor loadings

Because all these stress actions can act concurrently, the state of stress within the joint is most complex. Thus, it is not rational to treat the stresses resulting from the different loadings separately. However, very little published information is available on wall-floor connections, and there is no design procedure available that will account for the interaction of these force actions. Horizontal connections are designed mainly on the empirical basis. Therefore, a qualitative assessment of connections of Building 10 will be given.

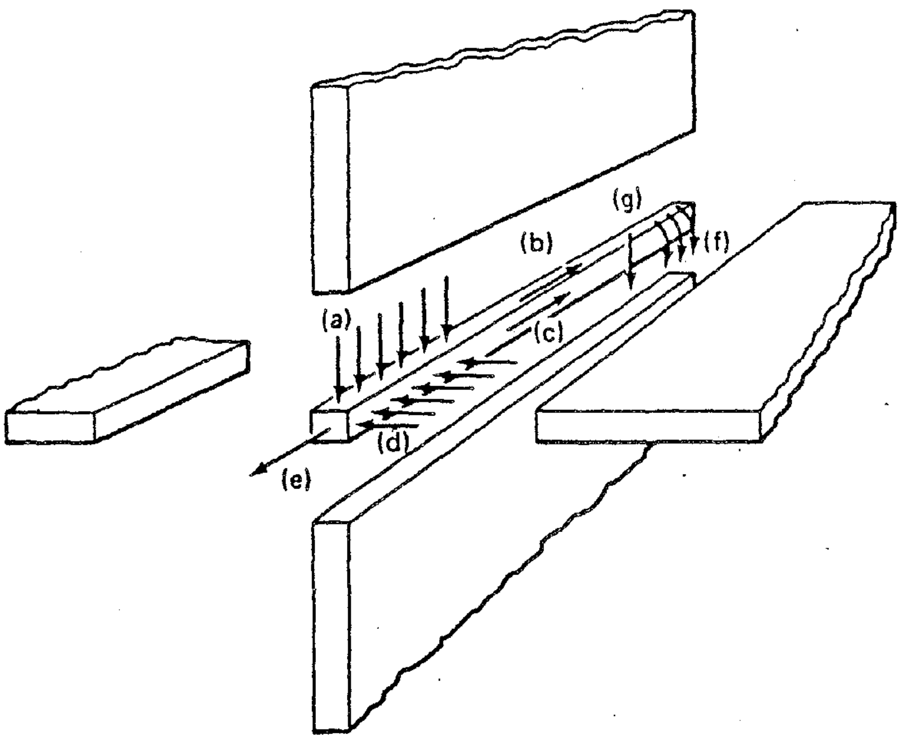

FIGURE 7-2. EXPLODED VIEW OF HORIZONTAL CONNECTION SHOWING FORCE ACTIONS

7.5.2 ASSESSMENT OF CONNECTIONS OF BUILDING 10

A qualitative assessment was made of connections and construction details by reviewing the available drawings. Some selected details are shown in Figures 7-3 through 7-10. Figures 7-3 and 7-4 illustrate interior and exterior wall-to-beam connections as built (1954). These figures show continuity of wall reinforcement in the beams. Figure 7-3b illustrates the current code of practice and indicates that connections of Figure 7-3a and 7-4 satisfy the current code of practice.

Figures 7-5 and 7-6 provide a comparison of wall-to-wall connections for the 1954 hospital construction and the present code of practice. The requirements of current practice are satisfied.

Figure 7-7 indicates adequate detail of parapets. Figure 7-8 shows wall reinforcement details, which illustrate adequate reinforcement around openings and the 45-bar diameter embedment for dowels. Minimum steel reinforcement ratio to gross area of section in shear walls was found to be 0.0007 in the horizontal direction and 0.0017 in the vertical direction. These two ratios add up to a total of 0.0024, which is larger than the 0.002 required by the 1979 Uniform Building Code. Figure 7-9 shows pier reinforcement including additional reinforcement at edge of pier.

Reinforcing steel in columns contributes to the load-carrying capacity of the member because the ties prevent it from buckling. The code requires that the minimum steel shall not be less than four No. 3 bars in a column. The maximum steel ratio shall be no more than 0.04 (4%) and the maximum size bars shall be No. 10. For these cases, steel ratio is the area of steel divided by the gross area of column. Figure 7-10 shows adequate detailing for a typical interior brick wall column as built in 1954.

The overall qualitative assessment indicates that connections were adequately designed and detailed.

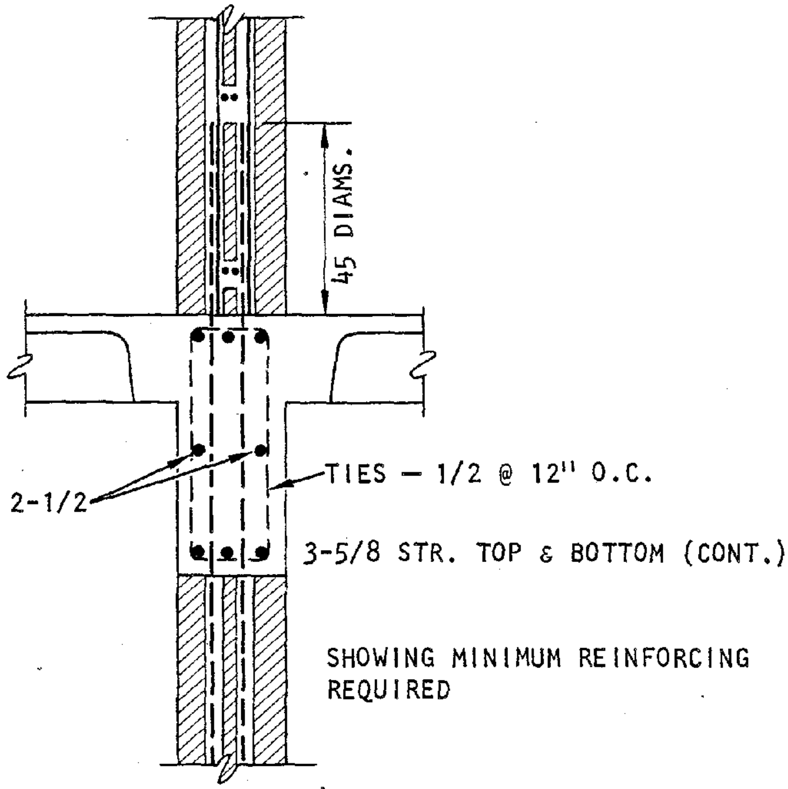

(a) Typical as built, 1954

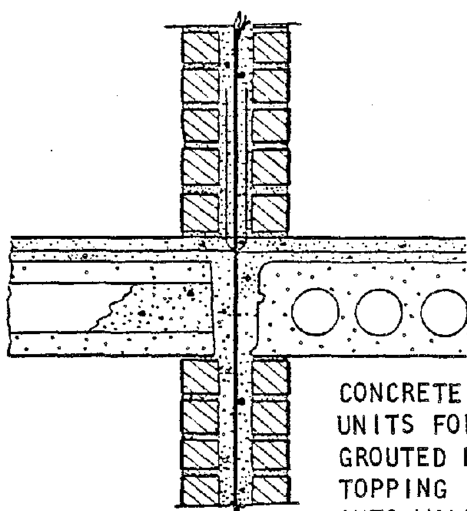

(b) Current recommended standard detail

FIGURE 7-3. WALL BEAM DETAIL (INTERIOR WALL)

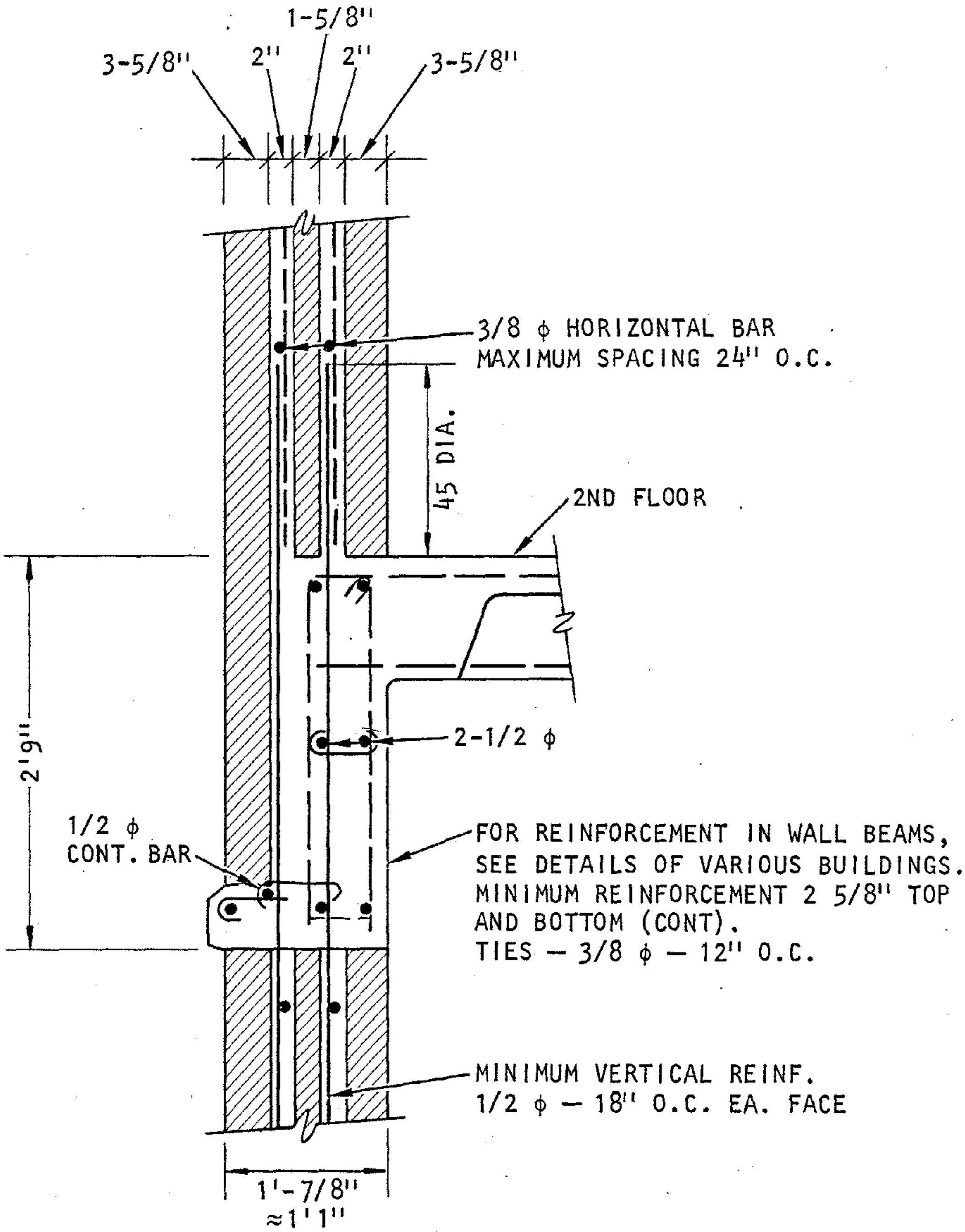

FIGURE 7-4. TYPICAL DETAIL OF WALL-BEAM (AS BUILT, 1954)

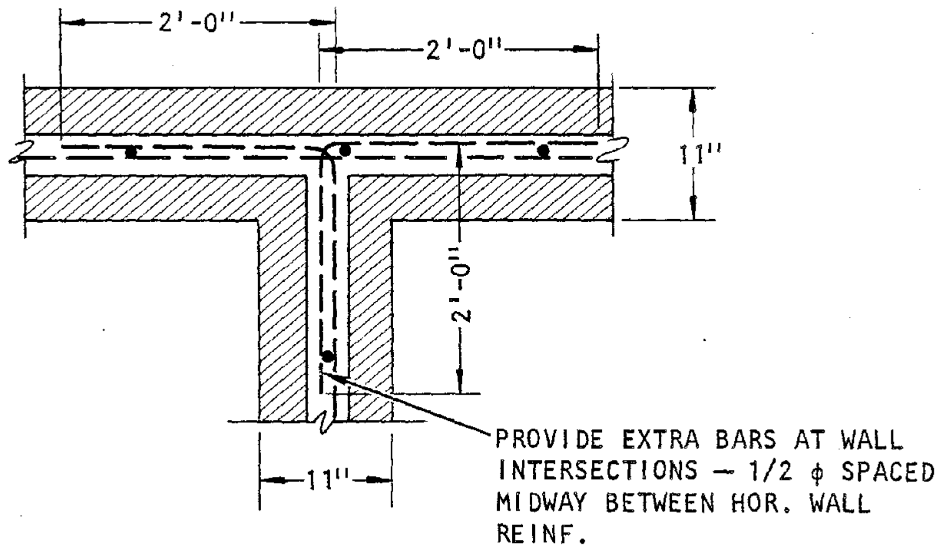

(a) Detail of wall intersections (as built, 1954)

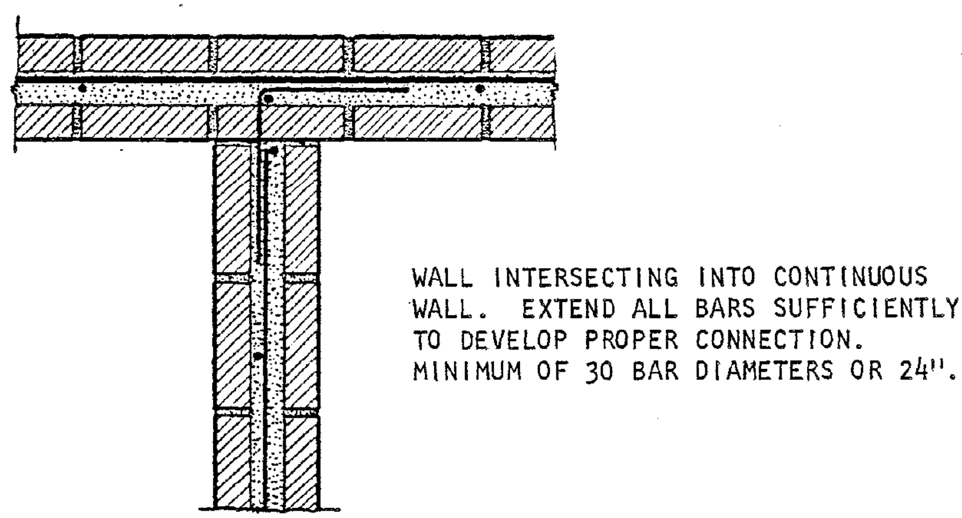

(b) Current standard detail

FIGURE 7-5. WALL INTERSECTIONS DETAIL

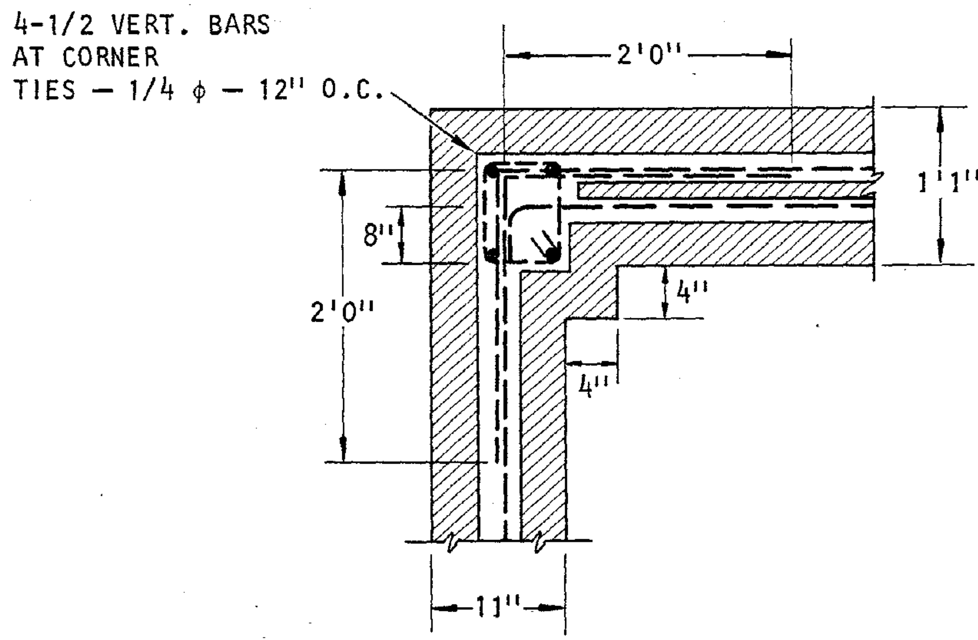

(a) Typical detail of corner piers (as built, 1954)

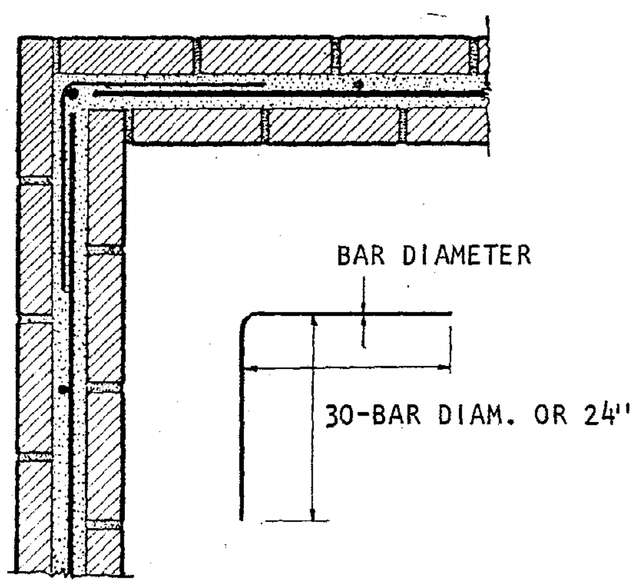

(b) Current standard detail of corner walls

FIGURE 7-6. DETAILS OF CORNER CONNECTIONS

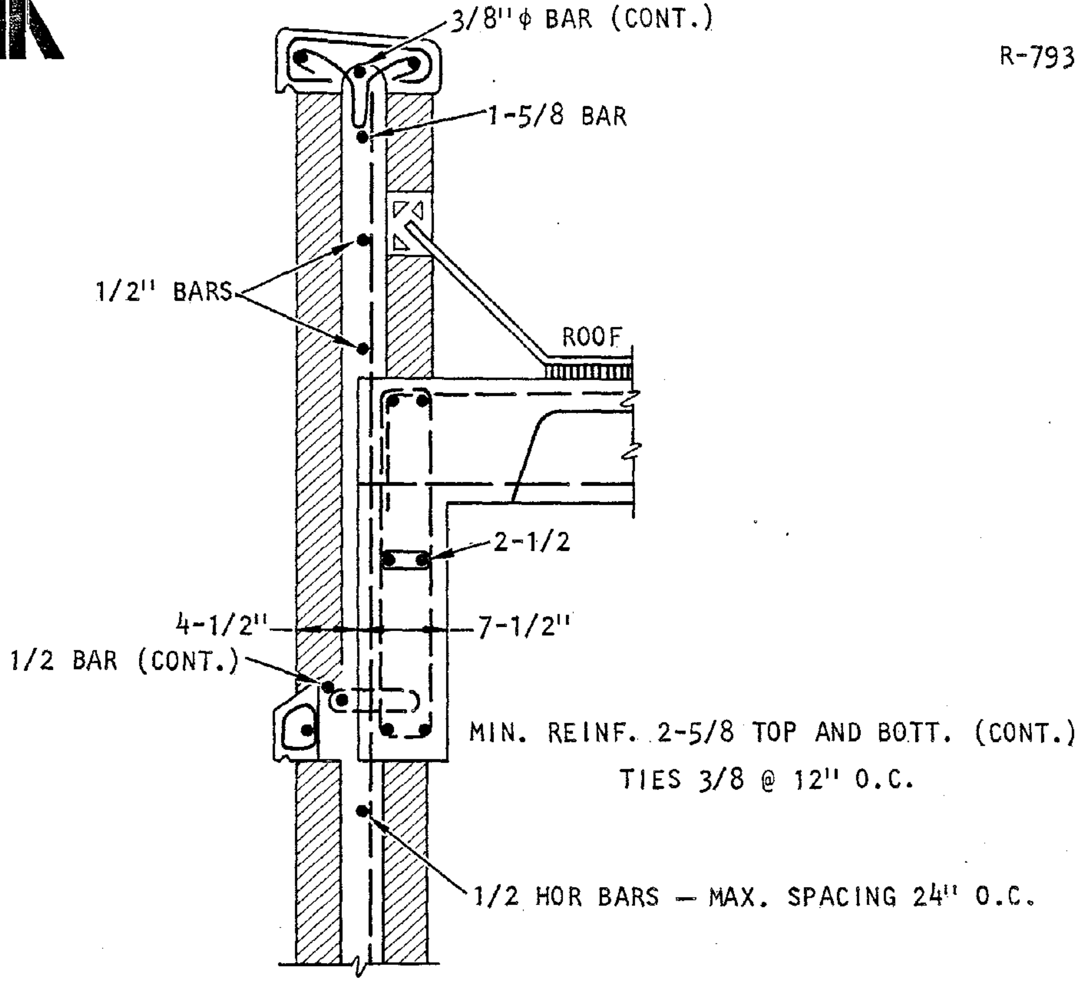

(a) Detail as built (1954)

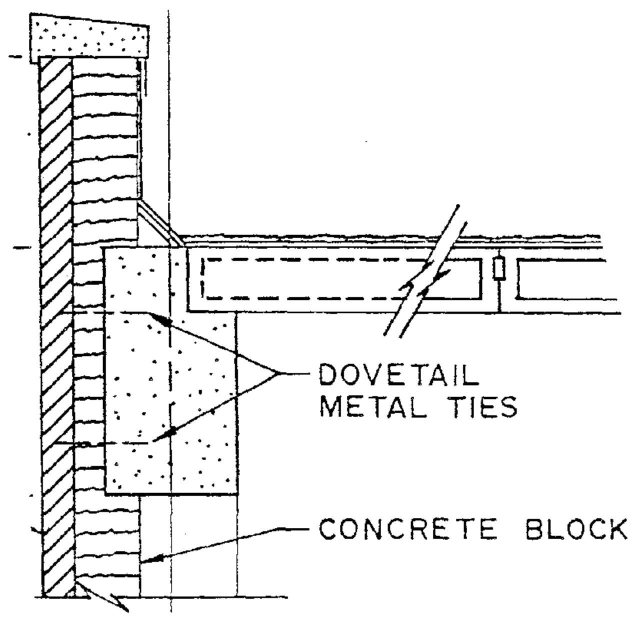

(b) Current standard detail

FIGURE 7-7. PARAPET DETAIL

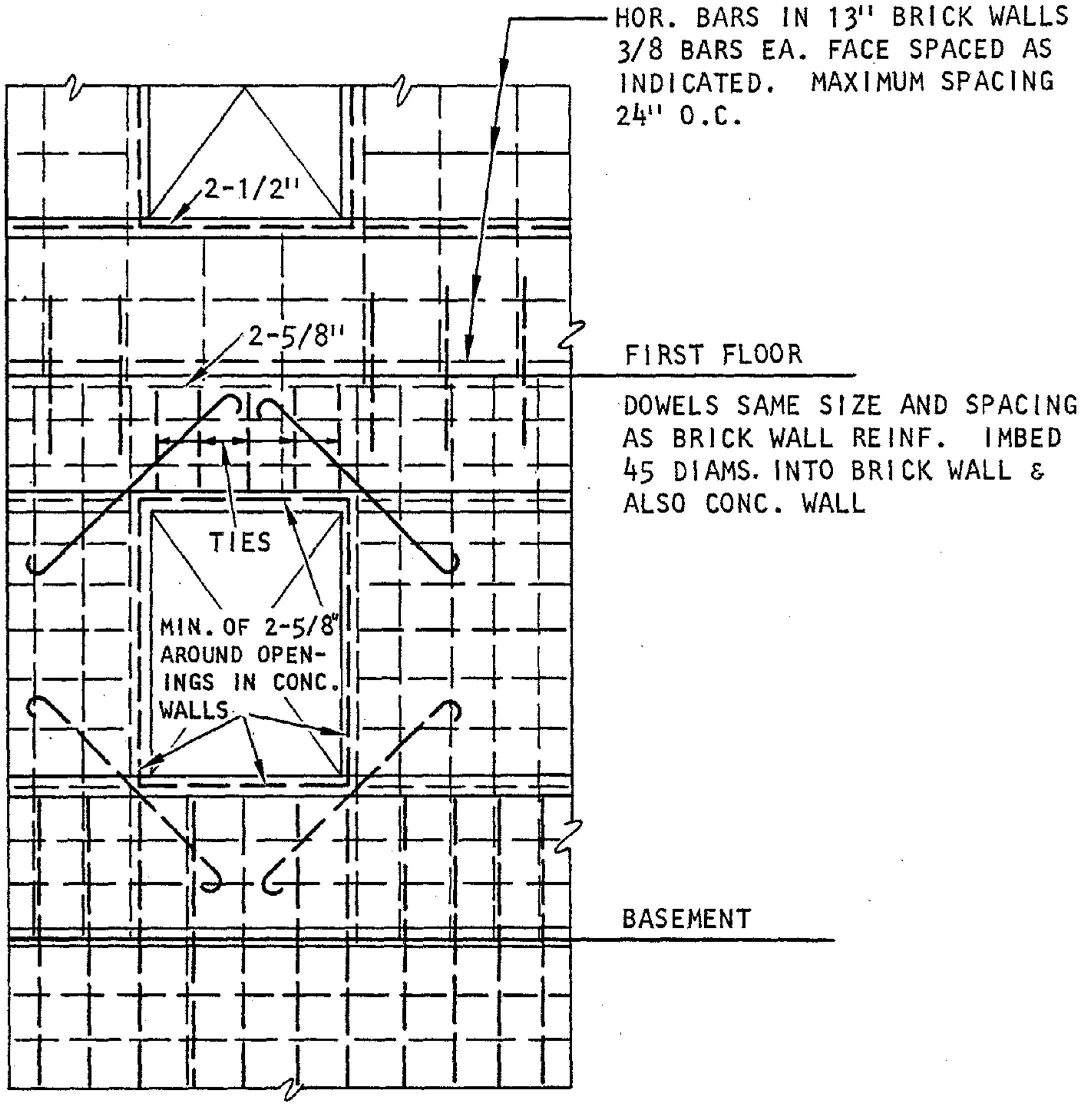

BARS AROUND WINDOW OR DOOR OPENINGS SHALL EXTEND AT LEAST 45 DIAMS., BUT NOT LESS THAN 24" BEYOND THE CORNER OF OPENINGS.
LAP BARS 45 DIAMS. AT SPLICES.

FIGURE 7-8. WALL REINFORCEMENT DETAIL (AS BUILT, 1954)

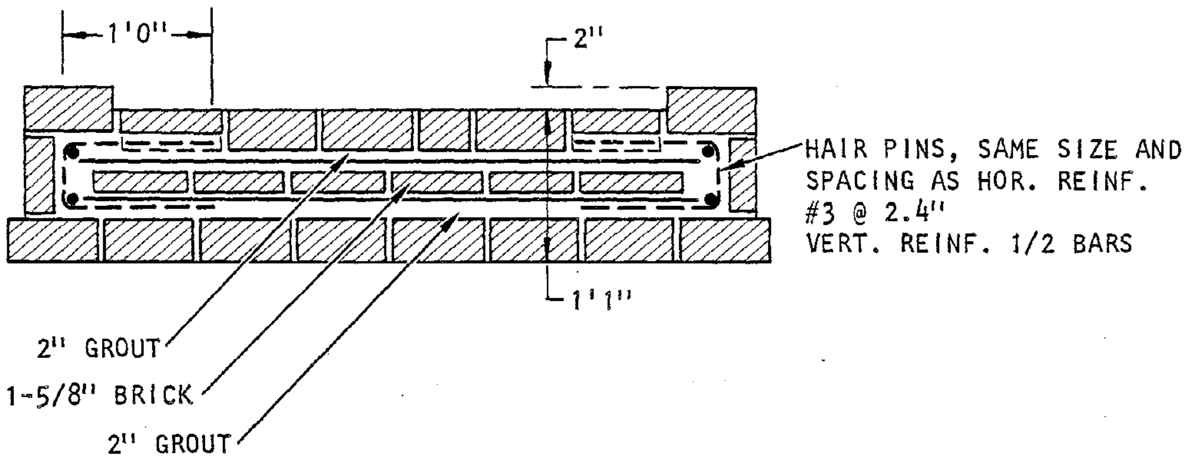

FIGURE 7-9. PIER SECTION SHOWING TYPICAL DETAIL AT JAMBS FOR 13" BRICK WALLS

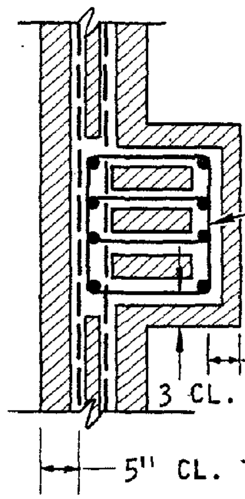

FIGURE 7-10. TYPICAL DETAIL OF INTERIOR BRICK WALL COLUMN (AS BUILT, 1954)

7.6 EFFECT OF EXPANSION JOINTS

Maximum stresses in shear wall elements 71, 81, and 90 resulting from the analysis are given in Table 7-2 for Building 10 with and without expansion joints. All columns numbered (1) provide results for Building 10 with expansion joints. These results were obtained from the analysis of Segment 10A only and represent the as-built configuration of Building 10. All columns numbered (2) provide results of Building 10 without expansion joints, i.e., all Segments A, B, and C were tied together in the model.

The results of the analysis indicate that stresses were increased by 28% for Element 71, 75% for Element 81, and 42% for Element 90 when Segments A, B, and C were tied together. However, Element 81 has a performance factor as low as 1.20 for the case when Building 10A is not tied to 10B or 10C as shown in Table 7-1. Performance factors of 1.30 and 1.35 were shown in this table for the same case for Elements 71 and 90, respectively. Therefore, the analyses results indicate that if Segments A, B, and C of Building 10 had been tied together (i.e., no expansion joints), this building would have suffered numerous cracks and probably considerable damage during the 1971 San Fernando earthquake.

7.7 COMPARISON OF HOSPITAL BUILDINGS SEISMIC REQUIREMENTS DURING THE 1971 SAN FERNANDO EARTHQUAKE AND ORIGINAL AND CURRENT SEISMIC DESIGN REQUIREMENTS

The variation of the equivalent static lateral force coefficient with building period for a structural system in which the required lateral forces are resisted by shear walls or moment resisting frames is shown in Figure 7-11 for several design criteria. These include VA (1973) earthquake resistant requirements and the requirements of the UBC (1979). ATC (1978) spectra for Los Angeles Area are given for 5 and 10 percent damping. These spectra are compared to the spectrum for the 0.40 g scaled

TABLE 7-2. COMPARISON OF STRESSES IN BUILDING 10 WITH AND WITHOUT EXPANSION JOINTS

El. No.	σ_y					σ_x		S_{xy}		Principal Stresses			
	Dead Load	Seismic		Total						σ_1†		σ_2†	
		1	2	1	2	1	2	1	2	1	2	1	2
71	31.2	4.9	17.4	36.1	48.6	2.6	7.0	84.9	109.4	146.7	190.2	-110.6	-141.6
81	27.5	19.2	1	46.7	28.5	4.5	19.9	94.0	141.6	166.3	227.6	-119.6	-199.1
90	30.0	5.9	19.8	35.9	49.8	3.8	8.4	81.3	115.4	141.2	199.8	-105.3	-150.0

(-) Sign denotes tension

* Stresses are in psi

1 Building with expansion joints (existing configuration)

2 Building without expansion joints (Parts A, B, and C tied together)

† $$\sigma_{1,2} = \frac{\sigma_y}{2} \pm \sqrt{\left(\frac{\sigma_y}{2}\right)^2 + \left(1.5\, S_{xy}\right)^2}$$

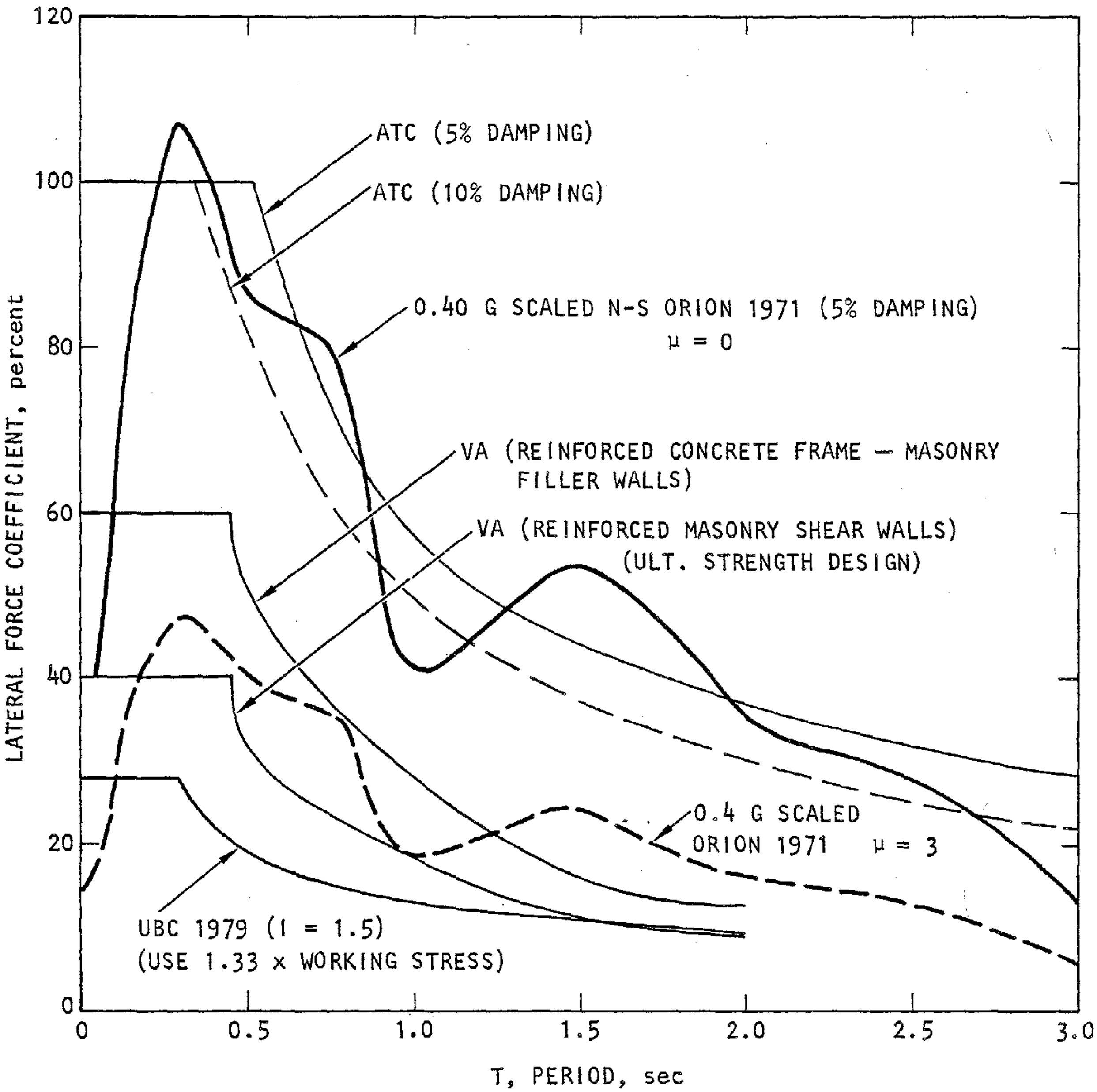

FIGURE 7-11. COMPARISON OF SEPULVEDA HOSPITAL DERIVED, 1971 SEISMIC INPUT AND ATC, VA, AND UBC SEISMIC DESIGN REQUIREMENTS

N-S 1971 Orion record used for seismic input to the analyses performed in this study. This spectrum was adjusted by ductility factor for masonry shear walls and compared to the VA and UBC criteria. Culver et al. (1975) provided a ductility factor (Table 3-21 of this reference) of 5 for average masonry construction. However, this factor is associated with extreme damage to the shear walls and should be reduced to 3 at the Sepulveda hospital because of life safety and function considerations. Based on the empirical equations recommended by Newmark (1970), a ductility modification factor of $1/\sqrt{2\mu-1}$ would be used. The resulting modified spectrum is compared in Figure 7-11 to the VA seismic criteria for reinforced masonry structural walls.

It is noted that the UBC represents a lower-bound loading condition, in contrast to the VA criteria. This is consistent with the philosophy of the UBC which is to provide minimum requirements for life safety. Also, the allowable UBC stresses are increased by a factor of 33% for seismic conditions as compared to the VA citeria which is based on ultimate strength considerations. The 0.4 g scaled 1971 Orion, adjusted by a ductility factor of 3, provides a good correlation with the VA criteria.

The uniform code of the Pacific Coast Building Official's Conference (UBC, 1946) was used for earthquake design requirements in determining the horizontal static forces which the hospital buildings were designed to resist (Guard, 1954). The hospital was designed in 1952 for requirements of seismic Zone 3. Forces were obtained from the formula:

$$F = CW \tag{7-5}$$

in which F is the horizontal force in pounds; W, the total dead load tributary to the point under consideration; and C, a numerical constant. This constant C is obtained from the formula:

$$C = \frac{60}{N + 4.5} \tag{7-6}$$

where N is the number of stories above the story under consideration.

For bearing walls:

$$C = 0.20 \tag{7-7}$$

According to Equation 7-7, reinforced masonry bearing walls were designed for 0.20 g lateral force. This can be visualized as a horizontal line going through 20% in Figure 7-11. These design requirements were associated with a 33% increase in allowable stresses. The hospital design criteria (1952) is lower than the current design requirements particularly in range of periods below 1.0 second. However, it is evident that the quality of construction, connections, and detailing allowed the hospital buildings to resist the 1971 earthquake forces with only minor damage.

SECTION 8

CONCLUSIONS AND RECOMMENDATIONS

8.1 CONCLUSIONS

Conclusions are summarized as follows:

1. Based on analysis results, performance factors ranging from 1.2 to 1.8 were experienced during the San Fernando earthquake.

2. Calculated stresses were increased by a factor ranging from 28% to 67% when expansion joints were eliminated from Building 10, and various parts of the building tied together.

3. No liquefaction potential was noted for the site at the time of the 1971 earthquake.

4. Expansion joints have been effective in reducing stresses below damaging levels and contributed to the survival of the hospital buildings.

5. Excellent connections and detailing resulted in adequate resistance to the 1971 San Fernando earthquake.

6. The deep alluvium in the San Fernando Valley provided a soft cushion that absorbed part of the high frequency energy of the earthquake. Therefore, higher stresses may have resulted if the same buildings were subjected to earthquake motions with higher frequency content, such as the scaled 1971 Castaic record.

7. The use of adequate grout in shear walls between the outer and inner wythes of brick provided adequate bond for the outer wythe. This bond resulted in mobilization of the full thickness of the brick shear wall to resist earthquake forces

and prevented the spalling and instability of the outer wythe which was observed in some masonry buildings during past earthquakes.

8. The inclusion of soil spring in the analytical model of shear wall buildings is necessary to provide a more realistic model of the soil-building system.

9. The use of more refined shear and biaxial failure criteria provides a more refined tool for evaluating state of stress in the building.

8.2 RECOMMENDATIONS

The following recommendations are given as a guide to improve earthquake resistance of masonry structures:

1. Adequate bond should be provided between outer and inner wythes of a 13-in. brick wall to mobilize all shear wall resistance during an earthquake.

2. Continuity of wall reinforcement through the beams should be provided for beam-wall connections.

3. Adequate anchoring of parapets and careful detailing of connections are needed to mobilize an integral structure during an earthquake.

4. Brick should be laid with full head and bed joints to achieve higher shear resistance during earthquakes.

5. Use of expansion joints is advantageous under similar soil and building configurations.

6. Detailed subsurface soil and shear wall test data are needed for refining analysis results such as relative displacements at the expansion joints.

7. Use of other types of earthquake input would provide information on the resistance of this type of construction to other possible earthquake environments.

8. Survey of effect of expansion joints on response of buildings during earthquakes can be combined with the results of this study to provide guidelines for their use.

9. Survey of other masonry buildings that survived other damaging earthquakes would generate a data base for providing specific recommendations for the design and construction of such buildings.

10. Compilation of results of current and past research programs on connections should be combined with the results of this research to provide a manual for preferred earthquake resistant connections and details.

REFERENCES

Abel, M.A. (1973) "Unreinforced Masonry Buildings," *San Fernando, California, Earthquake of February 9, 1971, Vol. I, Effects on Building Structures*, L.M. Murphy(Sci. Coordinator). Washington DC: National Oceanic and Atmos. Admin., Dept. of Commerce, pp 639-654.

Adham, S.; Bhaumik, A.; and Isenberg, J. (1975) *Reinforced Concrete Constitutive Relations*, AFWL-TR-74-72. El Segundo, CA: Agbabian Assoc., Feb.

Agbabian Assoc. (AA).(1973) *Procedures and Criteria for Increasing the Earthquake Resistance Level of Electrical Substations and Special Installations*, R-7211-13-2859. El Segundo, CA: AA, Sep.

----. (AA). (1976) *User's Guide for TRI/SAC Code*, 2nd rev. ed., R-7128-4-4102. El Segundo, CA: AA, May.

Alewine, R.W. (1974) *Application of Linear Inversion Theory Toward the Estimation of Seismic Source Parameters*, Ph.D. dissertation. Pasadena, CA: Calif. Inst. of Tech.

Allen, C.R.; Hanks, T.C.; and Whitcomb, J.H. (1973) "Seismological Studies of the San Fernando Earthquake and Their Tectonic Implications," *San Fernando, California, Earthquake of February 9, 1971*, Bull. 196, edited by G.B. Oakeshott. Sacramento, CA: Calif. Div. of Mines and Geology.

American Concrete Inst. (ACI).(1973) *Building Code Requirements for Reinforced Concrete*, ACI 318-71. Detroit, MI: ACI.

Balachandran, K. (1974) *An Investigation of the Strength of Concrete Masonry Shear Wall Structures*. Ph.D. dissertation, Univ. of Florida.

Barrows, A.G. et al. (1973) "Map of Surface Breaks Resulting from the San Fernando, California, Earthquake of February 9, 1971," *San Fernando California, Earthquake of February 9, 1971, Vol. III, Geological and Geophysical Studies*, L.M. Murphy(Sci. Coordinator). Washington DC: National Oceanic and Atmos. Admin., Dept. of Commerce, pp 127-136.

Benjamin, J.R. and Williams, H.A. (1958) "The Behavior of One-Story Brick Shear Walls," *Jnl Struct. Div, ASCE*, 84:ST4, Jul, pp 1923-1-1723-30.

Brandow & Johnston Assoc.(1972) Letter to Mr. V.P. Miller, Veteran's Admin., dated February 17, 1972.

Canitez, N. and Toksoz, M.N. (1972) "Static and Dynamic Study of Earthquake Source Mechanism: San Fernando Earthquake," *Jnl Geophys. Res.*, 77, pp 2583-2594.

Clough, R.W. and Penzien, J. (1975) *Dynamics of Structures*. New York: McGraw-Hill.

Dickey, W.L. (1972) "Now for the Good Part, or Veterans Administration's Wise Decision," *Masonry Industry*. Los Angeles, CA: Masonry Ind., Jan.

Guard, R.E. (1954) "Reinforced Brick Masonry Chosen for California," *Civil Engineering*. New York: ASCE, Oct.

Haller, P. (1969) "Load Capacity of Brick Masonry," *Designing Engineering and Constructing with Masonry Products*. Houston, TX: Gulf Pub. Co.

Hanks, T.C. (1972) *The Faulting Mechanism of the San Fernando Earthquake and Identification of the Initial Rupture Radiation*, Ph.D. Dissertation Chapter 5. Pasadena, CA: Calif. Inst. of Tech.

----. (1974) "The Faulting Mechanism of the San Fernando Earthquake," *Jnl Geophys. Res.*, 79, pp 1215-1229.

----. (1975) "Strong Ground Motion of the San Fernando, California Earthquake: Ground Displacements," *Bull. Seismol. Soc. of Amer.*, 65:1,pp 193-225.

Hedstrom, R.O. (1961) "Load Tests of Patterned Concrete Masonry Walls," *ACI Jnl*, 57, Apr, p 1265.

Hegemier, G.A. (1975) *Mechanics of Reinforced Concrete Masonry: A Literature Survey*, AMES-NSF-TR-75-5. San Diego, CA: Univ. of Calif.

Hegemier, G.A. et al. (1978) "On the Behavior of Joints in Concrete Masonry," *Proc. North Amer. Masonry Conf., Boulder, Colorado, August 14-16, 1978*, p 4.

Jennings, C.W. and Strand, R.G. (1969) *Geologic Map of California, Olaf P. Jenkins Edition, Los Angeles Sheet*, Scale 1:250,000. Sacramento, CA: Calif. Div. Mines and Geology.

Kamb, B. et al. (1971) "Pattern of Faulting and Nature of Fault Movement in the San Fernando Earthquake," *San Fernando, California, Earthquake of Feb 9, 1971: A Preliminary Report*, USGS Professional Paper 733. Reston, VA: U.S. Geological Survey.

Lew, H.S.; Leyendecker, E.V.; and Dikkers, R.D. (1971) "Engineering Aspects of the 1971 San Fernando Earthquake," *NBS Building Sci. Ser. 40*. Washington, DC: Nat. Bureau of Standards, Dec.

Maley, R.P. and Cloud, W.K. (1973) "Strong-Motion Accelerograph Records," *San Fernando, California, Earthquake of February 9, 1971, Vol. III, Geological and Geophysical Studies*, L.M.Murphy(Sci. Coordinator). Washington DC: National Oceanic and Atmos. Admin., Dept. of Commerce, pp 325-348.

Mayes, R.L. and Clough, R.W. (1975) *State-of-the-Art in Seismic Strength of Masonry - An Evaluation and Review*, EERC Report No. 75-21. Berkeley, CA: Univ. of Calif.

Morrill, B.J. (1973) "Seismoscope Results," *San Fernando, California, Earthquake of February 9, 1971, Vol. III, Geological and Geophysical Studies*, L.M. Murphy(Sci. Coordinator). Washington DC: National Oceanic and Atmos. Admin., Dept. of Commerce, pp 353-364.

Murphy, L.M. (Sci. Coordinator). (1973) *San Fernando, California, Earthquake of February 9, 1971*, 3 vols. Washington DC: National Oceanic and Atmos. Admin., Dept. of Commerce.

Oakeshott, G.B. (1958) *Geology and Mineral Deposits of San Fernando Quadrangle, Los Angeles County, California*, Bull. 172. Sacramento, CA: Calif. Div. Mines and Geology.

Proctor, R.J. et al. (1972) "Relation of Known Faults to Surface Ruptures, 1971, San Fernando Earthquake, Southern California," *Bull. Geolog. Soc. of Amer.*, 83, pp 1601-1618.

Shannon & Wilson (SW) & Agbabian Assoc. (AA). (1978a) *Effects of Local Site Conditions on Earthquake Ground Motion Parameters*. Seattle, WA: SW & El Segundo, CA: AA, Mar.

----. (1978b) *Verification of Subsurface Conditions at Selected "Rock" Accelerograph Stations in California, Vol. 1*, NUREG/CR-0055. Seattle, WA: SW & El Segundo, CA: AA, May.

----. (1979) *Statistical Analysis of Earthquake Ground Motion Parameters*, NUREG/CR-1175. Seattle, WA: SW & El Segundo, CA: AA, Dec.

Seed, H.B. and Lee, K.L. (1973) "Slides in the San Fernando Dams," *San Fernando, California, Earthquake of February 9, 1971, Vol. I, Effects on Building Structures*, L.M. Murphy(Sci. Coordinator). Washington DC: National Oceanic and Atmos. Admin., Dept. of Commerce, pp 809-814.

Self, M.W. (1974) *The Structural Properties of Load-Bearing Concrete Masonry*, EIES Project D-622. Engineering and Industrial Exp. Stations, Univ. of Florida, Mar.

Steinbrugge, K.V. and Schader, E.E. (1973) "Earthquake Damage and Related Statistics," *San Fernando, California, Earthquake of February 9, 1971, Vol. I, Effects on Building Structures*, L.M. Murphy(Sci Coordinator). Washington DC: National Oceanic and Atmos. Admin., Dept. of Commerce, pp 691-724.

Veterans Administration (VA). (1952) Blueprints, "Plans, Elevations and Sections," Sepulveda (California) VA Hospital. Los Angeles, CA: VA, Div. Chief R.E. Guard, May 29, 1952.

Wentworth, C.M. and Yerkes, R.F. (1971) "Geologic Setting and Activity of Faults in the San Fernando Area, California, with a Section on Seismological Environment by Clarence R. Allen," *The San Fernando, California, Earthquake of February 9, 1971*, Geol. Survey Prof. Paper 733. Washington DC: U.S. Government Printing Office.

Woodward-Lundgren & Assoc. (1975) *Geologic, Seismologic, and Earthquake Engineering Investigations and Evaluations, Veterans Administration Hospital, Sepulveda, California*. Oakland, CA: Woodward-Lundgren & Assoc.

Yerkes, R.F. (1973) "Effects of San Fernando Earthquake as Related to Geology," *San Fernando, California, Earthquake of February 9, 1971, Vol. III, Geological and Geophysical Studies*, L.M. Murphy(Sci.Coordinator). Washington DC: National Oceanic and Atmos. Admin., Dept. of Commerce, pp 137-154.

Yorulmaz, M. and Sozen, M.A. (1967) *Behavior of Single-Story Reinforced Concrete Frames with Filler Walls*. Technical report to the Dept. of Defense, Office of Civil Defense, Urbana, Illinois.

Young, G.A. et al. (1972) *Response of Two Multistory Reinforced Concrete Masonry Buildings to Earthquake Ground Motion*, P72-131-2410. El Segundo, CA: Agbabian Assoc., Aug.

APPENDIX A

CALCULATIONS OF FINITE ELEMENT PROPERTIES AND SOIL SPRING STIFFNESS FOR BUILDING 3

AGBABIAN ASSOCIATES	SUBJECT BLDG. 3, UNIT B1 VETERANS HOSPITAL
	AUTHOR Y C LEE DATE 9/18/79 FILE NO.
	CHECKED BY DATE PAGE 1 OF

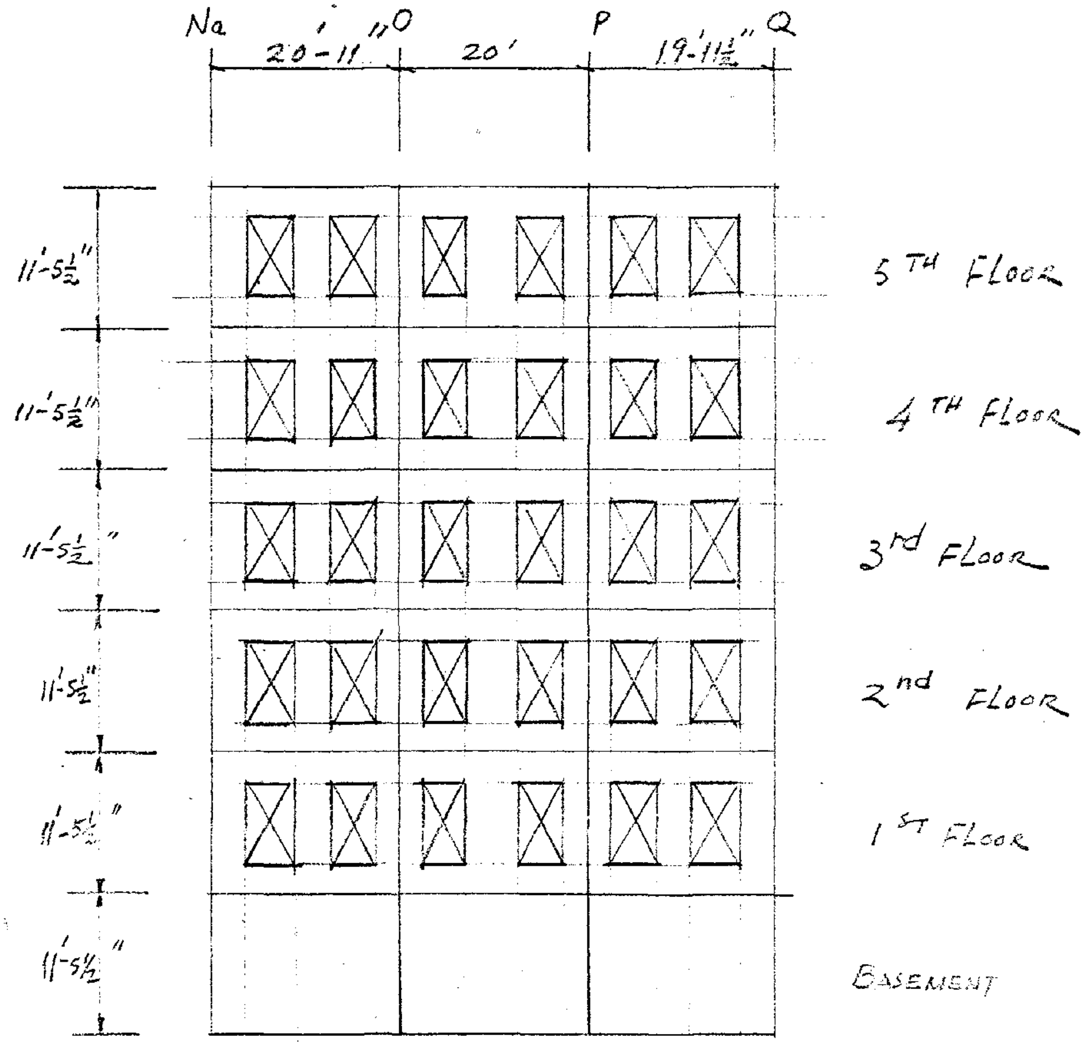

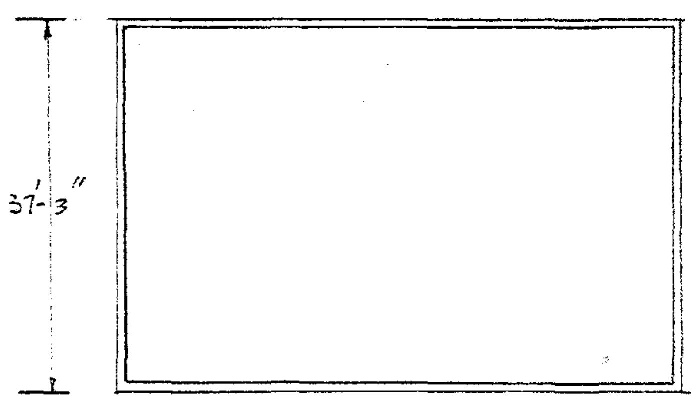

EAST OR WEST WALL

Reproduced from best available copy.

STIFFNESS OF WALLS

WALL BETWEEN Na AND O

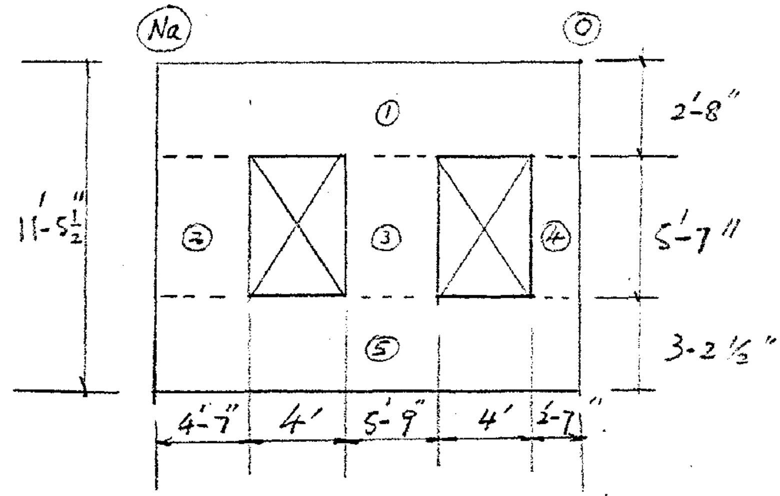

EQUIVALENT THICKNESS OF WALL

$$\Delta = \frac{Vh^3}{12EI} + \frac{1.2\,Vh}{AG}$$ DEFORMATION FOR FIXED ENDS

$$Et\Delta = \left(\frac{h}{L}\right)^3 + 2.76\left(\frac{h}{L}\right)$$

WHERE h = HEIGHT
L = WIDTH
t = THICKNESS
$V = 10^6$
$E = 2.3\,G$

TO FIND THE DEFORMATION OF THE PLATE SHOWN IN ABOVE FIGURE, WE CALCULATE DEFORMATION OF EACH REGION.

AGBABIAN ASSOCIATES

SUBJECT: BLDG 3 UNIT B1

AUTHOR: Y C LEE DATE: 9/20/79 FILE NO.

CHECKED BY: DATE: PAGE: 10 OF

MASS OF FLOOR

a) ROOF

1. AIRCONDITIONER

$W = 15,000\ \#$

2. A/C ENCLOSURE

DIMENSION $33'-9'' \times 24' \times 10.5'$

SURFACE AREA $= 2 \times 10.5 \times (33.75 + 24) + 33.75 \times 24$

$= 2021\ \square'$

ASSUMING AVERAGE WEIGHT $= 12\ lb/FT^2$

$W = 12 \times 2021 = 24260\ \#$

TOTAL WEIGHT $= 15000 + 24260 = 39260\ \#$ DISTRIBUTED BETWEEN P & Q

3. ROOF SLAB

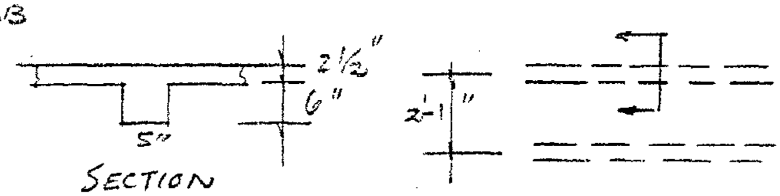

SECTION

SLAB & RIB

$$W = 2.5 \times 12 + (5 \times 6)\frac{145}{144}\frac{1}{2.08} = 45 \ \#/\square'$$

ROOFING MATERIAL

$7 \ \#/\square'$

BEAMS & STIFFENER

ASSUMING 10% OF SLAB WEIGHT $4 \ \#/\square'$

TOTAL $= 56 \ \#/\square'$

AREA $= 61 \times 38 = 2318 \ FT^2$

$W = 2318 \times 56 = 129808 \ \#$ UNIFORMLY DISTRIBUTED ALONG ENTIRE WIDTH

c) NORTH & SOUTH WALLS

PARAPET

DIMENSIONS $h \doteq 2'$ $l = 38'$ $t = $ 1'-2" SOUTH, 8½" NORTH

ASSUMING AVERAGE WEIGHT OF $135 \ \#/FT^2$ FOR SOUTH WALL

$W = 38 \times 2 \times .71 \times 145 = 7824 \ \#$ NORTH

$W = 38 \times 2 \times 1.16 \times 135 = 11900 \ \#$ SOUTH

Reproduced from best available copy.

WALL BETWEEN FLOOR & ROOF

NORTH WALL (8½" THICK, CONCRETE)

GROSS $A_1 = 38 \times 11.48 = 436$ FT^2

OPENING $A_2 = 8 \times 8.33 = 66.6$ FT^2

$A_n = A_1 - A_2 = 369$ FT^2

$W = 369 \times .71 \times 145 = 37988$ #

SOUTH WALL (8½" CONCRETE + 5½" BRICK)

GROSS $A_1 = 436$ FT^2

OPENINGS $A_2 = 3 \times 4 \times 5.6 = 67.2$ FT^2

$A_n = 369$ FT^2

$W = 369 \times 1.16 \times 135 = 57750$ #

DISTRIBUTION

$W_N = \frac{1}{2}\, 37988 + 7824 = 26821$ # @ Na

$W_S = \frac{1}{2}\, 57750 + 11900 = 40775$ # @ ℘

b) FLOORS

ALL FLRS HAVE APPROXIMATELY SAME MASS

1) PARTITION WALL

LENGTH $\ell = 220'$
HEIGHT $h = 10'$ } ASSUMING
AREA $A = 220' \times 10' = 2200$ □'

ASSUMING THE UNIT WEIGHT OF WALL = 20 #/□'

$W = 20 \times 2200 = 44{,}000$ # UNIFORMLY DISTRIBUTED

2) FLOOR SLAB

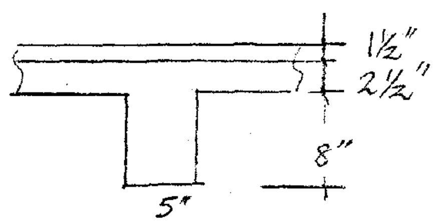

SLAB

$$W_1 = 2.5 \times 12 + (5 \times 8)\frac{145}{144} \times \frac{1}{2.08} = 49.2 \ \#/\square'$$

FINISH

$$W_2 = 1.5 \times 12 \qquad = 18 \ \#/\square'$$

BEAM & STIFFENER

$$W_3 = .1 W_1 \qquad = 5 \ \#/\square'$$

$$\text{TOTAL} = 72.2 \ \#/\square'$$

$$W = 2318 \times 72.2 = 167360 \ \#$$

EQUIVALENT THICKNESS OF PLANE STRESS ELEMENTS

ELEMENT NO.	THICKNESS (IN.)	EQUIV. THICKNESS (IN)	EQUIV. DENSITY (LB-SEC²/IN⁴)	REMARKS	Te (2-WALLS) (IN.)
1, 2, 3	12	12	.000217	NO OPENINGS	24
4	12	7.58	.000391	WITH OPENINGS	15.2
5	12	7.16	.000411		14.3
6	12	7.18	.000409		14.3
7, 10	10	6.32	.000414		12.6
8, 11	10	6.0	.000434		12.
9, 12	10	6.0	.000433		12.
13, 16	8.5	5.37	.000438		10.7
14, 17	8.5	5.07	.000460		10.1
15, 18	8.5	5.08	.000459		10.2

$E = w^{1.5}\, 33 \sqrt{f_c'}$ $\quad \nu = .15 \quad$ $G = E/2.3$

FOR $w = 145$ $\quad f_c' = 3000$ psi

$E = 3{,}160{,}000$ psi $\qquad G = 1{,}370{,}000$ psi

AGBABIAN ASSOCIATES	SUBJECT BLDG. 3 UNIT B1
	AUTHOR Y C Lee DATE 9/20/79 FILE NO.
	CHECKED BY DATE PAGE 17 OF

FLOOR AND ROOF MASS DISTRIBUTION

NODE NO.	SLAB (LB)	PARTITION (LB)	NORTH & SOUTH WALL ABOVE (LB)	BELOW (LB)	TOTAL (LB)	OTHERS (LB)	TOTAL WT. / TOTAL M.
5	27893	7333	26752	36898	63650		98876 (256.2)
6, 7	55786	14666					70451 (182.5)
8	27893	7333	37125	31627	68752		101978 (264.2)
9	27893	7333	22294	26752	49046		84272 (218.3)
10, 11, 14, 15	55786	14666					7045 (182.5)
12	27893	7333	32200	37125	69325		104551 (270.8)
13	27893	7333			44587		79813 (206.8)
16	27893	7333			64400		103406 (267.9)
17	27893	7333	18994	22293	41287		76513 (198.2)
18, 19, 23, 22	55786	14666					70451 (182.5)
20	27893	7333	28875	32200	61075		96301 (249.5)
21	27893	7333			37988		73214 (189.7)
24	27893	7333			57750		92976 (240.9)
25	21634				26821		48254 (125.5)
26	43269						43269 (112.1)
27	43269					19630	62899 (162.9)
28	21634				40775	19630	82039 (213.5)

Reproduced from best available copy.

AGBABIAN ASSOCIATES	
	SUBJECT Bldg 3, Unit 81 Veteran Hospital
	AUTHOR Y. C. Lee DATE 11/1/79 FILE NO.
	CHECKED BY DATE PAGE OF

RESULTS FROM F. E. ANALYSIS

1. MAXIMUM FLOOR DISPLACEMENT

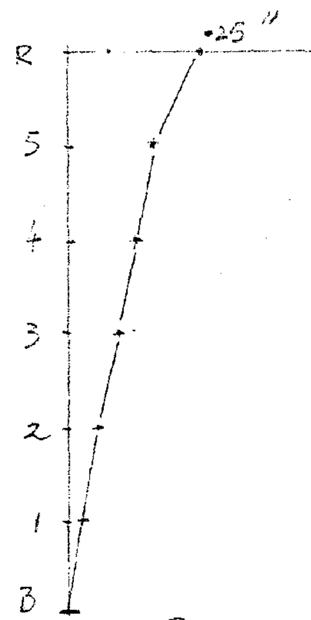

2. MAXIMUM SHEAR STRESSES (psi)

Floor	Na–O	O–P	P–Q
6–5		50	
5–4		95	
4–3		118	
3–2		147	
2–1		128	
1–B	75	52	73

3. FREQ

1st MODE, 5.8 Hz. 2nd MODE, 13.8 Hz.

SOIL SPRING

ASSUMING

$G = 5000$ KIPS/FT^2 $\nu = .3$

FOR ROTATIONAL STIFFNESS OF A RECTANGULAR FOUNDATION

$$K\psi = \frac{G}{1-\nu}\beta_\psi 8 c d^2$$

(REF.)

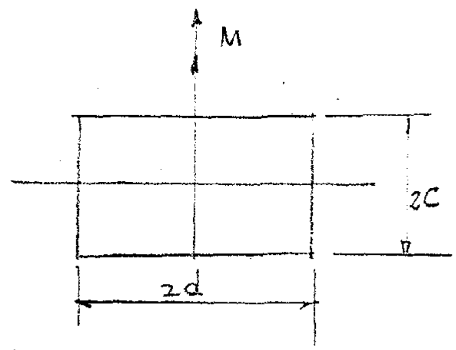

FOR BUILDING 3B1

$2c = 37.25'$

$2d = 60.75'$

$d/c = 1.63$

$\beta\psi = .6$

$$K\psi = \frac{5000}{.7} \times .6 \times \frac{37.25 \times (60.75)^2}{\cancel{8}}\cancel{8} = 5.89 \times 10^8 \text{ KIPS-FT}$$

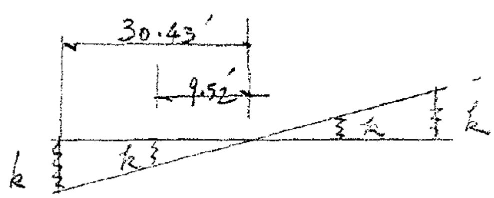

$$2k(30.43^2 + 9.52^2) = 5.89 \times 10^8 \text{ KIPS-FT}$$

AGBABIAN ASSOCIATES

SUBJECT Bldg 3, Unit B1
VA Hospital

AUTHOR Y C Lee DATE 9/18/79 FILE NO.

CHECKED BY DATE PAGE 17 OF

$k = 2.89 \times 10^5$ kips/ft

$= 2.4 \times 10^7$ lb/in

AGBABIAN ASSOCIATES

SUBJECT VA Hospital / Buildg 3B2

AUTHOR Y C Lee DATE 10/24/79 FILE NO.

CHECKED BY DATE PAGE 1 OF

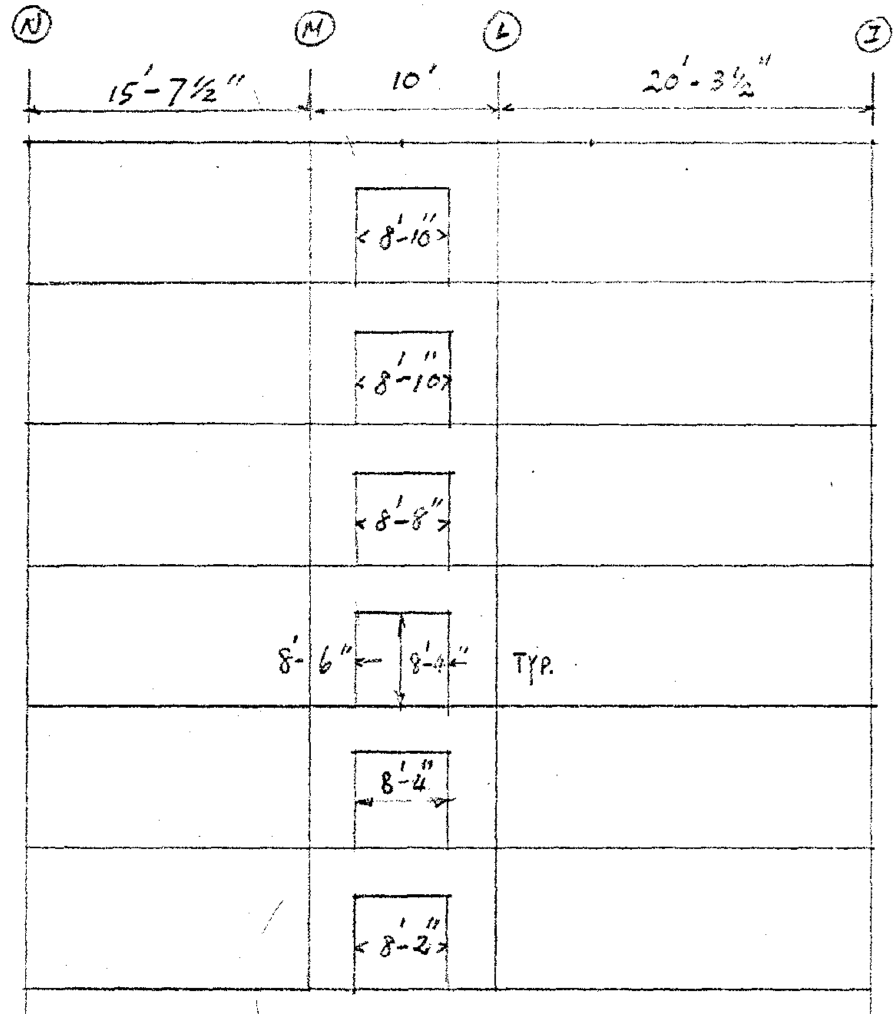

.17 12·8/46 = .28 15·1/46 = .33

10·1/46 = .22

EAST - WALL

AGBABIAN ASSOCIATES	SUBJECT V A HOSPITAL / BUILDING 3B2
	AUTHOR Y C LEE DATE 10/24/72 FILE NO.
	CHECKED BY DATE PAGE 2 OF

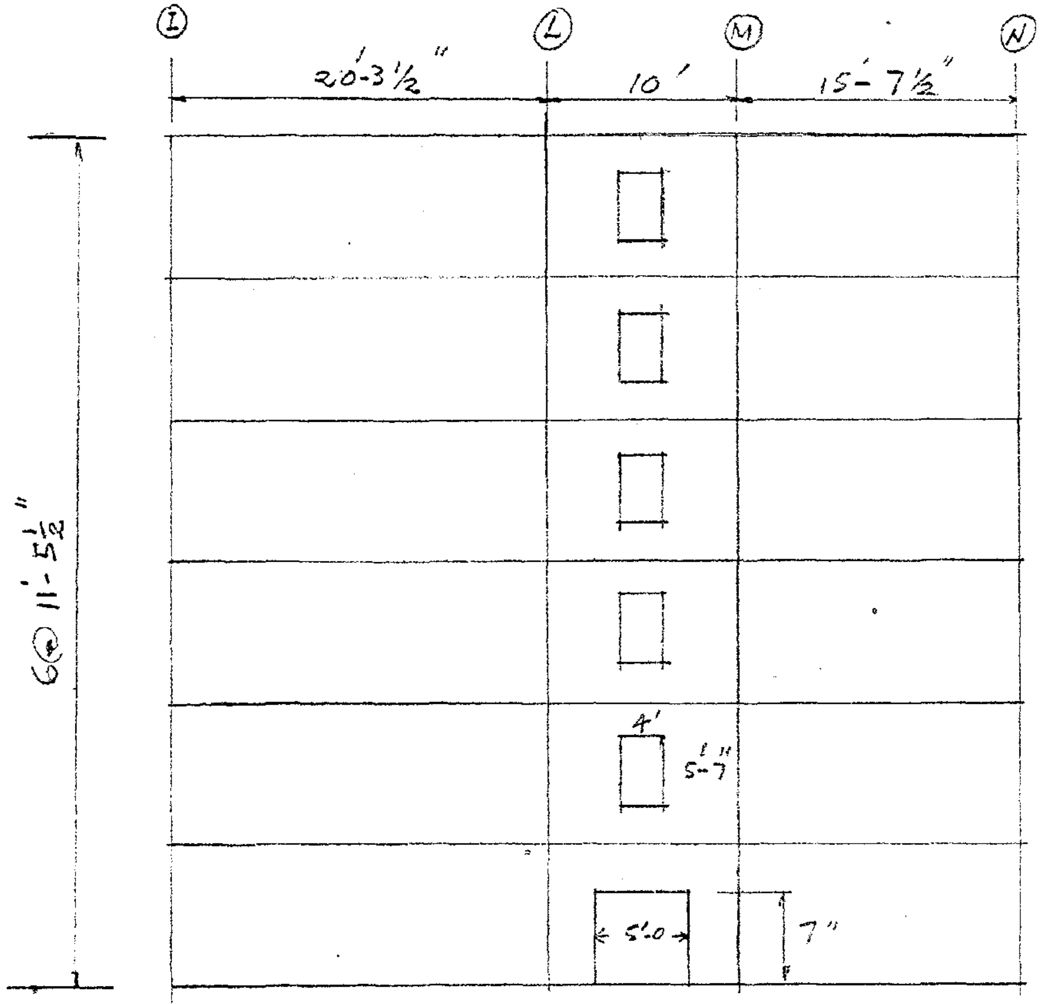

WEST WALL

AGBABIAN ASSOCIATES

SUBJECT: VA HOSPITAL BLDG 382

AUTHOR: Y C LEE DATE: 10/24/79 FILE NO.

CHECKED BY: DATE: PAGE: 3 OF

STIFFNESS CALCULATION

1) WEST WALL BETWEEN L & M (1st TO 5TH FLR)

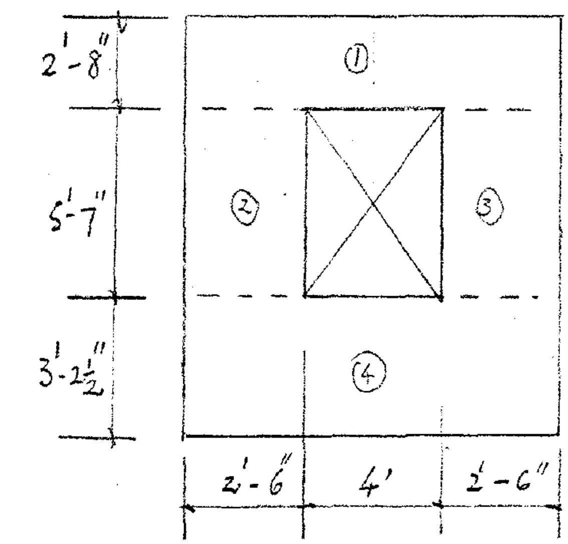

EQUIVALENT THICKNESS OF WALL

$$\Delta = \frac{Vh^3}{12EI} + \frac{1.2\,Vh}{AG}$$

$$Et\Delta = \left(\frac{h}{L}\right)^3 + 2.76\left(\frac{h}{L}\right)$$

WHERE h = HEIGHT
L = WIDTH
t = THICKNESS
$E = 2.3G$

REGION 1 $h_1 = 2.67'$ $L_1 = 10.$ $\frac{h_1}{L_1} = .267$

$Et\Delta_1 = .756$

REGION 2 & 3 $h_2 = 5.58'$ $L_2 = 2.5'$ $\frac{h_2}{L_2} = 2.232$

$Et\Delta_2 = 17.279$

AGBABIAN ASSOCIATES	SUBJECT VA Hospital Bldg 3R2		
	AUTHOR V C Lee	DATE 10/24/79	FILE NO.
	CHECKED BY	DATE	PAGE 9 OF

EQUIVALENT THICKNESS OF PLANE STRESS ELEMENTS

EL. NO.	THICKNESS (IN.)				EQUIV. (IN) THICKNESS	EQUIV. (LB-S²/IN) DENSITY	REMARKS
	E WALL	W-WALL	STAIR	OTHERS			
1	14	14	8 (2)		44	.000217	
2	1.2	0			1.2	.00222	
3	14	14			28.	.000217	
4	12	12	8 (2)		40.	.00026	
5	5.45	0	0		5.45	.00054	
6	12	12	0		24	.00026	
7,10,13	10	10	8 (2)		36	.000245	
8,11,14	4.54	0	0		4.54	.000571	
9,12,15	10	10	0		20	.000268	
16	8.5	8.5	8 (2)		33	.000248	
17	3.86	0	0		3.86	.000665	
18	8.5	8.5	0		17.	.000278	

AGBABIAN ASSOCIATES	SUBJECT V A Hospital 332
	AUTHOR Y C LEE DATE 10/24/79 FILE NO.
	CHECKED BY DATE PAGE 11 OF

$l = 194'$

$A = hl = 194 \times 15.5 = 3007 \ \square'$

$W = 3007 \times 161 = 484{,}127 \ \#$

$W_{TOTAL} = 484{,}127 + 108{,}000 = 592{,}127. \ \#$

ROOF

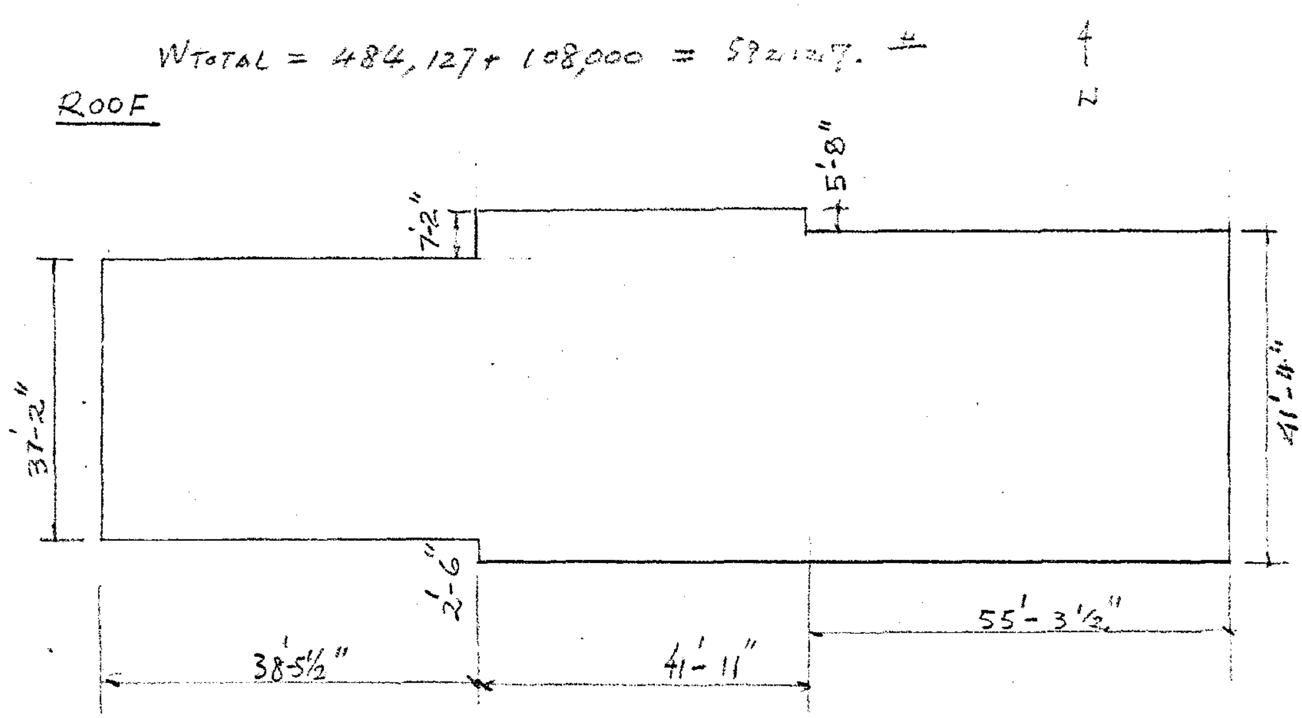

$$37.167 \times 38.46 = 1429.44 \ \square'$$
$$47 \times 41.92 = 1970.02$$
$$55.3 \times 41.33 = 2285.55$$
$$\overline{\quad 5685. \ \square' \quad}$$

SLAB	50
ROOFING & FLOORING	15
BEAM & STIFFENER	5
	70 #/□'

AGBABIAN ASSOCIATES	SUBJECT V A Hospital Bldg 3B2
	AUTHOR Y C Lee DATE 10/24/79 FILE NO.
	CHECKED BY DATE PAGE 17 OF

Floor & Roof Mass Distribution

Node #	Slab (#) & Partition	Partition (#)	North & South Wall (#) Above	Below	Total	Others	Total Wt # Mass (LB-S²/IN)
5	131252.		146,200	103800			381252. 988.
6	196878						196878 510.
7	167048						167048 433.
8	101422		133500	95000			329922 855.
9	131,252	—	129000	146,200			406452. 1053.
10	196878						196878 510
11	167,048						167048 432
12	101422		118,000	133,500			352922 914
13, 17	131252				257000		388252 1005.
14, 18	196878						196878 510
15, 19	167048						167048 432
16, 20	101422				235,400		336822 872.
21	131252		116,000	129,000			376252. 975.
22	196878						196878 510

AGBABIAN ASSOCIATES

SUBJECT: VA Hospital Bldg 382

AUTHOR: Y C Lee DATE: 10/24/79 FILE NO.

CHECKED BY: DATE: PAGE 18 OF

NODE #	SLAB (#) PARTITION	PARTITION (#)	NORTH & SOUTH WALL (#)			OTHERS	TOTAL WT. (#) MASS (LB-SEC²/IN)
			ABOVE	BELOW	TOTAL		
23	167048						167048. 432.
24	101422		106,000	117,700			325122. 842.
25	88547		40,250	116,000		134,000	378797 982.
26	132821					202,000	334820 867
27	112697					171,400	284097 736.
28	68423		32,200	106,000		104,000	310623 804.

AGBABIAN ASSOCIATES	SUBJECT VA Hospital Bldg 38
	AUTHOR Y C Lee DATE 10/24/79 FILE NO.
	CHECKED BY DATE PAGE 19 OF

Soil spring

$$K_\psi = \frac{G}{1-\nu}\beta_\psi\, 8 c d^2$$

$2c = 136'$

$2d = 47'$

$d/c = .35$

$\beta_\psi = .45$ $G = 5000$ ksf

$$K_\psi = \frac{5000}{.7} \times .45 \times 136 \times 47^2 = 9.6565 \times 10^8 \text{ kip-ft}$$

$$k(2.75^2 + 2\times 23^2 + 7.25^2) = 9.6565\times10^8 \qquad k = 8.636\times10^5\ k/ft$$

$k = 71969$ KIP/in

AGBABIAN ASSOCIATES	SUBJECT: BLDG 3, UNIT B2 VETERAN HOSPITAL
AUTHOR: Y. C. LEE	DATE: 11/1/79 FILE NO.
CHECKED BY	DATE PAGE OF

RESULTS FROM F.E. ANALYSIS

1. MAXIMUM FLOOR DISPLACEMENT

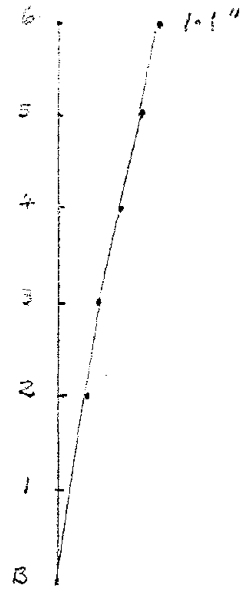

2. MAXIMUM SHEAR STRESSES (psi)

(I)–(L)	(L)–(M)	(M)–(N)
154		166
233		246
241		292
247		274
281		360

3. FREQ.

1st MODE, 3.1 Hz. 2nd MODE, 10.3 Hz.

APPENDIX B

ADDITIONAL DATA ON MODEL FOR BOILER HOUSE (BUILDING 40)

AGBABIAN ASSOCIATES

SUBJECT: SEISMIC ANALYSIS OF BOILER HOUSE, V. A. HOSPITAL
AUTHOR: Y C LEE   DATE: 2/27/81   FILE NO.
CHECKED BY: DATE:

SIMPLE HAND CALCULATION

1. HORIZONAL MOTION

MASSES

a) ROOF

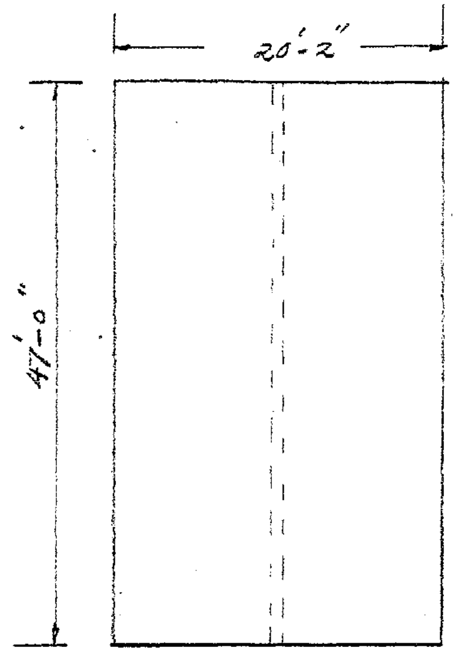

$$V = \left[\frac{47 \times 12}{25} \times (5 \times 8) \times (20 \times 12 + 2) \right]$$

$$+ 47 \times 12 \times 5 \times 8 \times 2$$

$$+ 2\tfrac{1}{2} \times 47 \times 12 \times (12 \times 20 + 2)$$

$$= 604720 \ IN^3$$

$$(MASS)_1 = 604720 \times 145 / 1728 \times 386$$

$$= 131.5 \ lb\text{-}sec^2/in$$

ROOFING = $6 \times 47 \times 20.2 = 5696$ lbs.

$$(MASS)_2 = 14.8 \ lb - sec^2/in$$

TOTAL MASS (10% ADDITIONAL MASS ON ROOF)

$$M_r = (131.5 + 14.8) \times 1.1 = 160.9 \ lb - sec^2/in$$

b) PLATFORM

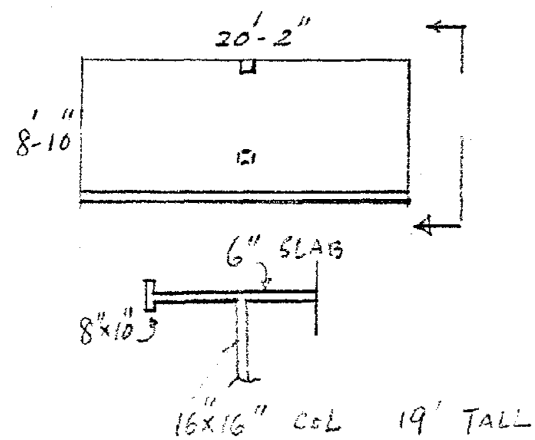

$$V = \left[\frac{19}{2} \times 12 \times 16 \times 16 + 6 \times 242 \times 106 \right.$$

$$\left. + 242 \times 8 \times 10 \right] = 202456 \ in^3$$

$$M = V \times 145 / 1728 \times 386 = 44 \ lb - sec^2/in$$

Reproduced from best available copy.

AGBABIAN ASSOCIATES

SUBJECT: Seismic Analysis of Boiler House VA Hospital

AUTHOR: Y C Lee DATE: 3/2/81 FILE NO.

CHECKED BY: DATE: PAGE 2 OF 11

Add 20% for steel platform

$M_p = 1.2 \times 44 = 53 \ \text{lbs-sec}^2/\text{in}$

c) Wall

$t = 13''$

$\gamma = 120 \ \text{lb}/\text{FT}^3$

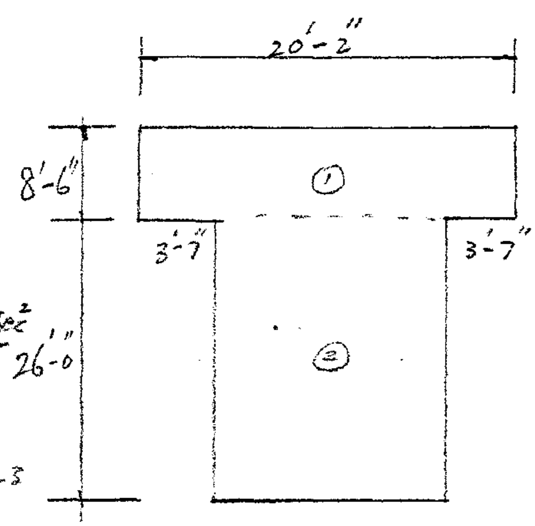

$V_1 = 8.5 \times 20.2 \times \frac{13}{12} = 186 \ \text{FT}^3$

$M'_w = 186 \times 120 \times \frac{1}{386} = 57.82 \ \frac{\text{lb-sec}^2}{\text{in}}$

$V_2 = 26 \times 14 \times \frac{13}{12} = 394.3 \ \text{FT}^3$

$M''_w = 394.3 \times 120 \times 1/386 = 122.6 \ \frac{\text{lb-sec}}{\text{in}}$

Mass Distribution

Top

$M = 160.9 + \frac{53}{2} + 2 \times 57.8 + 2(122.6/3) = 384.7 \ \text{lb-sec}^2/\text{in}$

Frame

$V_b = 2(2278 \times 8 + 1606 \times 12 + 1155 \times 12 + 902 \times 12 + 838 \times 24$

$+ 774 \times 60 + 710 \times 60 + 78 \times 598) - 47 \times 12 \times 150 = 351424 \text{ in}^3$

$m_b = 351424 \times \frac{144}{1728} \times \frac{1}{386} = 75.9 \quad \text{lb-sec}^2/\text{in}$

$V_c = 2(60 \times 480 + 72 \times 512 + 24 \times 544 + 12 \times 672 + 12 \times 832$

$+ 12 \times 1248 + 8 \times 1920) = 254208 \text{ in}^3$

$m_c = 54.9$

$\text{TOTAL MASS @ TOP} = 384.7 + 75.9 + 27.5 = 488.1 \frac{\text{lb-sec}^2}{\text{in}}$

STIFFNESS CALCULATION

$K = \frac{P}{\Delta} = \frac{6}{h^2 \left[\frac{h}{EI_h} + \frac{\ell}{2EI_\ell}\right]}$

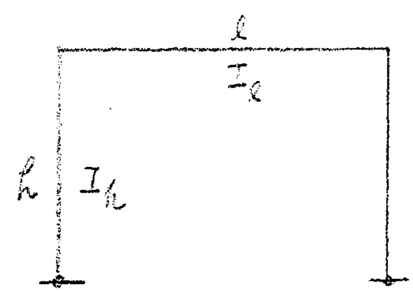

$h = 422''$

$\ell = 47 \times 12 = 564''$

$I_h = 4390 \text{ in}^4$

$I_\ell = 97810 \text{ in}^4$

$$K = \frac{P}{\Delta} = \frac{6}{422^2\left[\frac{422}{3\times10^6\times 43490} + \frac{564}{2\times3\times10^6\times 97810}\right]} = \frac{18\times10^6}{422^2[.102]}$$

$= 8030 \quad lb/in$

FREQUENCY OF FRAME

$$f = \frac{1}{2\pi}\sqrt{\frac{k}{m}} = \frac{1}{2\pi}\sqrt{\frac{6534}{488}} = .64 \text{ cps}$$ VS. .67 FROM COMPUTER RESULT

SPECTRUM ANALYSES

Apply Orion Response Spectrum NOOW Scaled to .4 g

$f = .64$ cps

$a = .55\,g$

SHEAR @ COLUMN

$S = \frac{m}{2}\cdot .55\,g = \frac{1}{2}488\times .55\times 386 = 51801$ lb COMPARED WITH 37250 lb FROM COMPUTER

Reproduced from best available copy.

STATIC LOAD

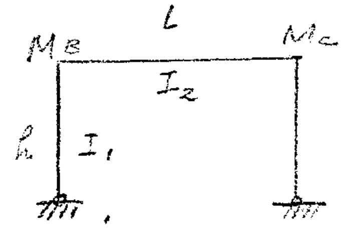

$H = M_B / h$

$M_B = WL / 4N_1$

$N_1 = 2\alpha + 3 = 2 \dfrac{I_2}{I_1} \dfrac{h}{L} + 3$

ASSUMING $\quad I_2/I_1 = 97810 / 43490 = 2.25$

$h/L = 422/538 = .784$

$N_1 = 2 \times 1.763 + 3 = 6.53$

$M_B = WL/4N_1 = (538/4 \times 6.53)\ W = 20.597\ W$

$H = (20.6/422)\ W = .0488\ W$

$W = (160 + 76)\ 386 = 91096.$ lb

$H = 4445$ lb

TOTAL SHEAR STRESS

$V_T = S + H = 51801 + 4445$

$= 56246$ lb.

SHEAR STRESS

$$v = \frac{V}{bd} = 56246/448 = 125 \text{ psi}$$

2) VERTICAL MOTION

MASS

$$m_t = \text{ROOF} + \text{BEAM} + \tfrac{1}{2}(\text{COLUMN}) + \tfrac{1}{2}(\text{WALL})$$

$$= 160.9 + 75.9 + \tfrac{1}{2}(54.9) + 57.82 = 318.2$$

STIFFNESS

$$k_c = \frac{AE}{\ell} = \frac{480 \times 3 \times 10^6}{422.9} = 3.41 \times 10^6 \text{ LB/IN}$$

$$k_b = \frac{384}{5}\frac{EI}{\ell^3} = \frac{384 \times 3.0 \times 10^6 \times 97810}{5 \times 564^3}$$

$$= 125611 \text{ LB/IN}$$

$$1/k = \frac{1}{\frac{1}{k_c} + \frac{1}{k_b}} = 8.254 \times 10^{-6} \qquad k = 121148 \text{ LB/IN}$$

FREQUECY

$f = \frac{1}{2\pi}\sqrt{\frac{k}{m}} = 3.1$ cps COMPARE WITH 3.3 FROM FINITE ELEMENT

SPECTRUM ANALYSIS

APPLY ORION VERTICAL WITH $f = 3.1$ cps

$a = 1.0\,g$

$F = ma = 318.2 \times 386 = 122825$ LB

$V_d = \frac{1}{2} F = 61412$ LB

STATIC SHEAR

$V_s = 30470$ LB

$V_t = 91883$

$v_c = \frac{V}{bd} = \frac{91883}{705} = 130$ psi

SHEAR STRESS BY FINITE ELEMENT METHOD

a) COLUMN

AT NODE #6

DYN. SHEAR = 32800 LB (FROM TABLE A·2)

STATIC

$H = .0488\ W$

$W = 91400$ LB

$H = 4450$ LB

$V_T = 32800 + 4450 = 37250$ LB

$$v = \frac{V}{bd} = \frac{37250}{448} = 84 \text{ psi}$$

b) BEAM

AT NODE #15

DYN. SHEAR = 82570 LB (FROM TABLE A·2)

STATIC

$H = \frac{1}{3} W = 30470$ LB (ESTIMATED)

AGBABIAN ASSOCIATES	SUBJECT V A Hospital Boiler Building
	AUTHOR Y C Lee DATE 3/3/81 FILE NO.
	CHECKED BY DATE PAGE 9 OF 11

$V = 82570 + 45700 = 113{,}40$ LB

$$v_c = \frac{V}{bd} = \frac{113040}{705} = 160 \text{ psi}$$

Allowable Shear Stress of Concrete

a) Column

From Finite Element Analysis, at Node #6

$N = 85{,}000$ LB. (Table A·2)

$V = 32800$ LB

$M = 20.3 \times 10^6$ IN-LB

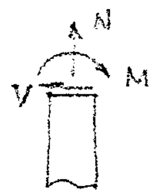

Forces from Dead Load

Weight of Beam

$W_b = 75.9 \times 386 = 29{,}200$ LB

Weight of Roof

$W_r = 160.9 \times 386 = 62{,}200$ LB

$W = W_b + W_r = 91400$ LB

Axial Force

$N' = \frac{1}{2} W = 45700$ LB

$N_R = N + N' = 85000 - 45700 = 39300$ LB TENSION

$A_g = 16(32-4) = 488$

$v_c = 2(1 + .002 \frac{N_u}{A_g})\sqrt{f_c'}$

TYPE 'B' CONCRETE

$f_c' = 2500$ psi

$v_c = 2(1 - 002 \frac{39300}{448})\, 50 = 82$ psi

b) BEAM

AT NODE # 15

N = 21170 LB
V = 82570 LB
M = 1599,0000 IN-LB

$A_g = 16(48-4) = 16 \times 44 = 705$

$v_c = 2(1 + .002 \frac{21170}{705})\, 50 = 94$ psi

APPENDIX C

ADDITIONAL DATA ON MODEL FOR BUILDING 10

AGBABIAN ASSOCIATES	SUBJECT NSF / BLDG-10 / SEISMIC ANALYSIS
	AUTHOR O.B. DATE 10-12-79 FILE NO. 7933
	CHECKED BY DATE PAGE B-1 OF

PHYSICAL CHARACTRISTICS

Building NO. 10 is one of the many Veterans Administration Hospital buildings which have been built since 1952 in the San Fernando Valley. It is a Reinforced Brick Masonry building.

AGBABIAN ASSOCIATES	SUBJECT: NSF / BLDG-10 / SEISMIC ANALYSIS		
	AUTHOR: O.B.	DATE: 10-12-79	FILE NO. 7933
	CHECKED BY:	DATE:	PAGE B-2 OF

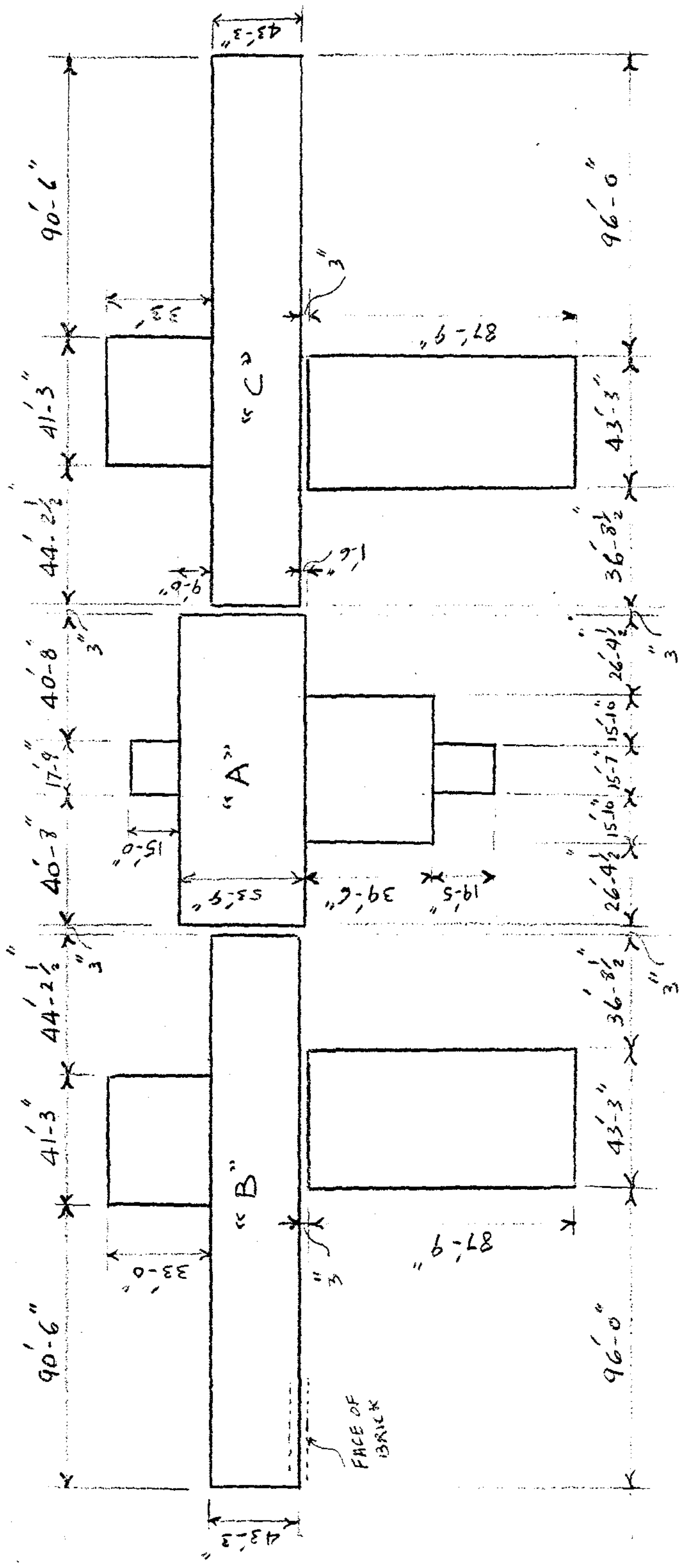

BUILDG -10

Reproduced from best available copy.

AGBABIAN ASSOCIATES

SUBJECT: NSF / BLDG 10 / SEISMIC ANALYSIS
sec. "B"

AUTHOR: O.B. DATE: 10-12-79 FILE NO. 7933

CHECKED BY: DATE: PAGE B-4 OF

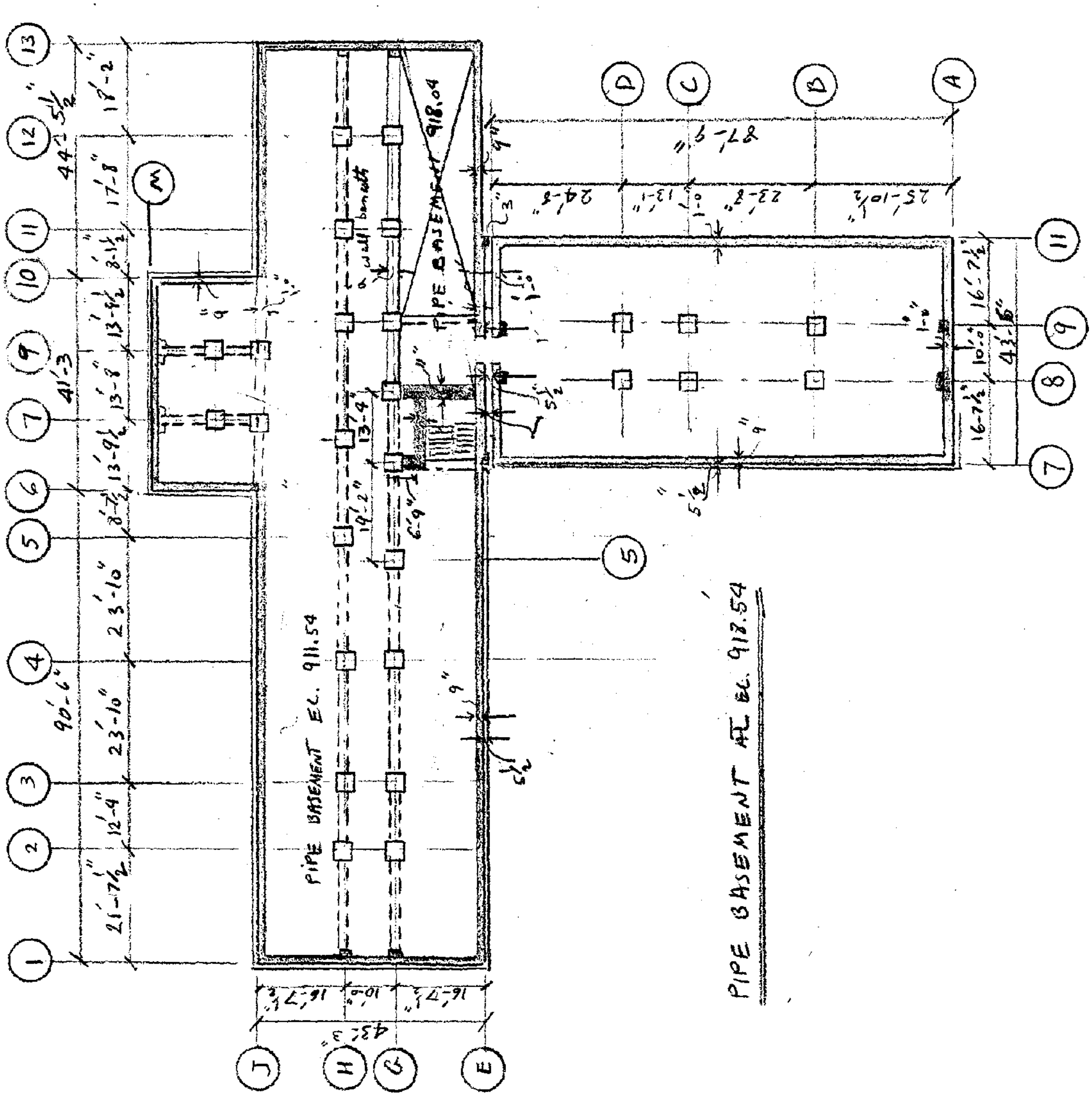

AGBABIAN ASSOCIATES

SUBJECT: NSF / BLDG-10 / SEISMIC ANALYSIS
SEC "B"

AUTHOR: O.B. DATE: 10-12-79 FILE NO. 7933

CHECKED BY: ______ DATE: ______ PAGE B-5 OF ______

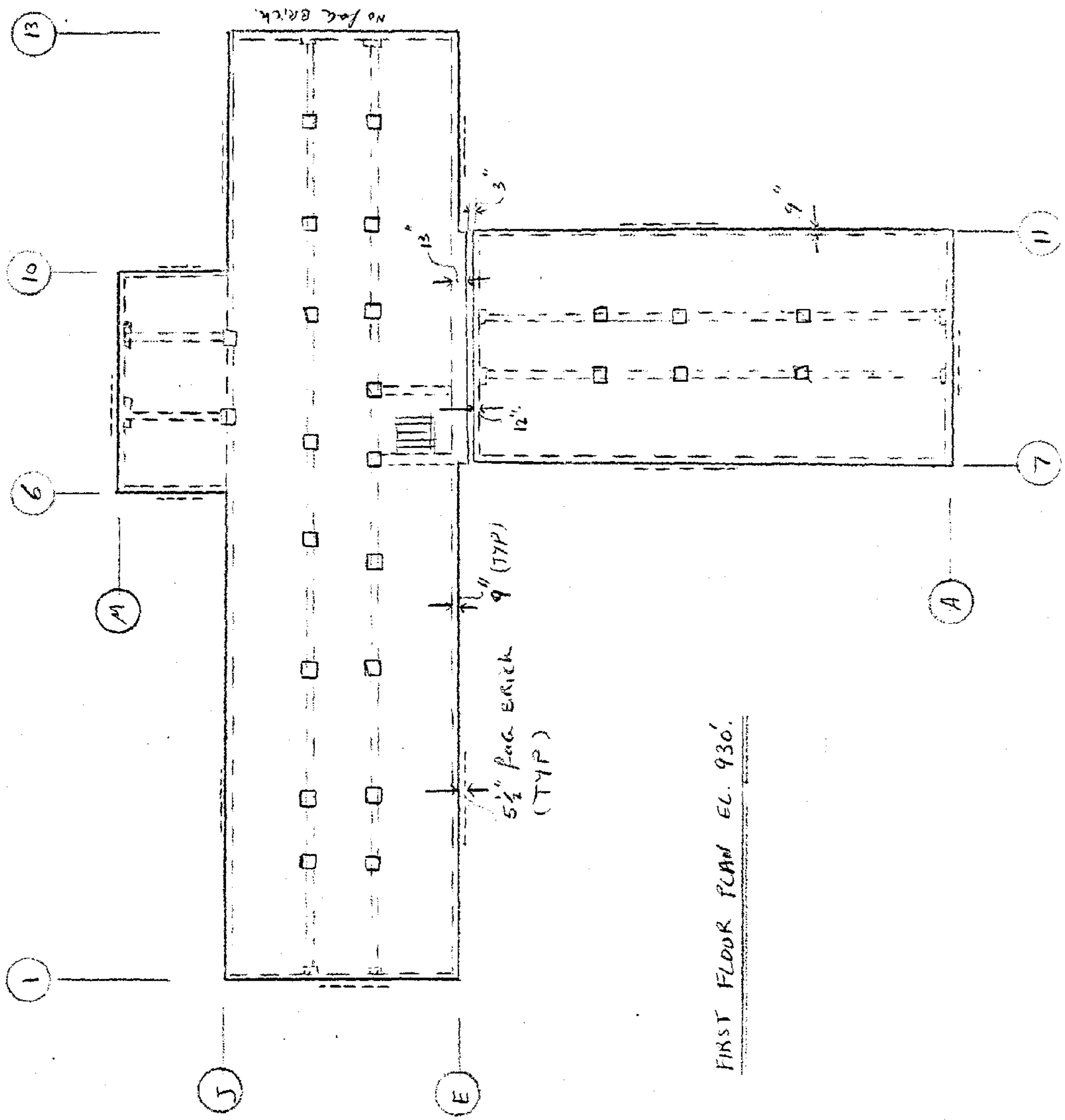

FIRST FLOOR PLAN EL. 930'

Reproduced from best available copy.

AGBABIAN ASSOCIATES

SUBJECT NSF / BUILDG 10 / SEISMIC ANALYSIS

SEC "A"

AUTHOR OB DATE 10-15-79 FILE NO. 7933

CHECKED BY DATE PAGE A-3 OF

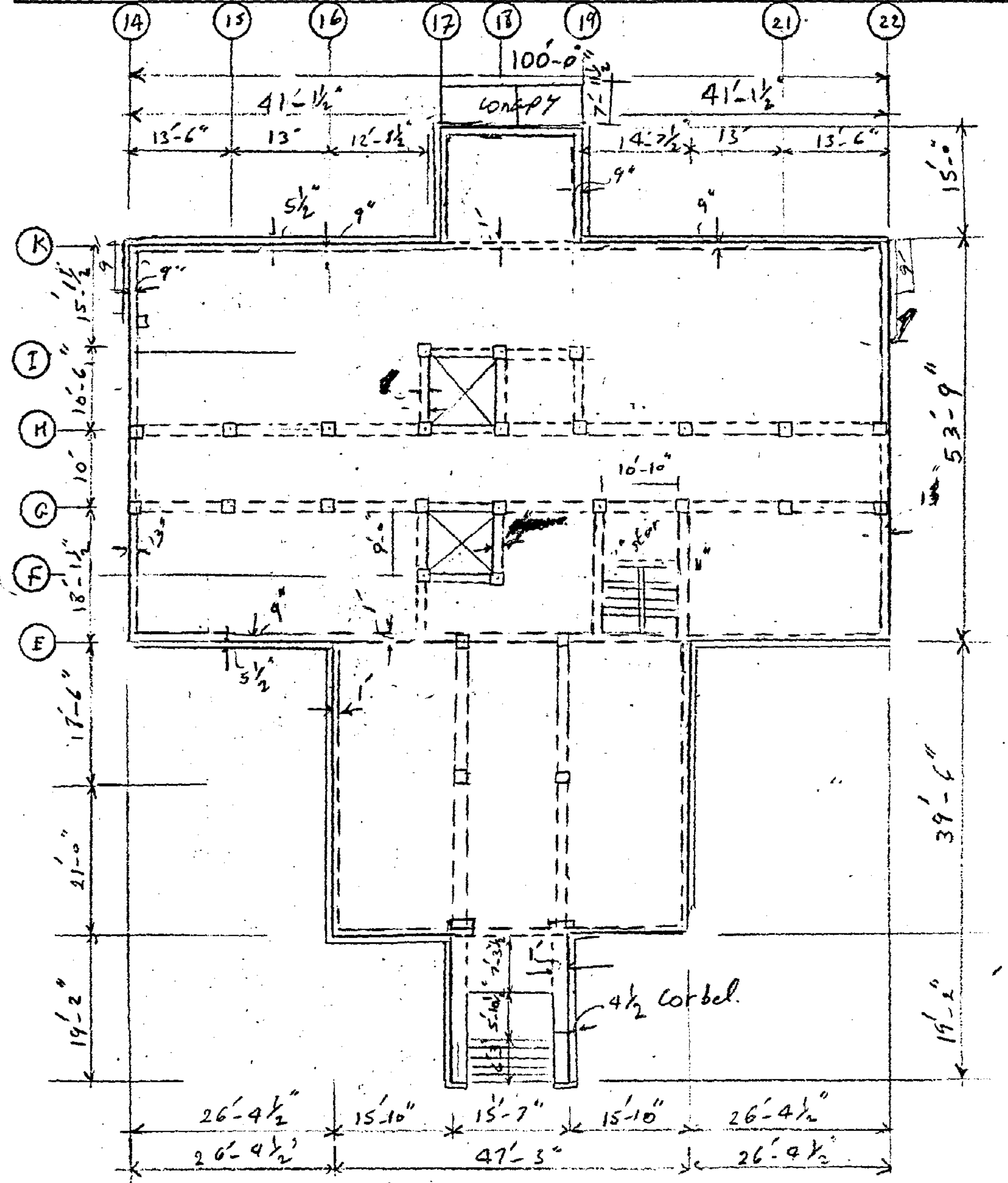

FIRST FLOOR PLAN @ EL 930'-0"

AGBABIAN ASSOCIATES

SUBJECT NSF / BLDG 10 / SEISMIC ANALYSIS
SEC. "A"
AUTHOR OB DATE 10-16-79 FILE NO. 7933
CHECKED BY ____ DATE ____ PAGE A-11 OF ____

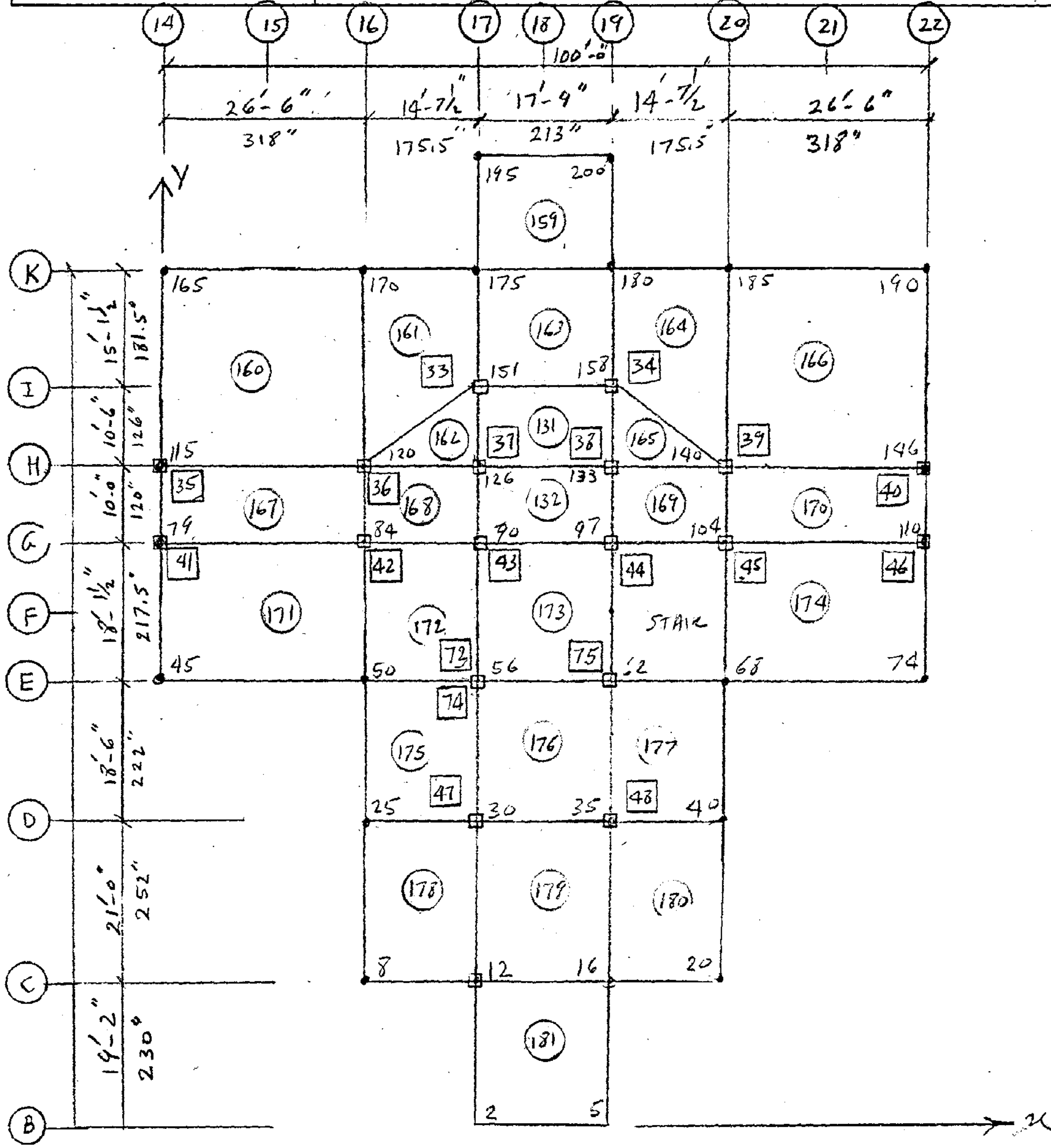

FIRST FLOOR MODEL EL. 930'-0"

□ column

○ SLAB

C-6

AGBABIAN ASSOCIATES

SUBJECT NSF / BLDG 10 / SEISMIC ANALYSIS
SEC. "A"

AUTHOR OB. DATE 10-16-79 FILE NO. 7933

CHECKED BY ______ DATE ______ PAGE 415 OF ______

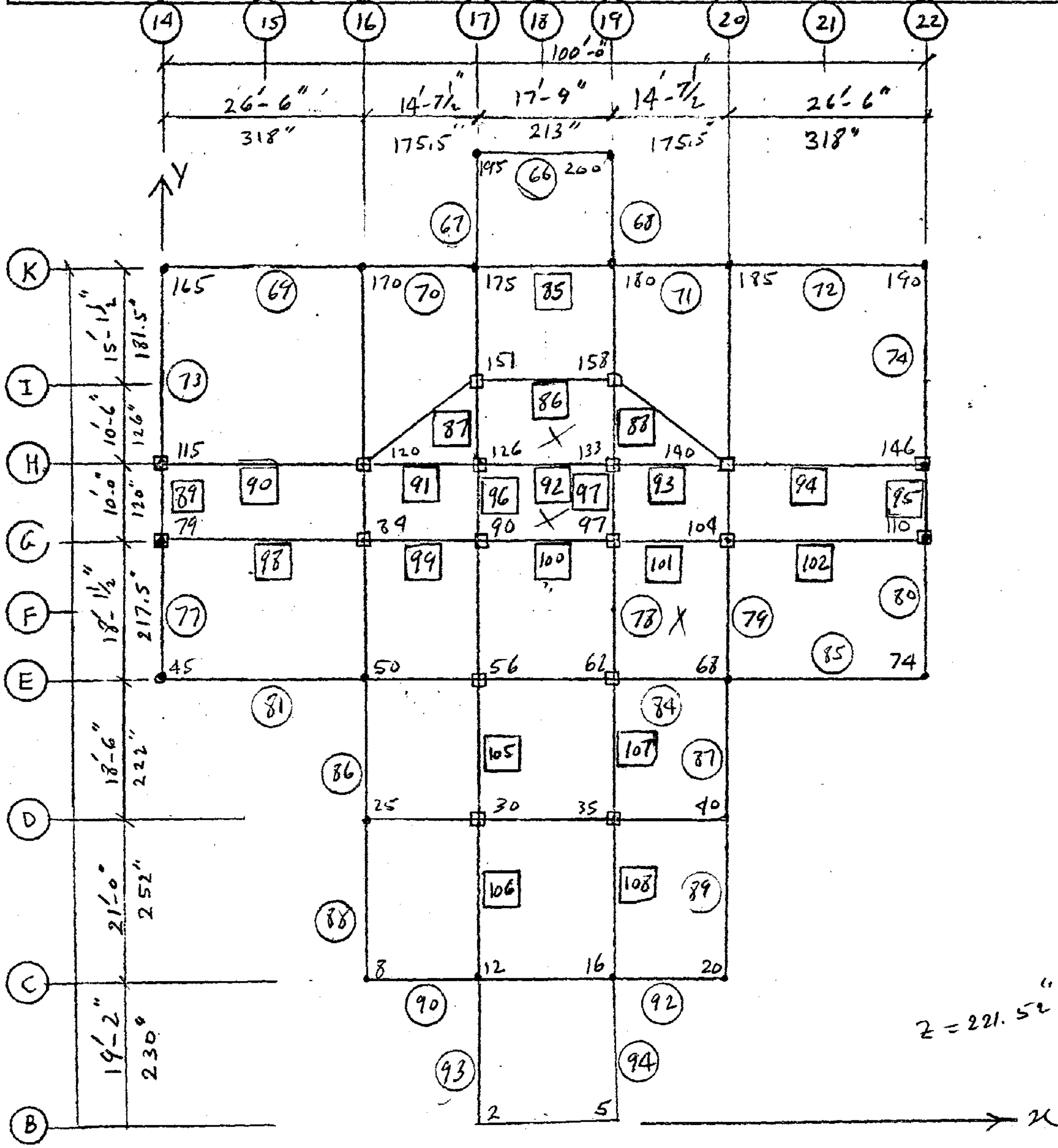

FIRST FLOOR PLAN EL. 930'-0"

AGBABIAN ASSOCIATES	
	SUBJECT NSF / BLDG 10 / SEISMIC ANALYSIS SEC "A"
	AUTHOR O.B. DATE 10-23-79 FILE NO. 7933
	CHECKED BY DATE PAGE A-19 OF

WALL SECTIONS TYPICAL

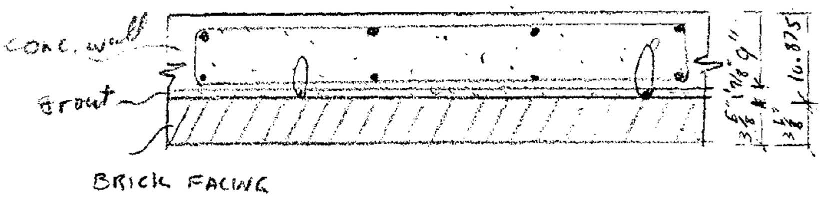

(1) TYP 14 1/2" WALL (CONC.)

in model: $t = 10.875"$
ignore the facing just add the mass to model
$f'_c = 3000$ psi
$w_{conc.} = 145$ pcf
$E_c = 33 w^{1.5} \sqrt{f'_c} = 3.16 \times 10^6$ psi
$G_c = 1.37 \times 10^6$ psi
$\gamma_{m\,wall} = 0.000277 \; \frac{lb\text{-}sec^2}{in^4}$

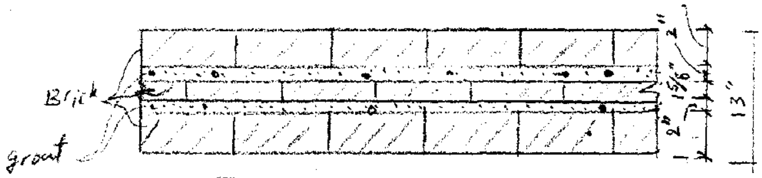

(2) TYP 13" WALL (BRIC)

in model: $t = 13"$
assume the whole act as a brick wall
$E_m = 2.5 \times 10^6$ psi
$G_m = 1.04 \times 10^6$ psi
$\nu = 0.2$
$w_{brick} = 120$ pcf
$\gamma_{m\,wall} = 0.000192 \; \frac{lb\text{-}sec^2}{in^4}$

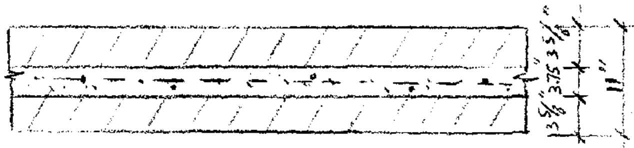

(3) TYP 11" WALL (BRIC

in model: $t = 11"$
assume the whole wall act as a brick wall
$E_m = 2.5 \times 10^6$ psi
$G_m = 1.04 \times 10^6$ psi
$\nu = 0.2$
$w_{brick} = 120$ pcf
$\gamma_{m\,wall} = 0.000193 \; \frac{lb\text{-}sec^2}{in^4}$

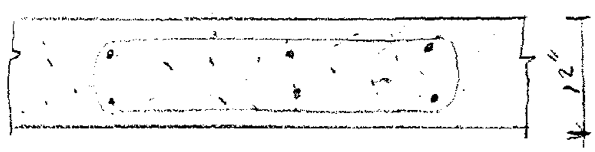

12" conc. wall

in model $t = 12"$
$f'_c = 3000$ psi
$w = 145$ pcf
$\gamma_m = 0.0002173 \; \frac{lb\text{-}sec^2}{in^4}$
$E = 33 w^{1.5} \sqrt{f'_c}$
$=$

Reproduced from best available copy.